THE UNIVERSITY OF CALGARY

Applications of Micromechanics in Granular Sand and Swelling Clay

by

Xiaoxiong Zhong

A THESIS

SUBMITTED TO THE FACULTY OF GRADUATE STUDIES

IN PARTIAL FULFILMENT OF THE REQUIREMENT FOR THE

DEGREE OF MASTER OF SCIENCE

DEPARTMENT OF CIVIL ENGINEERING

CALGARY, ALBERTA

AUGUST, 1994

ISBN 0-315-99535-1

Name XIAOXIONG ZHONG

Dissertation Abstracts International is arranged by broad, general subject categories. Please select the one subject which most nearly describes the content of your dissertation. Enter the corresponding four-digit code in the spaces provided.

GEOTECHNICAL ENGINEERING — SUBJECT TERM

0543 — SUBJECT CODE

UMI

Subject Categories

THE HUMANITIES AND SOCIAL SCIENCES

COMMUNICATIONS AND THE ARTS
Architecture 0729
Art History 0377
Cinema 0900
Dance 0378
Fine Arts 0357
Information Science 0723
Journalism 0391
Library Science 0399
Mass Communications 0708
Music 0413
Speech Communication 0459
Theater 0465

EDUCATION
General 0515
Administration 0514
Adult and Continuing 0516
Agricultural 0517
Art 0273
Bilingual and Multicultural 0282
Business 0688
Community College 0275
Curriculum and Instruction 0727
Early Childhood 0518
Elementary 0524
Finance 0277
Guidance and Counseling 0519
Health 0680
Higher 0745
History of 0520
Home Economics 0278
Industrial 0521
Language and Literature 0279
Mathematics 0280
Music 0522
Philosophy of 0998
Physical 0523
Psychology 0525
Reading 0535
Religious 0527
Sciences 0714
Secondary 0533
Social Sciences 0534
Sociology of 0340
Special 0529
Teacher Training 0530
Technology 0710
Tests and Measurements 0288
Vocational 0747

LANGUAGE, LITERATURE AND LINGUISTICS
Language
General 0679
Ancient 0289
Linguistics 0290
Modern 0291
Literature
General 0401
Classical 0294
Comparative 0295
Medieval 0297
Modern 0298
African 0316
American 0591
Asian 0305
Canadian (English) 0352
Canadian (French) 0355
English 0593
Germanic 0311
Latin American 0312
Middle Eastern 0315
Romance 0313
Slavic and East European 0314

PHILOSOPHY, RELIGION AND THEOLOGY
Philosophy 0422
Religion
General 0318
Biblical Studies 0321
Clergy 0319
History of 0320
Philosophy of 0322
Theology 0469

SOCIAL SCIENCES
American Studies 0323
Anthropology
Archaeology 0324
Cultural 0326
Physical 0327
Business Administration
General 0310
Accounting 0272
Banking 0770
Management 0454
Marketing 0338
Canadian Studies 0385
Economics
General 0501
Agricultural 0503
Commerce-Business 0505
Finance 0508
History 0509
Labor 0510
Theory 0511
Folklore 0358
Geography 0366
Gerontology 0351
History
General 0578
Ancient 0579
Medieval 0581
Modern 0582
Black 0328
African 0331
Asia, Australia and Oceania 0332
Canadian 0334
European 0335
Latin American 0336
Middle Eastern 0333
United States 0337
History of Science 0585
Law 0398
Political Science
General 0615
International Law and Relations 0616
Public Administration 0617
Recreation 0814
Social Work 0452
Sociology
General 0626
Criminology and Penology 0627
Demography 0938
Ethnic and Racial Studies 0631
Individual and Family Studies 0628
Industrial and Labor Relations 0629
Public and Social Welfare 0630
Social Structure and Development 0700
Theory and Methods 0344
Transportation 0709
Urban and Regional Planning 0999
Women's Studies 0453

THE SCIENCES AND ENGINEERING

BIOLOGICAL SCIENCES
Agriculture
General 0473
Agronomy 0285
Animal Culture and Nutrition 0475
Animal Pathology 0476
Food Science and Technology 0359
Forestry and Wildlife 0478
Plant Culture 0479
Plant Pathology 0480
Plant Physiology 0817
Range Management 0777
Wood Technology 0746
Biology
General 0306
Anatomy 0287
Biostatistics 0308
Botany 0309
Cell 0379
Ecology 0329
Entomology 0353
Genetics 0369
Limnology 0793
Microbiology 0410
Molecular 0307
Neuroscience 0317
Oceanography 0416
Physiology 0433
Radiation 0821
Veterinary Science 0778
Zoology 0472
Biophysics
General 0786
Medical 0760

EARTH SCIENCES
Biogeochemistry 0425
Geochemistry 0996
Geodesy 0370
Geology 0372
Geophysics 0373
Hydrology 0388
Mineralogy 0411
Paleobotany 0345
Paleoecology 0426
Paleontology 0418
Paleozoology 0985
Palynology 0427
Physical Geography 0368
Physical Oceanography 0415

HEALTH AND ENVIRONMENTAL SCIENCES
Environmental Sciences 0768
Health Sciences
General 0566
Audiology 0300
Chemotherapy 0992
Dentistry 0567
Education 0350
Hospital Management 0769
Human Development 0758
Immunology 0982
Medicine and Surgery 0564
Mental Health 0347
Nursing 0569
Nutrition 0570
Obstetrics and Gynecology 0380
Occupational Health and Therapy 0354
Ophthalmology 0381
Pathology 0571
Pharmacology 0419
Pharmacy 0572
Physical Therapy 0382
Public Health 0573
Radiology 0574
Recreation 0575
Speech Pathology 0460
Toxicology 0383
Home Economics 0386

PHYSICAL SCIENCES
Pure Sciences
Chemistry
General 0485
Agricultural 0749
Analytical 0486
Biochemistry 0487
Inorganic 0488
Nuclear 0738
Organic 0490
Pharmaceutical 0491
Physical 0494
Polymer 0495
Radiation 0754
Mathematics 0405
Physics
General 0605
Acoustics 0986
Astronomy and Astrophysics 0606
Atmospheric Science 0608
Atomic 0748
Electronics and Electricity 0607
Elementary Particles and High Energy 0798
Fluid and Plasma 0759
Molecular 0609
Nuclear 0610
Optics 0752
Radiation 0756
Solid State 0611
Statistics 0463

Applied Sciences
Applied Mechanics 0346
Computer Science 0984
Engineering
General 0537
Aerospace 0538
Agricultural 0539
Automotive 0540
Biomedical 0541
Chemical 0542
Civil 0543
Electronics and Electrical 0544
Heat and Thermodynamics 0348
Hydraulic 0545
Industrial 0546
Marine 0547
Materials Science 0794
Mechanical 0548
Metallurgy 0743
Mining 0551
Nuclear 0552
Packaging 0549
Petroleum 0765
Sanitary and Municipal 0554
System Science 0790
Geotechnology 0428
Operations Research 0796
Plastics Technology 0795
Textile Technology 0994

PSYCHOLOGY
General 0621
Behavioral 0384
Clinical 0622
Developmental 0620
Experimental 0623
Industrial 0624
Personality 0625
Physiological 0989
Psychobiology 0349
Psychometrics 0632
Social 0451

Nom ______________________________

Dissertation Abstracts International est organisé en catégories de sujets. Veuillez s.v.p. choisir le sujet qui décrit le mieux votre thèse et inscrivez le code numérique approprié dans l'espace réservé ci-dessous.

______________________________ SUJET   ☐☐☐☐ CODE DE SUJET   U·M·I

Catégories par sujets

HUMANITÉS ET SCIENCES SOCIALES

COMMUNICATIONS ET LES ARTS

- Architecture 0729
- Beaux-arts 0357
- Bibliothéconomie 0399
- Cinéma 0900
- Communication verbale 0459
- Communications 0708
- Danse 0378
- Histoire de l'art 0377
- Journalisme 0391
- Musique 0413
- Sciences de l'information 0723
- Théâtre 0465

ÉDUCATION

- Généralités 515
- Administration 0514
- Art 0273
- Collèges communautaires 0275
- Commerce 0688
- Économie domestique 0278
- Éducation permanente 0516
- Éducation préscolaire 0518
- Éducation sanitaire 0680
- Enseignement agricole 0517
- Enseignement bilingue et multiculturel 0282
- Enseignement industriel 0521
- Enseignement primaire. 0524
- Enseignement professionnel 0747
- Enseignement religieux 0527
- Enseignement secondaire 0533
- Enseignement spécial 0529
- Enseignement supérieur 0745
- Évaluation 0288
- Finances 0277
- Formation des enseignants 0530
- Histoire de l'éducation 0520
- Langues et littérature 0279
- Lecture 0535
- Mathématiques 0280
- Musique 0522
- Orientation et consultation 0519
- Philosophie de l'éducation 0998
- Physique 0523
- Programmes d'études et enseignement 0727
- Psychologie 0525
- Sciences 0714
- Sciences sociales 0534
- Sociologie de l'éducation 0340
- Technologie 0710

LANGUE, LITTÉRATURE ET LINGUISTIQUE

- Langues
  - Généralités 0679
  - Anciennes 0289
  - Linguistique 0290
  - Modernes 0291
- Littérature
  - Généralités 0401
  - Anciennes 0294
  - Comparée 0295
  - Mediévale 0297
  - Moderne 0298
  - Africaine 0316
  - Américaine 0591
  - Anglaise 0593
  - Asiatique 0305
  - Canadienne (Anglaise) 0352
  - Canadienne (Française) 0355
  - Germanique 0311
  - Latino-américaine 0312
  - Moyen-orientale 0315
  - Romane 0313
  - Slave et est-européenne 0314

PHILOSOPHIE, RELIGION ET THEOLOGIE

- Philosophie 0422
- Religion
  - Généralités 0318
  - Clergé 0319
  - Études bibliques 0321
  - Histoire des religions 0320
  - Philosophie de la religion 0322
- Théologie 0469

SCIENCES SOCIALES

- Anthropologie
  - Archéologie 0324
  - Culturelle 0326
  - Physique 0327
- Droit 0398
- Économie
  - Généralités 0501
  - Commerce-Affaires 0505
  - Économie agricole 0503
  - Économie du travail 0510
  - Finances 0508
  - Histoire 0509
  - Théorie 0511
- Études américaines 0323
- Études canadiennes 0385
- Études féministes 0453
- Folklore 0358
- Géographie 0366
- Gérontologie 0351
- Gestion des affaires
  - Généralités 0310
  - Administration 0454
  - Banques 0770
  - Comptabilité 0272
  - Marketing 0338
- Histoire
  - Histoire générale 0578
  - Ancienne 0579
  - Médiévale 0581
  - Moderne 0582
  - Histoire des noirs 0328
  - Africaine 0331
  - Canadienne 0334
  - États-Unis 0337
  - Européenne 0335
  - Moyen-orientale 0333
  - Latino-américaine 0336
  - Asie, Australie et Océanie 0332
- Histoire des sciences 0585
- Loisirs 0814
- Planification urbaine et régionale 0999
- Science politique
  - Généralités 0615
  - Administration publique 0617
  - Droit et relations internationales 0616
- Sociologie
  - Généralités 0626
  - Aide et bien-àtre social 0630
  - Criminologie et établissements pénitentiaires 0627
  - Démographie 0938
  - Études de l' individu et de la famille 0628
  - Études des relations interethniques et des relations raciales 0631
  - Structure et développement social 0700
  - Théorie et méthodes. 0344
  - Travail et relations industrielles 0629
- Transports 0709
- Travail social 0452

SCIENCES ET INGÉNIERIE

SCIENCES BIOLOGIQUES

- Agriculture
  - Généralités 0473
  - Agronomie. 0285
  - Alimentation et technologie alimentaire 0359
  - Culture 0479
  - Élevage et alimentation 0475
  - Exploitation des péturages 0777
  - Pathologie animale 0476
  - Pathologie végétale 0480
  - Physiologie végétale 0817
  - Sylviculture et faune 0478
  - Technologie du bois 0746
- Biologie
  - Généralités 0306
  - Anatomie 0287
  - Biologie (Statistiques) 0308
  - Biologie moléculaire 0307
  - Botanique 0309
  - Cellule 0379
  - Écologie 0329
  - Entomologie 0353
  - Génétique 0369
  - Limnologie 0793
  - Microbiologie 0410
  - Neurologie 0317
  - Océanographie 0416
  - Physiologie 0433
  - Radiation 0821
  - Science vétérinaire 0778
  - Zoologie 0472
- Biophysique
  - Généralités 0786
  - Medicale 0760

SCIENCES DE LA TERRE

- Biogéochimie 0425
- Géochimie 0996
- Géodésie 0370
- Géographie physique 0368
- Géologie 0372
- Géophysique 0373
- Hydrologie 0388
- Minéralogie 0411
- Océanographie physique 0415
- Paléobotanique 0345
- Paléoécologie 0426
- Paléontologie 0418
- Paléozoologie 0985
- Palynologie 0427

SCIENCES DE LA SANTÉ ET DE L'ENVIRONNEMENT

- Économie domestique 0386
- Sciences de l'environnement 0768
- Sciences de la santé
  - Généralités 0566
  - Administration des hipitaux 0769
  - Alimentation et nutrition 0570
  - Audiologie 0300
  - Chimiothérapie 0992
  - Dentisterie 0567
  - Développement humain 0758
  - Enseignement 0350
  - Immunologie 0982
  - Loisirs 0575
  - Médecine du travail et thérapie 0354
  - Médecine et chirurgie 0564
  - Obstétrique et gynécologie 0380
  - Ophtalmologie 0381
  - Orthophonie 0460
  - Pathologie 0571
  - Pharmacie 0572
  - Pharmacologie 0419
  - Physiothérapie 0382
  - Radiologie 0574
  - Santé mentale 0347
  - Santé publique 0573
  - Soins infirmiers 0569
  - Toxicologie 0383

SCIENCES PHYSIQUES

Sciences Pures

- Chimie
  - Genéralités 0485
  - Biochimie 487
  - Chimie agricole 0749
  - Chimie analytique 0486
  - Chimie minérale 0488
  - Chimie nucléaire 0738
  - Chimie organique 0490
  - Chimie pharmaceutique 0491
  - Physique 0494
  - PolymÇres 0495
  - Radiation 0754
- Mathématiques 0405
- Physique
  - Généralités 0605
  - Acoustique 0986
  - Astronomie et astrophysique 0606
  - Electronique et électricité 0607
  - Fluides et plasma 0759
  - Météorologie 0608
  - Optique 0752
  - Particules (Physique nucléaire) 0798
  - Physique atomique 0748
  - Physique de l'état solide 0611
  - Physique moléculaire 0609
  - Physique nucléaire 0610
  - Radiation 0756
- Statistiques 0463

Sciences Appliqués Et Technologie

- Informatique 0984
- Ingénierie
  - Généralités 0537
  - Agricole 0539
  - Automobile 0540
  - Biomédicale 0541
  - Chaleur et ther modynamique 0348
  - Conditionnement (Emballage) 0549
  - Génie aérospatial 0538
  - Génie chimique 0542
  - Génie civil 0543
  - Génie électronique et électrique 0544
  - Génie industriel 0546
  - Génie mécanique 0548
  - Génie nucléaire 0552
  - Ingénierie des systämes 0790
  - Mécanique navale 0547
  - Métallurgie 0743
  - Science des matériaux 0794
  - Technique du pétrole 0765
  - Technique minière 0551
  - Techniques sanitaires et municipales 0554
  - Technologie hydraulique 0545
- Mécanique appliquée 0346
- Géotechnologie 0428
- Matières plastiques (Technologie) 0795
- Recherche opérationnelle 0796
- Textiles et tissus (Technologie) 0794

PSYCHOLOGIE

- Généralités 0621
- Personnalité 0625
- Psychobiologie 0349
- Psychologie clinique 0622
- Psychologie du comportement 0384
- Psychologie du développement 0620
- Psychologie expérimentale 0623
- Psychologie industrielle 0624
- Psychologie physiologique 0989
- Psychologie sociale 0451
- Psychométrie 0632

THE UNIVERSITY OF CALGARY

FACULTY OF GRADUATE STUDIES

The undersigned certify that they have read, and recommend to the Faculty of Graduate Studies for acceptance, a thesis entitled " Applications of Micromechanics in Granular Sand and Swelling Clay " submitted by Xiaoxiong Zhong in partial fulfilment of the requirements for the degree of Master of Science.

Ron Wong

Chairperson, Dr. R.C. Wong
Department of Civil Engineering

NG Shrive

Dr. N.G. Shrive
Department of Civil Engineering

Dr. R.G. Wan
Department of Civil Engineering

M. Epstein

Dr. M. Epstein
Department of Mechanical Engineering

AUGUST 22, 1994

Date

ABSTRACT

The shear behaviours of a granular assembly of rigid particles in simple shear and biaxial compression conditions have been studied using the principle of micromechanics. Analytical solutions are derived to describe the stress ratio, the change in fabric distribution and orientation, and the strain ratio during the process of shearing deformation. The stress-strain relations of contact deformation for two-dimensional and three-dimensional regular packing assemblies are established. For random packing assembly the stress-strain relations under contact deformation are derived considering the fabric distribution and orientation, and micromechanics. In addition, a stress-strain model has been developed to predict anisotropic swelling behaviour of clay. The model predicts that the swelling is dependent of clay particle swelling properties, fabrics and imposed principal stresses.

ACKNOWLEDGEMENTS

I would like to express a great deal of gratitude to my supervisor, Dr. R.C.K. Wong, for his guidance, penetrating discussion, and support throughout this research project. I would also like to express my sincere appreciation to his invaluable comments in revising and polishing the manuscript of this thesis.

I wish to acknowledge to Dr. N.G. Shrive, Dr. R.G. Wan, and Dr. M. Epstein for their critical reviews of the thesis.

Special thanks to Dr. F. Guo, Mr. X. Pan, Mr. W. Dale, Mr. Z. Lin, Mr. J. Li, Dr. E. Wang for their helpful assistance.

The financial support from the Department of Civil Engineering at The University of Calgary through teaching assistantship is gratefully appreciated.

Finally, I would like to thank my wife, Anjuan Tian, for her encouragement, understanding and moral support.

TABLE OF CONTENTS

LIST OF TABLES

LIST OF FIGURES

LIST OF SYMBOLS

$a(\theta)$, $a(\gamma, \beta)$	density function
A, B	fabric constants for two-dimensional assemblies
A_0, B_0	initial values of A and B, respectively
A_{ijkl}	fourth-order constitutive tensor
b	dimension of sample
B_{ijkl}	fourth-order tensor related to normal vectors
C	fabric constant for two-dimensional assembly
C_2	constant
C_{ij}	second-order constitutive tensor
C_{ij}'	constitutive coefficient for three-dimensional regular packing
C_0	initial value of C
C_m	test parameter
C_{se}	swell coefficient
D	integral parameter
D_n	normal contact stiffness of particles
D_s, D_t, D_r	tangential contact stiffness of particles
E	Young's modulus of isotropic assembly
E_{ijkl}	fourth-order tensor related to normal vectors
E_{zz}	Young's modulus of a transversely isotropic assembly
$E(\theta)$	contact normal distribution for two-dimensional assemblies

$E(\Omega)$	contact normal distribution for three-dimensional assemblies
e	void ratio
Δe	incremental void ratio
f_0	test parameter
f^i	contact force component
f_i	parameter (i = 1, 2, 3)
f_n	normal contact force
f_n^i	normal component of contact force at i^{th} contact point for two-dimension assemblies
f_r	resultant tangential contact force
f_s, f_t	tangential contact force
f_t^i	tangential component of contact force at i^{th} contact point for two-dimension assemblies
g_0	test parameter
g_i	parameters (i = 1, 2, 3)
G	shear modulus of an isotropic assembly
G_μ	particle shear modulus
G_{xz}, G_{xy}	shear modulus of a transversely isotropic assembly
h_i	parameters (i = 1, 2, 3)
H	width of slip band for two-dimensional simple shear
H_i	parameters (i=1 to i=7)
HX_i, HY_i, HZ_i	parameters (i=0 to i=9)

I_i	parameter (i=1 to i=6)
J_i	parameter (i=1 to i=8)
K	bulk modulus of assembly
l	branch vector
l^i	branch length component
L	branch length for two-dimensional simple shear
L^i	branch length component for two-dimensional simple shear
m	coordination number
m_1	number of contact points within a microelement
Δm	incremental coordination number
M	total number of contact point
ΔM	incremental total number of contact point
M_0	initial value of M
n	unit contact normal vector
n'	unit normal branch vector
n_x, n_y, n_z	components of n in x-, y-, and z-directions, respectively
n_i, n_j	contact normal components
N	total number of particles
N_1	number of particles within a microelement
N_1, N_2	minimum and maximum principal fabric values for two-dimensional assemblies
N_{ij}	fabric tensor

Q	constitutive constant
r	radius of spherical or disc particle
R	constitutive constant
s	unit contact tangential vector
s_x, s_y, s_z	components of s in x, y, and z directions, respectively
S	area of shear plane for two-dimensional simple shear condition
S^i	i^{th} contact project area on shear plane
t	unit contact tangential vector
t_x, t_y, t_z	components of t in x-, y-, and z-directions, respectively
u_i	displacement component
Δu_i	incremental contact displacement component
Δu_x, Δu_y	particle sliding components
V	volume of assembly
V_0	initial volume of assembly
ΔV	incremental volume of assembly
W	work done by stress in unit volume
XX'	overall sliding plane
α^i	dilatancy angle at the i^{th} contact point
β	spherical coordinate angle, from 0 to 2π
β'	intermediate variable
γ	shear strain for two-dimension simple shear, or

	spherical coordinate angle, from 0 to π
$d\gamma$	incremental shear strain
$\Delta\gamma_{ij}$	incremental shear strain tensor
γ_{xy}, γ_{xz}, γ_{yz}	shear strain components
δ	swell of clay particle
δ^i	swell of i^{th} clay particle
δ_r	resultant tangential contact displacement
δ_{xx}, δ_{yy}	swell components for swelling clay
ε	strain
ε_1, ε_2, ε_3	principal strain
$\Delta\varepsilon_1$, $\Delta\varepsilon_3$	incremental principal strain for two-dimensional assemblies
ε_v	volumetric strain
ε_{xx}, ε_{yy}, ε_{zz}	strain components
$\Delta\varepsilon_{xx}$, $\Delta\varepsilon_{yy}$, $\Delta\varepsilon_{zz}$	incremental strain components
$d\varepsilon$	incremental strain
$d\varepsilon_v$	incremental volumetric strain
η	test parameter
θ	contact angle for two-dimensional assembly
θ_1, θ_2	principal fabric angles
θ^i	contact angle at i^{th} contact point
θ_s	inclined angle of sliding wedge
$\Delta\theta$	average incremental contact angle

$\Delta\theta^i$	incremental contact angle at the i^{th} contact point
Θ	average dilatancy angle
Θ_0	initial value of Θ
λ	principal fabric ratio
μ	interparticle friction coefficient
μ_{max}	maximum value of μ
ν	Poisson's ratio of assembly
ν_v	Poisson's ratio of particle
ξ	contact stiffness ratio
σ_1, σ_2, σ_3	principal stresses
σ^i	induced normal stress at the i^{th} particle for swelling clay model
σ_{xx}, σ_{yy}, σ_{zz}	stress components
σ_{xy}, σ_{xz}, σ_{yz}	shear stress components
$\Delta\sigma_{ij}$	incremental stress tensor
σ_s	swell pressure
τ	shear stress for two-dimensional simple shear
τ^i	induced shear stress at the i^{th} particle for swelling clay model
ϕ_{cv}	friction angle at constant volume
ϕ_f	friction angle
ϕ_m	average mobilized friction angle
ϕ_μ	interparticle friction angle
ψ	$= \theta - 90°$

Ω	solid angle
$\Delta\Omega$	incremental solid angle

CHAPTER 1

INTRODUCTION

1.1 INTRODUCTION

The mechanical behaviour of a particulate assembly, including granular sand composed of spherical or non-spherical particles and swelling clay composed of "plate-like" particles, is significantly influenced by its microstructure. Theories of continuum mechanics have limitations when used to describe the strength, stress and strain of these particulate assemblies. Hence, mathematical models based on micromechanics are required to be established. There are two approaches based on micromechanics, namely, the discrete element approach and the microstructural continuum approach. The discrete element approach solves the governing equations of each particle interacting with its surrounding particle. This simulation method, which stems from the field of molecular dynamics, calculates the movements of all particles based on a set of mechanics laws that are also simultaneously satisfied for each particle. However, this approach is cumbersome for systems composed of a large number of particles because a prohibitive amount of computing effort is required to trace the movements and the equilibrating forces of all particles. Therefore, it is desirable to represent the discrete system using a more tractable continuum model, i.e., the microstructural continuum approach. In this approach, the micro-features of the particulate assembly such as the spatial arrangement of particles, the distributions of contact normals and inter-particulate forces, are considered using some fabric functions. With these fabric functions, the micro-variables (contact force and contact displacement) can be related to the macro-variables (stress and strain). The microstructural continuum approach has advantages over the classical continuum method because the former approach takes into account the effect of microstructure or fabric on the deformation behaviour of particulate assembly.

1.2 OBJECTIVES

The main goal of the research is to explore the use of the microstructural continuum method to study the deformation behaviour of particulate assemblies such as sand and clay. This goal can be fulfilled by achieving the following objectives:

(1) to quantify the shear deformation of a granular assembly of rigid particles under simple shear and biaxial compression conditions,

(2) to derive stress-strain relations for regular and random packing assemblies of deformable particles under general loading conditions,

(3) to develop 2-D and 3-D anisotropic models for swelling clay, and

(4) to verify the proposed models with experimental data.

1.3 LITERATURE REVIEW

Particulate assemblies typically comprise a large number of particles with a large number of degrees of freedom. Development of theories on constitutive mechanics of such assemblies are built on two concepts: (1) the concept of the mobilized plane which is used to analyze the strength feature of the particulate assembly, and (2) the concept of the constitutive stiffness which establishes the stress-strain relation in terms of the contact stiffness of particles and fabric parameters of the particulate assembly.

The concept of the mobilized plane was first introduced by Coulomb (1773) to describe the resistance due to internal friction between particles (Figure 1.1a). Based on this concept, the theory of active and passive pressures was developed by Rankine (1857). Roynolds (1885) examined the dilatancy induced by shearing in granular masses composed of rigid particles. The corresponding limiting equilibrium for an ideal granular wedge was derived (Caquot, 1934). Taylor (1938) proposed that the stress-strain relation was specified independently on mobilized planes of various orientations within the assembly, and assumed that either the stresses on the mobilized plane are the resolved components of the macroscopic stress tensor, or the strains on the mobilized plane are the resolved components of the macroscopic strain tensor. In addition, Taylor (1948) and Bishop (1950) studied the sliding behaviour by using the mechanism of interlocking between particles of granular materials. Interlocking of particles restricts the degree of mobilization and the shear strength becomes larger. As a result of the interlocking, dilation occurs with sliding. This dilatancy theory was developed by Newland and Allely (1957). They suggested that the relative sliding direction between two blocks is not parallel to the mobilized plane, but rather at an inclined angle.

Under the biaxial compressional condition, Rowe (1962) postulated a minimum energy principle stating that particles tend to slide along the direction of minimum energy and derived the relative direction of sliding between two blocks of particles in a random packing assembly subjected to a triaxial loading condition. Based on this postulate, the angle between the sliding direction and the mobilized plane is a function of applied stress,

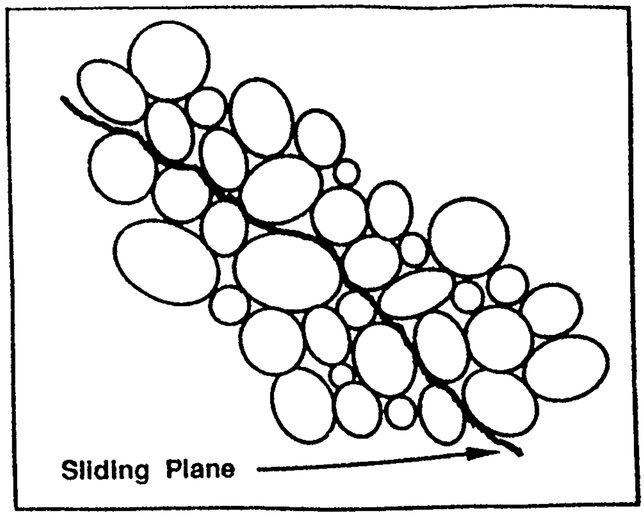

(a) Mobilized Plane Concept

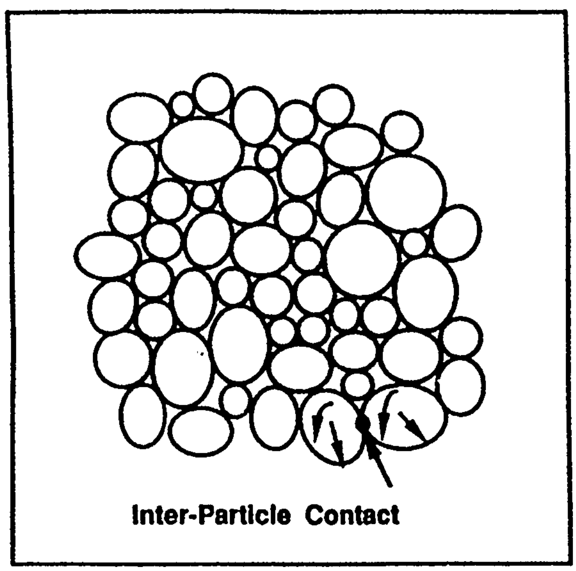

(b) Micromechanical Concept

Figure 1.1 Two Concepts in Constitutive Mechanics of Particulate Assembly

(After Chang et al., 1992a)

i.e.,

$$\frac{\sigma_1}{\sigma_3} = -\frac{\varepsilon_3}{\varepsilon_1}\tan^2(45° + \frac{\phi_\mu}{2}) \tag{1.1}$$

where ϕ_μ is inter-particle friction angle; σ_1 and σ_3 are applied stresses in the vertical and horizontal directions, respectively. Later, Horne (1965) studied Rowe's energy postulate by considering the sliding between pairs of particles in a random assembly.

Tokue (1979) and Nemat-Nasser (1980) assumed probability distributions function for the planes of sliding. Through an integration of this distribution, the average plane of sliding can be obtained. Chang (1985) also derived a similar dilatancy equation under simple shear condition, based on considering the deformation of a particle chain and assuming that the inclination of the mean sliding plane can be related to the mean inter-particle force vector of the assemblage. The derived dilatancy equation is given by

$$\frac{d\varepsilon}{d\gamma} = \frac{\tan\phi_\mu - \frac{\tau}{\sigma}}{1 + \frac{\tau}{\sigma}\tan\phi_\mu} \tag{1.2}$$

where $d\varepsilon$ is vertical strain; $d\gamma$ is horizontal shear strain; σ is vertical applied stress; and τ is horizontal applied shear stress.

In the concept of micromechanics (Figure 1.1b), the constitutive relations are defined at three levels, namely, contact, micro-element and representative-unit levels, as shown in Figure 1.2 and Figure 1.3 (Chang et al., 1992a).

At the contact level, the constitutive law is determined by micro-variables (contact force and contact displacement). At this level, the continuum concept has not yet been

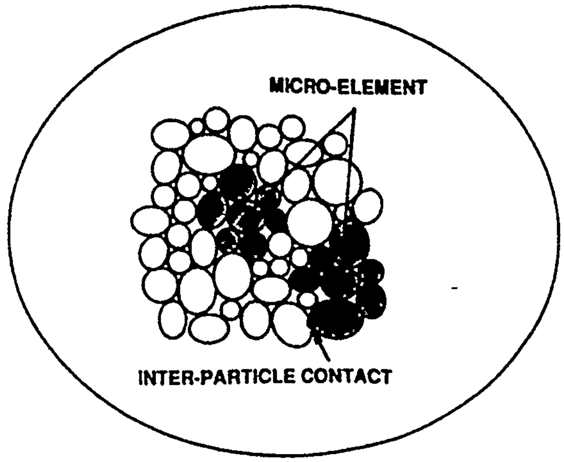

Figure 1.2 Schematic Representation of Three Levels of Particulate Assembly (After Chang et al., 1992a)

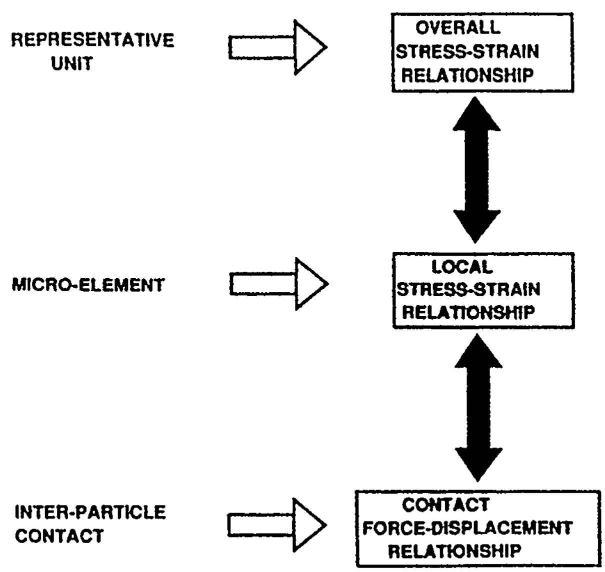

Figure 1.3 Micromechanics Approach for Modelling Mechanical Behaviour of Particulate Assembly (After Chang et al., 1992a)

introduced. The analysis at this stage is based on contact theory. If we assume that tangential (slip) contact stiffnesses and a normal (compression) contact stiffness being independent of one another, the relations between the shear contact forces (f_s, f_t) and the tangential contact displacements (δ_s, δ_t) are $f_s = D_s\delta_s$, and $f_t = D_t\delta_t$, respectively, where D_s and D_t are tangential contact stiffnesses in two directions perpendicular to each other, respectively. Likewise, the relation between the normal compressional force f_n and normal displacement δ_n is determined by $f_n = D_n\delta_n$, where D_n is normal contact stiffness. In this case, the stiffness tensor at the contact between particles takes a form of (Chang, 1990a, 1990c, 1992a)

$$D_{ij}=D_n\ n_in_j+D_s\ s_is_j+D_t\ t_it_j \tag{1.3}$$

where **n**, **s**, and **t** are basic unit vectors of the local coordinate system of each contact. If $D_s = D_t = D_r$, the resultant tangential shear force (f_r) is given by $f_r = D_r\delta_r$, where δ_r is the resultant shear displacement on the contact plane. So the equation (1.3) becomes

$$D_{ij}=D_n\ n_in_j+D_r\ (s_is_j+t_it_j) \tag{1.4}$$

When the contact force reaches the yield condition defined by the surface friction of particles, i.e., $f_r = f_n \tan\phi_\mu$, sliding occurs and D_r vanishes. When the contact force tends to be in tension, particle separation occurs and D_n vanishes. If linear behaviour is studied, we can choose the contact stiffnesses (D_n, D_s, and D_t) to be constants as shown in Figure 1.4. However, if we discuss non-linear contact, the contact stiffnesses are functions of the contact forces and contact area becomes more complicated. For a contact of two smooth spheres, the tangential stiffness under oscillating contact force was studied

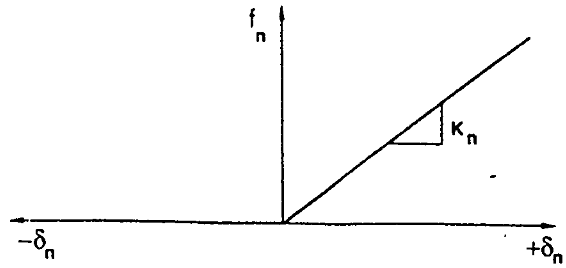

(a) Normal

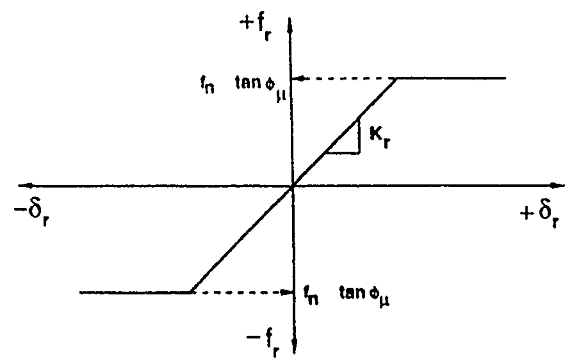

(b) Shear

Figure 1.4 Force and Displacement Relations (After Change et al., 1992a) by Mindlin and Deresiewicz (1953). They summarized some of the difficulties encountered and some results obtained in the course of development of a mathematical theory of small deformations of granular media. The medium is assumed to be composed of discrete, isotropic, elastic granules in direct contact under local forces which, in general, vary in the magnitude and in direction. The consideration of the effects of this variation served to distinguish the theory from several others (Hara, 1935; Iida, 1939; Gassmann, 1953) in which only normal components of the contact forces were taken into account.

A general expression for the tangential stiffness of two particles can be written as a function of the contact force and the particle properties as follows

$$D_r = C_1 D_n \left(1 - \frac{f_r}{f_n \tan\phi_\mu}\right)^{\frac{1}{3}} \tag{1.5}$$

where ν_μ is the particle Poisson's ratio; $C_1 = 2(1-\nu_\mu)/(2-\nu_\mu)$.

Considering the contact area to be circular with a parabolic pressure distribution, the deformation at the contact is obtained from the elasticity solution for pressure loads on semi-infinite space. This leads to the expression of normal stiffness as follows (Johnson, 1985)

$$D_n = 3^{\frac{1}{3}} \frac{C_2 r G_\mu}{1-\nu_\mu} \left[\frac{(1-\nu_\mu) f_n}{r^2 G_\mu}\right]^{\frac{1}{3}} \tag{1.6}$$

where r is the radius of the particles; G_μ is the particle shear modulus; C_2 is a constant.

At the micro-element level, the stress and strain are defined in connection with the resultant contact forces and the resultant displacements, respectively. The stress-strain relation is then obtained in terms of the contact stiffnesses. Obviously, for a regular packing assembly, the behaviour at the micro-element level is the same as that at representative-unit level. Some researchers have obtained different stress-strain relations for different regular packing assemblies, namely, Simth et al. (1929) suggested a configuration of a mixture of zones composed of face-cantered cubic and simple cubic packing. The micromechanical models are developed by Duffy and Mindlin (1957) for a face-centred cubic array of elastic spheres in contact, by Deresiewicz (1958) for a simple cubic array, and by Makhlouf and Stewart (1967) for a cubic-tetrahedral and a tetragonal spheroidal array.

Computer simulation has been used as a tool for micromechanics analysis at the micro-element level. Various types of discrete element methods have been developed (Serrano and Rodriguez-Ortiz, 1973; Cundall and Strack, 1979; Kishino, 1988; Bathurst and Rothenburg, 1988a and 1988b) and applied successfully to describe the behaviour of granular materials under various loading conditions (Cundall and Strack, 1979; Chang and Misra, 1989b; Ting and Corkum, 1988).

At the representative-unit level, since the assembly consists of a large number of particles, it is expedient to treat the system as a random packing system, Therefore, from the statistical point of view, a density function has to be introduced so that the micro-mechanical variables (contact force and contact displacement) can be connected with the macro-mechanical variables (stress and strain) by the intermediate fabric variables. Such a density function is introduced to describe the spatial distribution of branch vectors (the vectors joining the centroids of particles in contact), and of normal vectors at the inter-particle contacts. These concepts of vector distribution can be found in the work of Oda (1972a) and Oda et al. (1982). Along this line, Christofferson et al. (1981) defined an average stress in terms of inter-particle contact forces. The above micromechanical definitions can also be found in the work by Drescher and Dejosseline (1972), and a number of papers in Cowin and Satake (1978), Jenkins and Satake (1983), and Satake and Jenkins 1988). In addition, Digby (1981) obtained the effective elastic moduli of porous rocks by considering them to be composed of spherical particles with no shear force acting at the contact. Walton (1987) studied the moduli of isotropic packing of equal spheres under axi-symmetrical loading considering both normal and tangential compliancies at contact. Jenkins (1988) analyzed the volume change characteristics of assemblies of equal spheres under small axi-symmetrical deformation. Bathurst and Rothenburg (1988a and 1988b) studied the behaviour of disk packing with linear contact interactions. In recent years, the micromechanics of particulate assemblies has been greatly developed from a series of work by Chang, namely, a stress-strain theory for random packing has been developed (Chang, 1988; Chang et al., 1989a); The theory has been verified by computer simulation of disks (Chang and Misra, 1989b). The theory has been applied to the behaviour of sand (Chang et al., 1989b) and cemented sand (Chang et al., 1990e), with discussions of the fabric effects on initial moduli (Chang and Misra, (1990c).

The study presented in this thesis is based on a micromechanics approach at the micro-element (regular packing) and representative-unit levels (random packing).

1.4 ORGANIZATION

Chapter 1 covers the topic of investigation, objectives and literature review.

Chapter 2 investigates shear deformation of granular assemblies of rigid particles under simple shear and biaxial compression conditions. The relations between stress ratio and fabric constants, and the relations between strain ratio and fabric constants are established by introducing the density function of contact normals. Using the fabric constants as the intermediate variables, the relations between stress and strain are obtained. These relations are compared to those proposed in previous publications.

Chapter 3 studies the behaviour of a granular assembly under small strain. The relations between micro-mechanical quantities and micro-mechanical variables are analyzed, and the proposed stress-strain stiffness tensors are expressed in terms of the fabric quantities.

In Chapter 4 the stress-strain relations of small strain are analyzed for granular assemblies of random packing. The corresponding relations between the fabric tensor and the stiffness tensor are discussed. Finally the relations between the fabric tensor and the moduli of assemblies are given.

In Chapter 5, the micromechanics approach is used to study the behaviour of swelling clay. Constitutive relations for two-dimensional and three-dimensional anisotropic swelling are derived. Results predicted from the swelling model are compared to those observed in experiments.

Chapter 6 summarizes the major conclusions from this study and presents recommendations for further research.

CHAPTER 2

SHEAR DEFORMATION OF AN ASSEMBLY OF RIGID PARTICLES IN SIMPLE SHEAR AND BIAXIAL COMPRESSION CONDITIONS

2.1 INTRODUCTION

Sand is a particulate, discrete and frictional material forming a discontinuous medium. The discrete nature of sand facilitates fabric change or spatial rearrangement of particles as a result of external loading. Hence, micromechanics may be an appropriate approach to study the granular behaviour of sand. The deformation of an assembly of particles may be caused by: (1) the sliding and rolling between particles, (2) the deformation of solid particles, and (3) the crushing of particles (Ko and Scott, 1967). Shear deformation caused by particle sliding and rolling in simple shear and biaxial compression conditions will be studied in this chapter. Deformation of solid particles will be treated in Chapters 3 and 4. Crushing of sand particles is significant at high stress levels (Vesic and Clough, 1968) and is beyond the scope of this thesis.

In this chapter, by introducing the density function of normals at particle contacts, the relations between stress ratio and fabric constants, and the relations between strain ratio and fabric constants are established. Using the fabric constants as the intermediate variables, the relation between stress and strain are obtained for simple shear and biaxial compression.

2.2 MATHEMATICAL EXPRESSION OF FABRICS

2.2.1 Distribution of Contact Normals

The inter-particle forces between two particles are shown in Figure 2.1. The two components of contact force are the tangential contact force f_t^i and the normal contact force f_n^i at the i^{th} contact point, respectively. The tangential contact force f_t^i is parallel to the i^{th} contact plane and the normal contact force f_n^i perpendicular to the i^{th} contact plane. The contact normal **n** is defined as the vector perpendicular to the i^{th} contact plane of the particles. In order to describe the characteristic of the spatial arrangement of particles of a granular assembly, we define a density function:

$$\begin{aligned} E(\Omega) &= \frac{1}{D\pi} N_{ij} n_i n_j \\ &= \frac{1}{D\pi} (N_{xx} n_x n_x + N_{yy} n_y n_y + N_{zz} n_z n_z \\ &\quad + 2N_{xy} n_x n_y + 2N_{xz} n_x n_z + 2N_{yz} n_y n_z) \end{aligned} \tag{2.1}$$

where Ω is a solid angle; D=4 in the 3-D case and D=1 in the 2-D case; N_{ij} is a second-order fabric tensor; n_i and n_j are the components of the contact normal vectors in i and j directions, respectively. In two-dimensions, $n_x = \cos\theta$, and $n_y = \sin\theta$, where θ is the contact angle as defined in Figure 2.1. We let $A=N_{xx}$, $B=N_{yy}$ and $C=N_{xy}$, so the contact density function in the 2-D case becomes

$$E(\theta) = \frac{1}{D\pi} (A\cos^2\theta + B\sin^2\theta + C\sin 2\theta) \tag{2.2}$$

where θ is the contact angle; The fabric variables A, B, and C change with the change of stress or the rotation of principal stress axes caused by external loads.

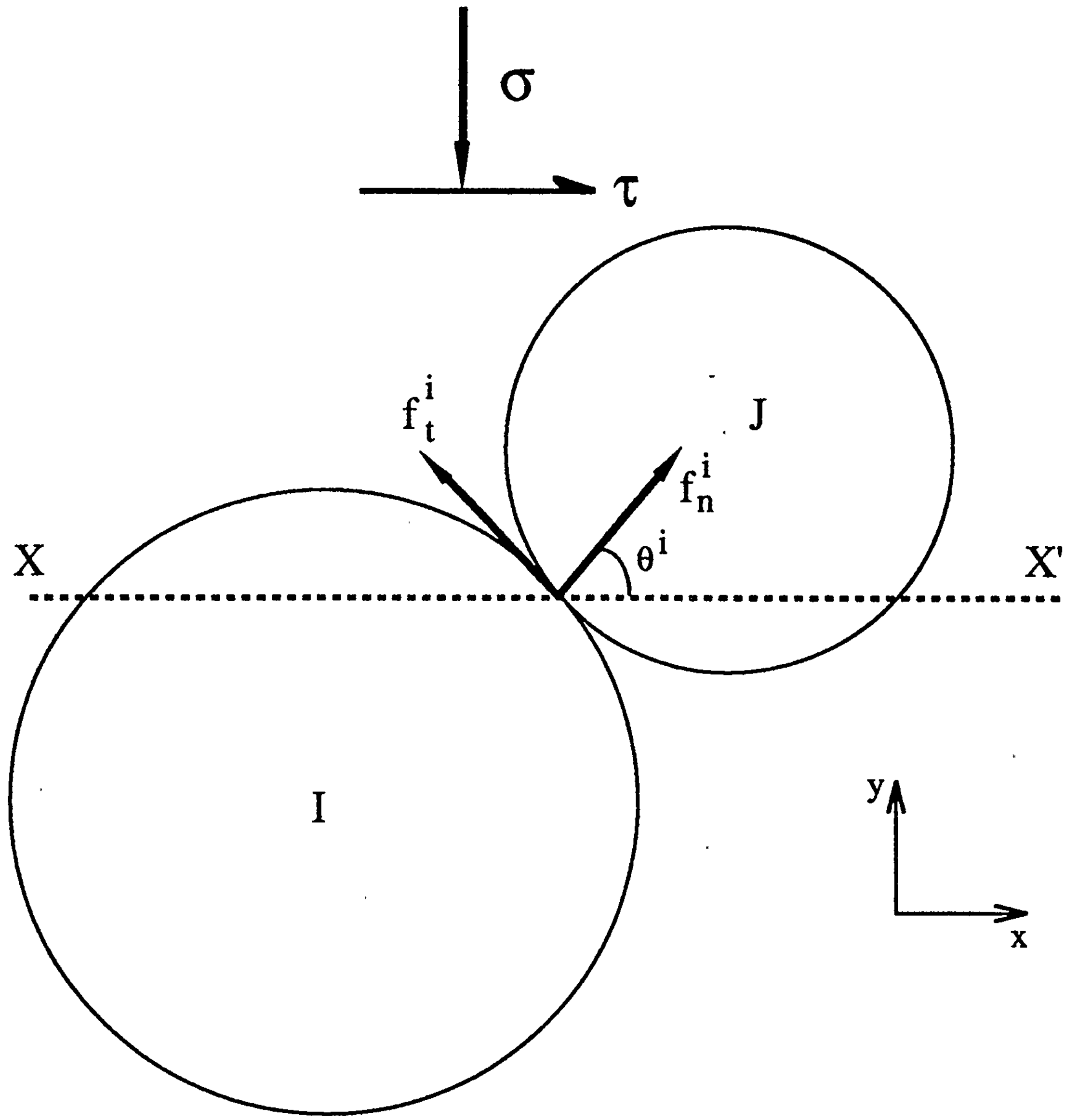

Figure 2.1 Schematic Diagram of Particle Interaction

According the statistical theory, the density function of contact normal must satisfy

$$\int_0^{\pi} E(\theta)d\theta = 1 \tag{2.3}$$

Obviously, we can consider the integral limits of θ to be from 0 to π or from $-\pi/2$ to $\pi/2$ due to the symmetry of the density function about the original point, i.e., $E(\theta)=E(\pi+\theta)$. In this case, equation (2.3) yields $A+B=2$ for $D=1$, $A+B=4$ for $D=2$, $A+B=6$ for $D=3$, and so on. In the following we assume $D=1$ and the integral limits are from 0 to π due to the contact angle varying from 0 to π . The distribution of $E(\theta)$ is shown in Figure 2.2. In this figure, N_1 and N_2 are the maximum and minimum principal fabric values along the principal fabric axes, namely, $N_1=E(\theta_1)$ and $N_2=E(\theta_2)$, respectively. The principal fabric angles, defined by the angles between the principal fabric axes and coordinate axes, are determined from the maximum and minimum values of equation (2.2):

$$\theta_{1,2} = \pm \frac{1}{2} \arctan \frac{2C}{A-B} \tag{2.4}$$

Substituting equation (2.4) into equation (2.2) yields

$$\begin{aligned} N_{1,2} &= \frac{1}{\pi}[1 \pm \frac{1}{2}\sqrt{(A-B)^2+4C^2}] \\ &= \frac{1}{\pi}(1 \pm \sqrt{(A-1)^2+C^2}) \end{aligned} \tag{2.5}$$

Since $N_1 \geq 0$ and $N_2 \geq 0$, from equation (2.5) we have

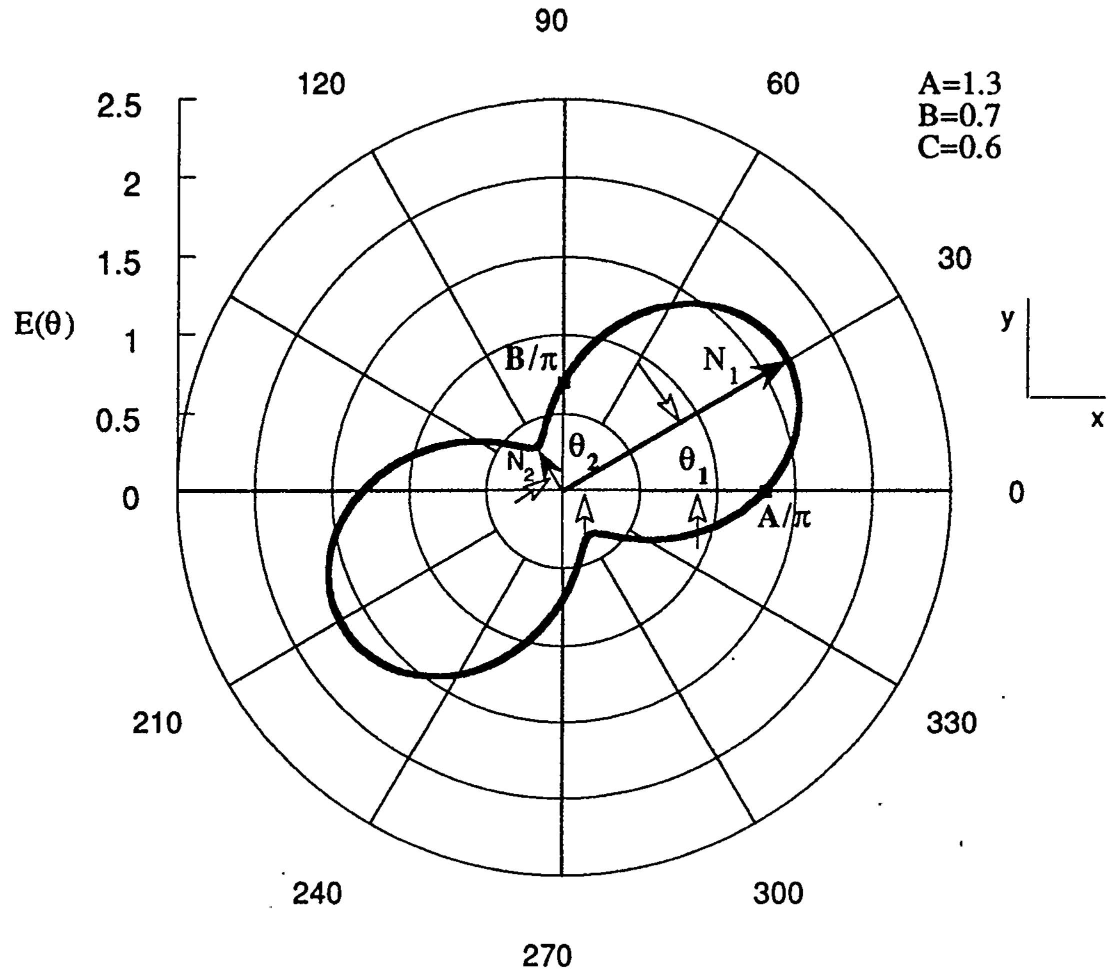

Figure 2.2 Distribution of Density Function $E(\theta)$

$$(A-1)^2+C^2 \le 1 \tag{2.6}$$

Therefore, the upper limits of N_1 and N_2 are $2/\pi$. In Figure 2.2, the density function intersects at A/π along x-axis and at B/π along y-axis. Thus, $A \ge 0$ and $B \ge 0$. Since $A+B=2$, $0 \le A \le 2$ and $0 \le B \le 2$. Substituting limits of A into equation (2.6) yields $-1 \le C \le 1$. In summary, the fabric constants A, B, C, N_1 and N_2 have limits as follows:

$$\begin{gathered} 0 \le A \le 2 \\ 0 \le B \le 2 \\ -1 \le C \le 1 \\ 0 \le N_{1,2} \le \frac{2}{\pi} \end{gathered} \tag{2.7}$$

If C=0, the principal fabric axes coincide with the coordinate axes. If A=B and C=0 the distribution of $E(\theta)$ is a circle. If $C \neq 0$ and $A = B$, $\theta_1 = 45°$ and $\theta_2 = 135°$. The magnitudes of deviation of the principal fabric axes from the coordinate axes are determined by the term 2C/(A-B).

Another way to define the fabric function is to use a principal fabric ratio λ which is defined as

$$\lambda = \frac{N_1}{N_2} = \frac{E(\theta_1)}{E(\theta_2)} = \frac{1+\sqrt{(A-1)^2+C^2}}{1-\sqrt{(A-1)^2+C^2}} \tag{2.8}$$

The above equation can be rearranged as

$$(A-1)^2+C^2=\frac{(\lambda-1)^2}{(\lambda+1)^2} \tag{2.9}$$

Equation (2.9) requires

$$|C|\leq\frac{\lambda-1}{\lambda+1} \tag{2.10}$$

The geometric meaning of equation (2.9) is a circle. Its radius equals $(\lambda-1)/(\lambda+1)$ and its centre is located at (1, 0) in axes A and C. If λ=1 and C=0, the circle reduces to a point which shows isotropic fabric. Obviously, the larger the radius of this circle, the larger is the anisotropy of the assembly.

2.2.2 Number of Contact Points

During the process of shear deformation, the number of contact points increases with shear compression and decreases with shear dilation. The relations among the number of contact points, shear strain and fabric constants will be discussed in section 2.3.3.

2.3 MODEL OF SIMPLE SHEAR DEFORMATION

2.3.1 Relation between Stress Ratio and Fabric Constants

In a test of simple shear on a sand specimen, a normal stress σ and a shear stress τ are applied to the specimen, as shown in Figure 2.3. The resultant forces in the horizontal direction and vertical direction are zero for equilibrium. When the shear deformation of a granular assembly occurs due to the action of external forces, the

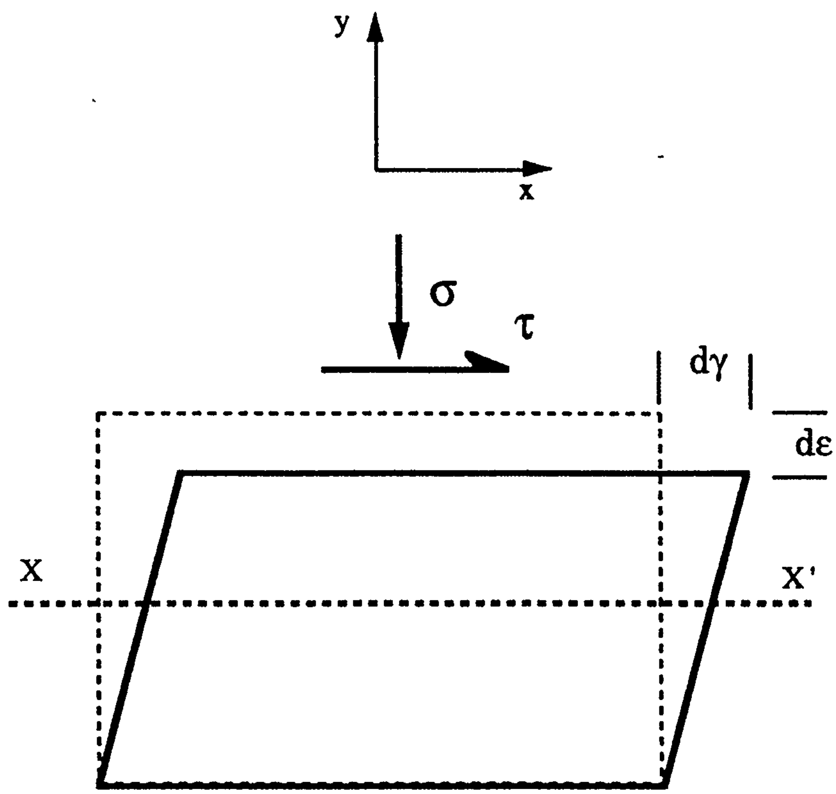

Figure 2.3 Schematic Diagram of Simple Shear

arrangement of the particles will change in succession, searching for a new equilibrium state. Therefore, the magnitudes and directions of contact forces change during the period of shear deformation. Here we assume that the particles are rigid, hence, the deformations of the particle assembly are mainly caused by the movement and rearrangement of particles. Every load increment causes a new change in fabrics during the shearing process.

During the process of shear deformation in the simple shear condition, the directions of sliding vary randomly from particle to particle, and the average direction of the overall sliding is denoted by the horizontal plane, XX' in Figure 2.3. This plane represents the inclination of the sliding plane and is related to both the stress conditions and the dilatancy behaviour of the assembly.

From the analysis of external force and inter-particle forces acting on the horizontal sliding plane XX' in Figure 2.1 we have

$$\begin{aligned} \sigma S^i &= f_n^i \sin\theta^i + f_t^i \cos\theta^i \\ \tau S^i &= -f_n^i \cos\theta^i + f_t^i \sin\theta^i \end{aligned} \tag{2.11}$$

where S^i is the projected area of the i^{th} contact section on XX' ; σ and τ are the effective normal stress and shear stress acting on the plane, respectively; M is the number of contact points intersected by the plane XX'. θ^i is the contact angle at the i^{th} contact point.

Along the plane XX' we obtain

$$\frac{\tau}{\sigma}=\frac{\sum_{i=1}^{M}\left(-\cos\theta^{i}+\frac{f_t^i}{f_n^i}\sin\theta^{i}\right)}{\sum_{i=1}^{M}\left(\sin\theta^{i}+\frac{f_t^i}{f_n^i}\cos\theta^{i}\right)} \tag{2.12}$$

In frictional materials, the maximum ratio of tangent contact force to normal contact force is related through an overall coefficient of limiting friction μ_{max} or friction angle ϕ_μ . At the contacts where there is no relative movement, the ratio is less than or equal to μ_{max} .

We assume that the friction angle ϕ at contacts satisfies

$$\tan\phi^{i}=\frac{f_t^i}{f_n^i} \tag{2.13}$$

where ϕ^i is the friction angle at the i^{th} contact point and varies from 0 to ϕ_μ. Substituting equation (2.13) into equation (2.12) yields

$$\frac{\tau}{\sigma}=\frac{-\sum_{i=1}^{M}\cos(\phi^{i}+\theta^{i})}{\sum_{i=1}^{M}\sin(\phi^{i}+\theta^{i})} \tag{2.14}$$

Because there are a large number of particles on the plane, we assume that the distribution of contact angles is continuous. Therefore the summation sign in equation (2.14) can be replaced by an integral sign. The integral limit of θ is from 0 to π, so equation (2.14) becomes

$$\frac{\tau}{\sigma}=\frac{-\int_0^{\pi}\cos(\phi_m+\theta)E(\theta)d\theta}{\int_0^{\pi}\sin(\phi_m+\theta)E(\theta)d\theta} \tag{2.15}$$

where ϕ_m is an average mobilized friction angle

Substituting equation (2.2) into equation (2.15) yields

$$\frac{\tau}{\sigma}=\frac{(A+2B)\tan\phi_m-2C}{A+2B+2C\tan\phi_m} \tag{2.16}$$

The above equation provides a relationship between the stress ratio and fabric constants. It shows that the change of stress ratio will cause the change of the fabric distribution for the case of simple shear. For C=0, $\tau/\sigma = \tan\phi_m$. For $C < 0$, the stress ratio exceeds the limiting value of $\tan\phi_m$ because of shear dilation.

2.3.2 Fabric Conditions of Shear Compression and Dilation

Consider the sliding mechanism between two particles as shown in Figure 2.4, the increment of contact angle caused by sliding at the i^{th} contact point is $\Delta\theta^i$, and L^i is the distance between two centres of the two contact particles and passes the i^{th} contact point. The distance L^i is also called branch length. The corresponding slip at the i^{th} contact point is $L^i\Delta\theta^i$, likewise, for L being the average branch length and $\Delta\theta$ the incremental contact angle. Therefore, the increments of the average horizontal displacement Δu_x and average vertical displacement Δu_y are given by

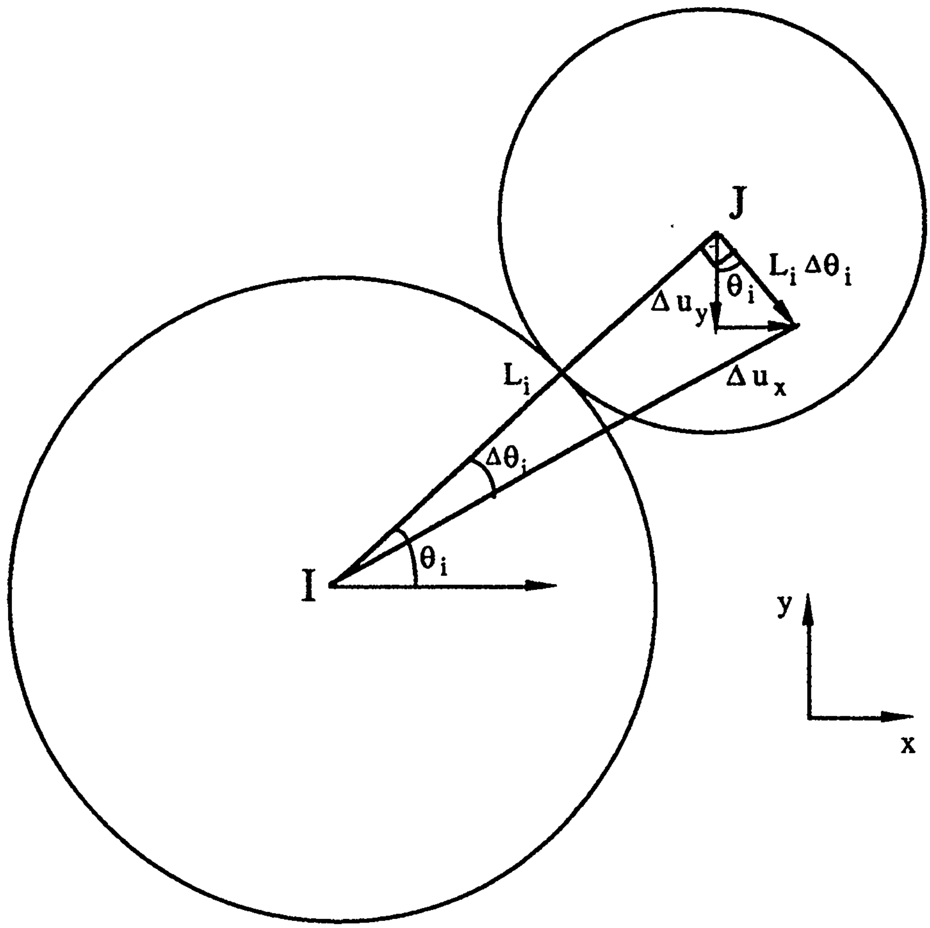

Figure 2.4 Schematic Diagram of Particle Sliding

$$\Delta u_x = -\int_0^{\pi} L\Delta\theta \sin\theta E(\theta) d\theta \tag{2.17}$$
$$= -\frac{2}{3\pi} L(A+2B)\Delta\theta$$

$$\Delta u_y = \int_0^{\pi} L\Delta\theta \cos\theta E(\theta) d\theta \tag{2.18}$$
$$= \frac{4}{3\pi} LC\Delta\theta$$

If $\Delta\theta^i$ is positive, Δu_x is negative and Δu_y is positive. We assume the average thickness of the slip plane to be H, i.e., the component of average branch length L in the vertical direction, $H=L_y$. Therefore we have

$$H = \int_0^{\pi} L \sin\theta E(\theta) d\theta \tag{2.19}$$
$$= \frac{2}{3\pi} L(A+2B)$$

According the definition of strain components, the increments of horizontal shear strain and vertical strains in simple shear are given by

$$d\gamma = \frac{\Delta u_x}{L_y} = \frac{\Delta u_x}{H} = -\Delta\theta \tag{2.20}$$

$$d\varepsilon = \frac{\Delta u_y}{L_y} = \frac{\Delta u_y}{H} = \frac{2C\Delta\theta}{A+2B} \tag{2.21}$$

Comparing equation (2.20) and equation (2.21) yields

$$\frac{d\varepsilon}{d\gamma} = -\frac{2C}{A+2B} \tag{2.22}$$

In equation (2.22), compressive and dilative strains correspond to the positive and negative values of C, respectively. Equation (2.18) indicates that there is no vertical deformation for C=0, i.e., shear dilation or compression does not occur for C=0. In other words, the shear dilation or shear compression is caused by the deviation of the principal fabric axes from the coordinate axes. The coordinate axes coincide with the σ- and τ-shear axes in this simple shear condition.

Now, we investigate under what condition shear dilation or compression will occur. Consider the sliding mechanisms as shown in Figure 2.5. The plane XX' denotes the average direction of the overall sliding. The angle θ^i is the i^{th} contact angle. The angle α^i is called the dilatancy angle at the i^{th} contact point and is the angle between the contact plane and horizontal plane. Since $\alpha^i = \pi/2 - \theta^i$, α^i varies from $-\pi/2$ to $\pi/2$. The sign convention of dilatancy angle α^i is defined in Figure 2.5. Shear compression and dilation occur with positive and negative dilatancy angles, respectively. There is no shear compression and dilation for $\alpha^i = 0$. In order to analyze the physical meaning of dilatancy angle α^i, we define Θ to be an overall dilatancy angle of the concerned particulate assembly. According to its definition, we have

$$\Theta=\int_{-\frac{\pi}{2}}^{\frac{\pi}{2}} \alpha \; E(\frac{\pi}{2}-\alpha) \; d(-\alpha)= -\frac{C}{2} \tag{2.23}$$

Therefore, equation (2.19) becomes

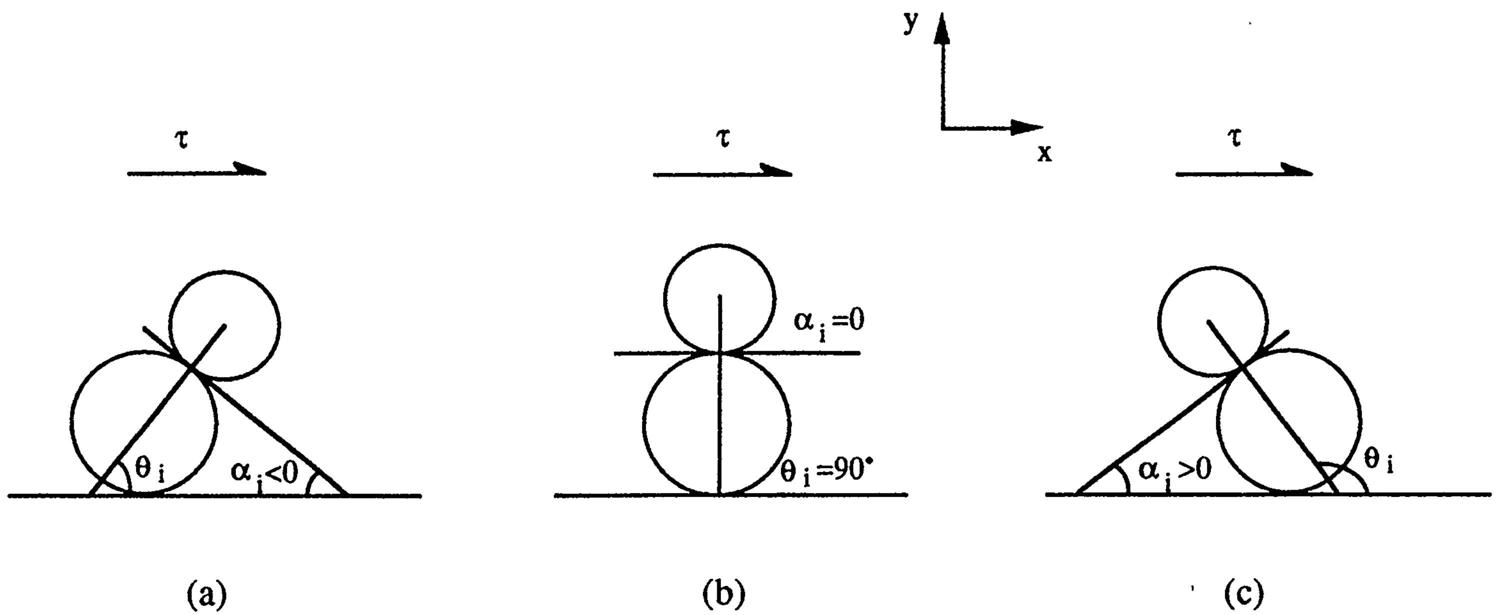

Figure 2.5 Relation between Dilatancy Angle and Volume Change (a) Shear Compression, (b) No Volume Change, and (c) Shear Dilation

$$\frac{d\varepsilon}{d\gamma}=\frac{4\Theta}{A+2B} \tag{2.24}$$

The physical meaning of equation (2.24) is: (1) If C=0, i.e., $\Theta = 0$, the principal fabric axes do not change, and there is no shear compression and dilation during the process of shear deformation. (2) If $C < 0$, i.e., $\Theta > 0$, shear dilation occurs, (3) If $C > 0$, i.e., $\Theta < 0$, shear compression occurs.

From the above analyses, it is a requisite condition for the occurrence of shear compression and dilation that the principal fabric axes do not coincide with the plane of sliding or the normal and shear stress axes in the simple shear condition, i.e., $\Theta \neq 0$.

2.3.3 Relation between Contact Number and Shear Strain

In the process of shear deformation the number of contacts may increase or decrease depending on the overall dilatancy angle Θ. Five typical cases shown in Figure 2.6 are explored.

The dilatancy angles are positive and negative in cases of Figures 2.6a and Figure 2.6b, respectively. Neither case has gain or loss of contact points during the slip of particle I relative to particle J. However, under external loading, dilation occurs in Figure 2.6a with positive dilatancy angle and compression occurs in Figure 2.6b with negative dilatancy angle. Although there is no net gain or loss of contact points in the case of Figure 2.6c, the total number of dilatancy points does change and the sign of the dilatancy

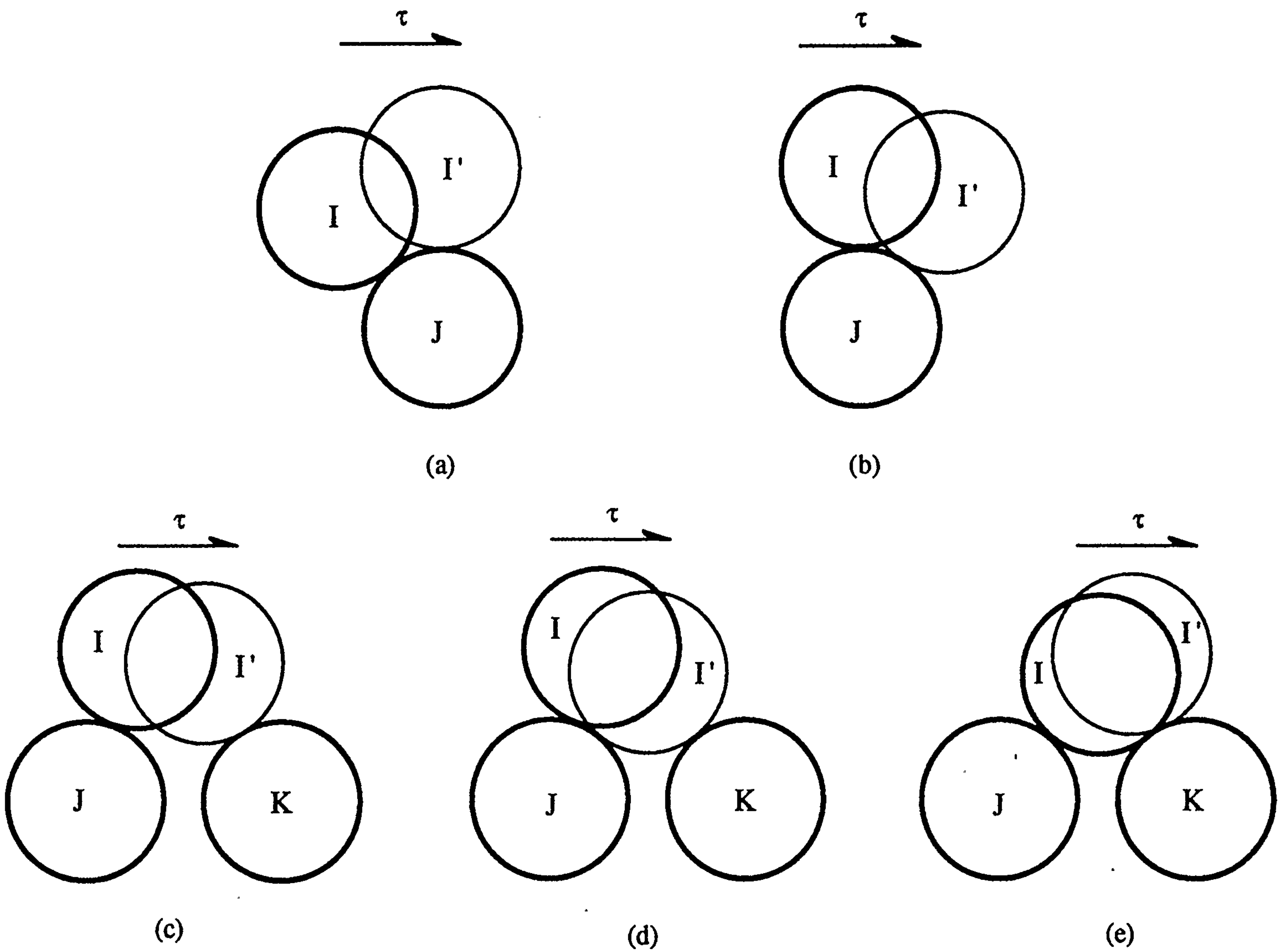

Figure 2.6 Gain and Loss of Contact Points

angle changes from negative to positive. For the case of Figure 2.6d, its number of contact points increases and the dilatancy angle changes from negative to positive. During the initial process of shear deformation in Figure 2.6d, compression occurs. If the shear deformation continues, dilation will occur as shown in Figure 2.6e. It is obvious that during the process of shear deformation, the numbers of positive and negative dilatancy angles are changing. The distribution of these contact points is described by the density function. We attempt to relate the number of contact points with the shear strain in the following section.

We define the initial volume V_0 and the deformation volume V. The definition of void ratio is given by

$$\frac{V-V_0}{V}=\frac{\Delta V}{V}=\frac{\Delta e}{1+e} \tag{2.25}$$

where ΔV and Δe are the increments of the volume and the void ratio of the particle assembly, respectively.

The average number of contact points between two adjacent particles is defined by an average coordination number, m. The relation between the coordination number and the void ratio satisfies (Field, 1963):

$$m=\frac{C_m}{1+e} \tag{2.26}$$

where C_m is a constant. Differentiation of the void ratio e with respect to the coordination number m yields

$$\Delta e = -\frac{\Delta m}{m^2} C_m = -\frac{\Delta m}{m}(1+e) \tag{2.27}$$

If we define compression strain to be positive, combining equations (2.25), (2.26) and equation (2.27) yields

$$d\varepsilon_v = d\varepsilon = -\frac{\Delta V}{V} = \frac{\Delta m}{m} = \frac{\Delta M}{M} \tag{2.28}$$

where M is the total number of contact points; $d\varepsilon_v$ is the incremental volumetric strain.

Obviously, $d\varepsilon = d\varepsilon_v$ under the simple shear condition. Equation (2.25) shows that the number of contact points decreases with the volumetric dilation and increases with the volumetric compression.

The total number of contact points, M, at any stage of the shearing process is a function of the initial fabric and the total deformation. The function for the contact number is assumed to be (Mogami, 1965):

$$M = M_0 e^{-[\gamma(f_0+1)+g_0(e^{-\frac{\gamma}{g_0}}-1)]} \tag{2.29}$$

where f_0 and g_0 are constants related to initial fabrics. γ is the total shear strain; M_0 is the initial number of contact points.

From equation (2.29) we differentiate M with respect to γ, and we obtain

$$\frac{dM}{d\gamma}=-M(f_0+1-e^{-\frac{\gamma}{g_0}}) \tag{2.30}$$

Combining equations (2.23), (2.28) and (2.30), the average dilatancy angle can be expressed as follows:

$$\Theta=\frac{1}{4}(A+2B)(f_0+1-e^{-\frac{\gamma}{g_0}}) \tag{2.31}$$

The constant f_0 can be determined from equation (2.31) using the initial conditions, e.g., $A=A_0$, $B=B_0$, and $\Theta=\Theta_0$ when $\gamma=0$. Hence

$$\begin{aligned} f_0&=\frac{4\Theta_0}{B_0+2} \\ &=\frac{4\Theta_0}{4-A_0} \end{aligned} \tag{2.32}$$

where constants A_0, B_0 are initial fabric constants; Θ_0 is the initial dilatancy angle. Equation (2.31) means that the average dilatancy angle is a function of the initial fabric constants, the induced fabric change, and the shear strain.

2.3.4 Stress-Strain Relation

Substituting the term 2C/(A+2B) from equation (2.22) into equation (2.16) we obtain a relation between the stress ratio and the strain ratio as follows:

$$\frac{\tau}{\sigma}=\frac{\frac{d\varepsilon}{d\gamma}+\tan\phi_m}{1-\frac{d\varepsilon}{d\gamma}\tan\phi_m} \tag{2.33}$$

Rearrangement of equation (2.33) yields

$$\frac{d\varepsilon}{d\gamma}=\frac{\frac{\tau}{\sigma}-\tan\phi_m}{1+\frac{\tau}{\sigma}\tan\phi_m} \tag{2.34}$$

Equation (2.31) is called as the dilatancy equation of a granular assembly in the simple shear condition. It is interesting to note that the relation between stress ratio and strain ratio is not related to the fabrics. However, the stress-strain relations are related to the fabrics, such as equation (2.16) and equation (2.22). Previous researchers (Tokue, 1979; Nemat-Nasser, 1980; Chang, 1982) have obtained a similar dilatancy equation using different methods. However, their shear models can be only used to analyze the relation between the stress ratio and strain ratio, not the volumetric strain and shear strains.

To obtain a stress-strain relation, we have to substitute the term $d\varepsilon/d\gamma$ expressed in terms of f_0, g_0 and γ from equation (2.30) into equation (2.33). The stress-strain relation for simple shear condition becomes

$$\frac{\tau}{\sigma}=\frac{\tan\phi_m+1+f_0-e^{-\frac{\gamma}{g_0}}}{1+(1-f_0-e^{-\frac{\gamma}{g_0}})\tan\phi_m} \tag{2.35}$$

The stress-strain curves obtained from the above equation are plotted in Figure 2.7 for different initial fabrics. In these numerical examples, the initial fabric f_0 is varied to

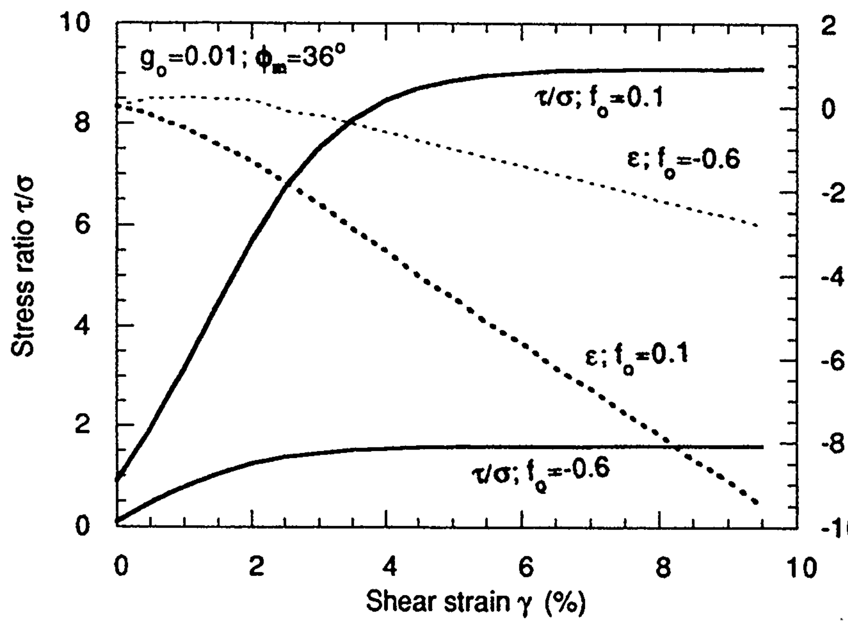

Figure 2.7 Stress-Strain Curves of Different Initial Fabrics

study its effects on the stress-strain curve while ϕ_m and g_0 are kept constant (ϕ_m =36° and g_0 =0.01). For f_0=-0.6, i.e., the average initial dilatancy angle is negative, shear compression is induced at the beginning of shearing. The stress ratio τ/σ reaches to the limiting value of tan ϕ_m when $d\varepsilon/d\gamma = 0$. The stress ratio continues to increase with increasing $d\varepsilon/d\gamma$, and levels off with no change in $d\varepsilon/d\gamma$. For f_0=0.1, i.e., the average dilatancy angle is positive, only shear dilatancy is induced. The stress ratio increases with increasing $d\varepsilon/d\gamma$ and γ. In both cases of f_0 =-0.6 and 0.1, the stress ratio starts from a finite value at zero shear strain because the initial fabric is anisotropic.

In the stress-strain model of equation (2.35), we take the fabrics into full account, by taking the fabric constants as the intermediate variables. Thus we can obtain the total volumetric strain ε and total shear strain γ. In fact, during the process of shear deformation, the fabric changes with different shearing load. Therefore, equations (2.16), (2.22) and (2.35) together describe the shearing process of a granular assembly in simple shear condition.

2.4 MODEL OF BIAXIAL COMPRESSION

2.4.1 Relation between Stress Ratio and Fabric Constants in Biaxial Compression Condition

In a biaxial compression test, compressive stresses acting on the specimen are σ_1 in the vertical direction and σ_3 in the horizontal direction as shown in Figure 2.8. The plane of sliding denoted by BC is assumed to follow the direction of the major principal fabric axes, N_1 because the number of contacts is the least along that direction. The

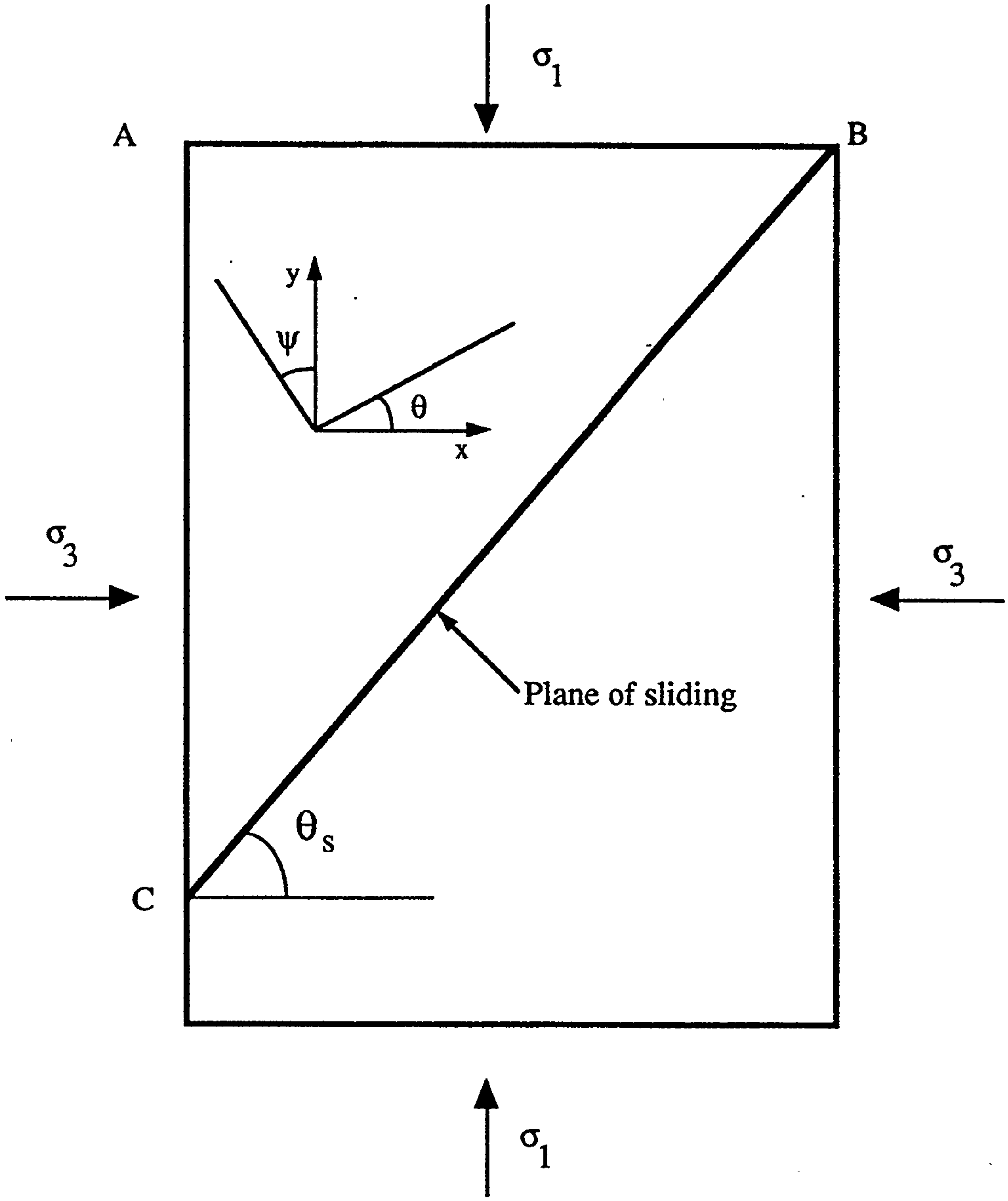

Figure 2.8 Schematic Diagram of Biaxial Compression

inclined angle of the sliding wedge is θ_s, given by equation (2.4).

Considering the external forces acting on planes AB and AC, the relations between external forces and internal contact forces are given by the two equilibrium equations in the vertical and horizontal directions. Therefore, stress ratio σ_1/σ_3 can be obtained using similar analytical steps to the simple shear case, and can be simplified to a form

$$\frac{\sigma_1}{\sigma_3}=\frac{\int_0^{\pi}(f_n\sin\theta+f_t\cos\theta)(A\cos^2\theta+B\sin^2\theta+C\sin 2\theta)d\theta}{\int_0^{\pi}(f_n\sin\psi+f_t\cos\psi)(A\sin^2\psi+B\cos^2\psi-C\sin 2\psi)d\psi}\tan\theta_s$$

$$=\frac{(A+2B)+2C\tan\phi_m}{(2A+B)-2C\tan\phi_m}\tan\theta_s \qquad (2.36)$$

where $\psi = \theta - 90°$.

2.4.2 Stress-Strain Relation

The derivation method for the strain in the biaxial compression condition is similar to that in the simple shear condition. In the biaxial compression condition, the strain ratio is expressed in terms of principal strains in the vertical and horizontal directions as follows:

$$\frac{\Delta\varepsilon_1}{\Delta\varepsilon_3}=\frac{\int_0^{\pi}\sin\theta(A\cos^2\theta+B\sin^2\theta+C\sin 2\theta)d\theta}{\int_0^{\pi}\sin\psi(A\sin^2\psi+B\cos^2\psi-C\sin 2\psi)d\psi}\frac{1}{\tan\theta_s}$$

$$=\frac{2A+B}{A+2B}\frac{1}{\tan\theta_s} \qquad (2.37)$$

Substituting equation (2.38) into equation (2.37) yields a relation between the stress ratio and the strain ratio

$$\frac{\sigma_1}{\sigma_3}=\frac{1+2C(A+2B)\tan\phi_m}{1-2C(A+2B)\tan\phi_m}\frac{\Delta\varepsilon_3}{\Delta\varepsilon_1} \tag{2.38}$$

If substituting equation (2.4) into equation (2.38) and using $\theta_1 = \theta_s$, we have

$$\frac{\sigma_1}{\sigma_3}=\frac{1+(A-B)(A+2B)\tan2\theta_s\tan\phi_m}{1-(A-B)(A+2B)\tan2\theta_s\tan\phi_m}\frac{\Delta\varepsilon_3}{\Delta\varepsilon_1} \tag{2.39}$$

Equation(2.39) and equation (2.40) provide a mathematical framework based on fabric mechanics to quantify the shearing process of a granular assembly in biaxial compression conditions. However, development of a stress-strain relation requires an additional relation linking fabric change with total strain (strain ratio with total strain). This subject is beyond the scope of this study.

2.4.3 Comparison with Rowe's Stress-Dilatancy Theory

Rowe (1962) investigated the shear deformation of a regular packing assembly and derived a theoretical relation between stress ratio and strain ratio for the case of biaxial compression

$$\frac{\sigma_1}{\sigma_3}=-\frac{\Delta\varepsilon_3}{\Delta\varepsilon_1}\tan^2(45°+\frac{\phi_\mu}{2}) \tag{2.40}$$

However, Rowe (1962) found that equation (2.41) had to be modified to match the test results observed in granular assemblies of random packing. His semi-empirical relation becomes

$$\frac{\sigma_1}{\sigma_3}=-\frac{\Delta\varepsilon_3}{\Delta\varepsilon_1}\tan^2(45°+\frac{\phi_f}{2}) \tag{2.41}$$

In equation (2.41), the friction angle ϕ_f is a variable which is a function of stress and strain. Comparison between (2.40) and (2.42) indicate that Rowe's model has several limitations: (1) the model does not consider the effect of initial fabrics on the shear deformation of granular assembly, (2) the model indicates the effect of fabric change implicitly using ϕ_f as a variable, and (3) the interparticle friction angle is not explicitly defined. The new stress-dilatancy relation of equation (2.40) is more comprehensive because the relation is a function of initial fabric, induced fabric change, and dilation rate.

2.4.4 Critical State

When a sand sample is sheared, its void ratio will decrease or increase depending on its initial void ratio. If the shear deformation is sufficiently large, the sample, loose or dense, will reach a state in which the arrangement of the particles is such that no volume change takes place during shearing. This particular void ratio is called the critical void ratio, The corresponding stress state is called the critical stress. Based on laboratory measurement, the critical stress can be expressed in an empirical correlation (Casagrande, 1936):

$$\frac{\sigma_1}{\sigma_3}=\tan^2(45°+\frac{\phi_{cv}}{2}) \tag{2.42}$$

where ϕ_{cv} is the friction angle at constant volume. The value of ϕ_{cv} varies among materials and is greater than the value of ϕ_μ .

The critical stress can be derived from equation (2.40) based on micromechanics by setting $\Delta\varepsilon_1/\Delta\varepsilon_3$=-1, i.e.,

$$\frac{\sigma_1}{\sigma_3}=\frac{(2+A)[4-A+2(A-1)\tan 2\theta_s \tan\phi_m]}{(4-A)[A+2-2(A-1)\tan 2\theta_s \tan\phi_m]} \tag{2.43}$$

Equation (2.44) indicates that the critical stress is dependent on the interparticle friction angle ϕ_m, fabric constant A or B, and the critical state fabrics θ_s , It can be seen that these two parameters ϕ_m and θ_s are implicitly described by the correlation parameter ϕ_{cv} in the empirical equation (2.43).

2.5 CONCLUSION

The shear behaviours of a assembly composed of rigid particles in simple shear and biaxial compression conditions have been studied using the principles of micromechanics. Analytical solutions are derived to describe the stress ratio, the change in fabric distribution and orientation, and the strain ratio during the process of shearing deformation. Development of a stress-strain model based on micromechanics requires an additional relation linking the change in fabrics, the change in contact number and the strain. The main advantages of this micromechanics model are that the model considers the effects of the fabric anisotropy, the rotation of principal fabric axes and the rotation of principal stress axes on the shear deformation of the granular medium. The model provides a sound basis to explain some empirical correlations in soil mechanics such as Rowe's stress-dilatancy law and critical state. Since the model includes the effects of fabrics, the model can be applicable to any granular assembly of particles of different size distribution.

CHAPTER 3

STRESS-STRAIN RELATION OF A REGULAR PACKING ASSEMBLY UNDER CONTACT DEFORMATION

3.1 INTRODUCTION

The total deformation of a granular assembly is the resultant of deformation caused by particle sliding, rolling, solid deformation, and grain crushing. In this chapter, we are concerned with the small strain deformation of a regular packing assembly of deformable particles due to solid deformation or contact deformation. This small strain deformation depends on the sizes of particles, fabrics of assembly, mechanical properties of particles, and loading condition. Recently, mathematical representations of this type of deformation on granular materials have been attempted by several researchers (e.g., Walton, 1987; Bathurst, 1985; Rothenburg and Bathurst, 1989). However, their models do not take into account the effects of the change of fabrics. In recent years, the micromechanics of granular materials has been greatly developed by Chang et al. (1990a, 1990b, 1990c, 1990d, 1992a, 1992b). Here, we take the complete anisotropy of the assembly into account. The research work presented in this chapter focuses on the stress-strain relations from fabric considerations. The relations between micromechanical quantities and micromechanical variables are analyzed, and the proposed stress-strain stiffness tensor is expressed in terms of the fabric quantities. Because the stress-strain relations of granular masses with different fabrics are derived under the condition that the directions of principal fabric axes are not the same as the principal stress axes, the relations are valid for general loading both in two-dimensional and three dimensional conditions. Five different types of regular packings are analyzed. Although all the stress-strain relations are derived from the contact theory of small strain, these constitutive laws can be used in the analyses of large deformation caused by the change of fabric quantities.

3.2 RELATION BETWEEN MICROMECHANICAL VARIABLES AND MACROMECHANICAL VARIABLES

3.2.1 Principle of Virtual Work for A Particulate Assembly

It is very difficult to measure contact force between two particles directly, so we have to find a description method to establish a relation between micro-mechanical quantities and macromechanical variables. Since granular materials form discontinuous media, stress at a point defined for a continuum is no longer valid for such media. Here the volume average stress quantities are defined. In the previous chapter we introduced a density function $E(\theta)$ for the case of two-dimensions. Here, $E(\theta)$ is replaced by $E(\Omega)$, where Ω is a solid angle in the spherical coordinate system for the case of three-dimension, i.e.,

$$d\Omega = \sin\beta \, d\beta \, d\gamma \tag{3.1}$$

where γ from 0 to π and β from 0 to 2π are spherical coordinates shown on Figure 3.1.

Obviously, the number of contact points within the solid angle from Ω to $\Omega+d\Omega$ is given by $ME(\Omega)d\Omega$, where M is the total number of contact points. We assume $f_i(\mathbf{r}^q,\mathbf{n}^q)$ to be the i^{th} component of the q^{th} contact force with position vector $\mathbf{r}^q$ and unit normal

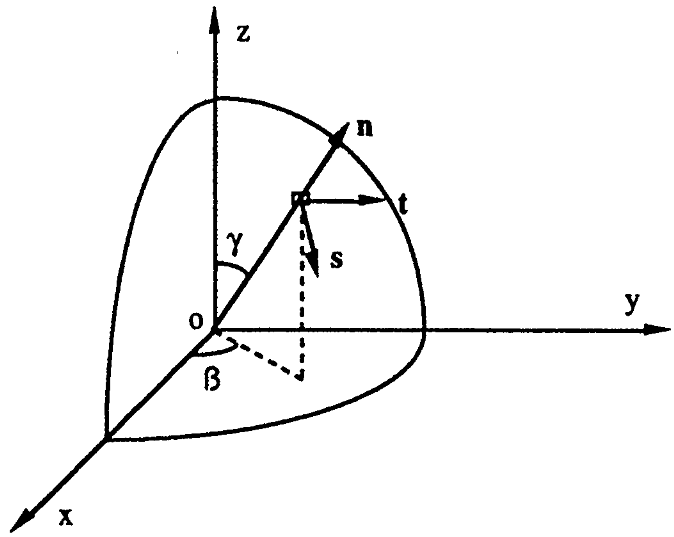

Figure 3.1 Signs of Coordinates

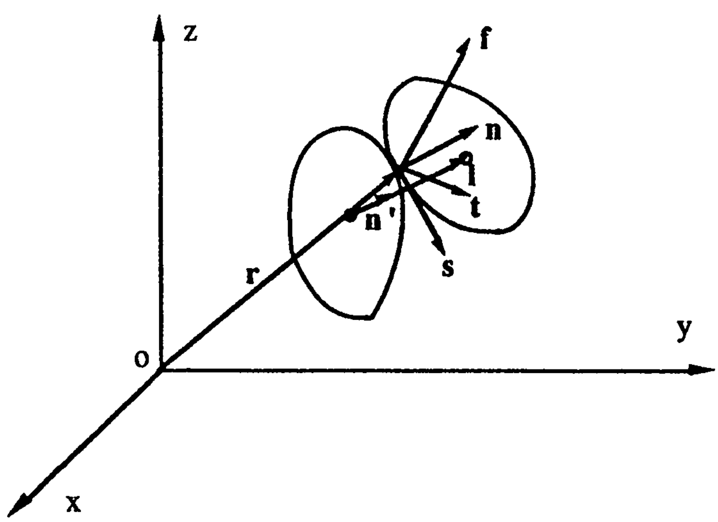

Figure 3.2 Contact between Particles

vector **n** (i=x, y, z). According to the equilibrium condition, the vector summation of contact forces must be zero, i.e.,

$$\sum_{q=1}^{M} f_i(r^q,\ n^q)=0 \qquad (i=x,\ y,\ z) \tag{3.2}$$

The contact forces in equation (3.2) are assumed to act at a point and consequently, transfer of moments across physical contacts is not considered. Obviously, we can establish the equilibrium equations of moment for every pair of the adjacent particles, and then get the vector summation for the whole assembly

$$\sum_{q=1}^{M} f_i(n^q)l_j(n'^q)=\sum_{q=1}^{M} f_j(n^q)l_i(n'^q) \qquad (i,\ j=x,\ y,\ z) \tag{3.3}$$

where l(**n'**) is the branch vector connecting two centres of adjoint particles, as shown in Figure 3.2. **n'** is the unit vector of this branch.

We assume that the overall strain field is uniform (Chang and Misra 1989a, 1990c), so the relation between the strain tensor $\varepsilon_{ij}(\mathbf{r}^q)$ and the displacement $u_i(\mathbf{r}^q)$ is given by

$$u_i(r^q)=\varepsilon_{ij}(r^q)l_j(r^q,\ n'^q) \qquad (i,\ j=x,\ y,\ z) \tag{3.4}$$

The virtual work done by the contact forces per unit volume is given by

$$W=\frac{1}{2V}\sum_{q=1}^{M} f_i(r^q,\ n^q)\varepsilon_{ij}(r^q)l_j(r^q,\ n'^q) \qquad (i,\ j=x,\ y,\ z) \tag{3.5}$$

The factor 2 is introduced to account for each contact point being included twice. If the sums of contact force components in equation (3.5) are calculated for any subregion of assembly, it would be different from subregion to subregion. However, these fluctuations can be expected to become smaller and smaller if the expression is used in an assembly consisting of a large number of particles with a large volume.

The work done by stress per unit volume is

$$W=\sigma_{ij}\varepsilon_{ij} \tag{3.6}$$

where σ_{ij} is a second symmetric tensor. Symmetry is due to the condition of moment equilibrium for each particle.

3.2.2 Contact Force and Average Stress

Combining equation (3.5) and equation (3.6) and according to the symmetry of stress tensor and strain tensor yields

$$\sigma_{ij}=\frac{1}{4V}\sum_{q=1}^{M}[f_i(r^q,\ n^q\ )l_j(r^q,\ n^{\prime q}\ )+f_j(r^q,\ n^q\ )l_i(r^q,\ n^{\prime q}\ )] \tag{3.7}$$

Equation (3.7) gives a relation between the macro-mechanical second-order stress tensor σ_{ij} and the micro-mechanical first-order contact force tensor. These equations can be used not only in cases of two-dimensions and three-dimensions but also in cases with different size and shape particles. However, $l_i(n^{\prime})$ may be a complex expression since it must include the influence of particle shape and particle size-distribution. The development leading to equation (3.7) shows that the macroscopic stress tensor for an assembly can be obtained from consideration of statically admissible contact forces and microstructure described by contact vectors. A similar equation has also been reported by Christoffersen (1981), and Chang (1990a, 1990b, 1990c).

Equation (3.7) can be simplified in an idealized assembly of the idealized particle with equal radius r. For the case of three-dimensions, we have

$$\begin{aligned} V &= V_s(1+e) \\ &= \frac{4N\pi r^3}{3}(1+e) \end{aligned} \tag{3.8}$$

where N is the total number of particles in volume V; V_s is the total volume of particles; e is void ratio.

Substituting equation (3.8) into equation (3.7) yields

$$\sigma_{ij}=\frac{3}{16N\pi r^3(1+e)}\sum_{q=1}^{M}[f_i(r^q,\ n^q)l_j(r^q,\ n^q)+f_j(r^q,\ n^q)l_i(r^q,\ n^q)] \tag{3.9}$$

Likewise, for the case of two-dimensions, we obtain

$$\sigma_{ij}=\frac{1}{4N\pi r^2(1+e)}\sum_{q=1}^{M}[f_i(r^q,\ n^q)l_j(r^q,\ n^q)+f_j(r^q,\ n^q)l_i(r^q,\ n^q)] \tag{3.10}$$

Figure 3.3 represents a four-point symmetric array in two-dimensions. In this case, we have

$$\begin{aligned} 1+e &= \frac{V}{V_s} \\ &= \frac{4r^2\sin(\theta_2-\theta_1)}{\pi r^2} \\ &= \frac{4\sin(\theta_2-\theta_1)}{\pi} \end{aligned} \tag{3.11}$$

Substituting Equation (3.11) into equation (3.10), we obtain

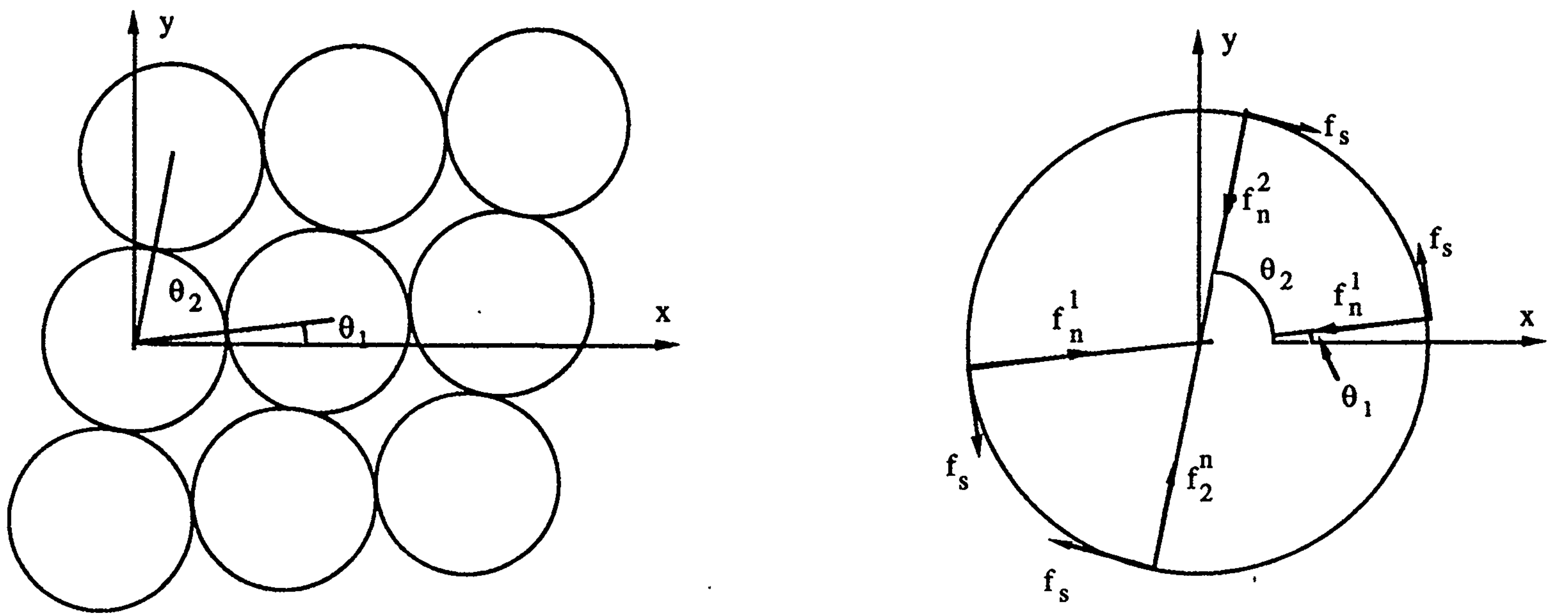

Figure 3.3 Two-Dimensional Regular Packing

$$\sigma_{ij}=\frac{1}{16Nr^2\sin(\theta_2-\theta_1)}\sum_{q=1}^{M}[f_i(r^q,\ n^q)l_j(r^q,\ n^q)+f_j(r^q,\ n^q)l_i(r^q,\ n^q)] \tag{3.12}$$

If the contact forces are divided into tangent contact forces f_s and normal contact forces f_n, we have

$$\sigma_{xx}=\frac{1}{2rsin(\theta_2-\theta_1)}[-f_s(\sin\theta_2\cos\theta_2 \\ -\cos\theta_1\sin\theta_1)+(f_n^1\cos^2\theta_1+f_n^2\cos^2\theta_2)] \tag{3.13}$$

$$\sigma_{yy}=\frac{1}{2rsin(\theta_2-\theta_1)}[f_s(\sin\theta_2\cos\theta_2 \\ -\cos\theta_1\sin\theta_1)+(f_n^1\sin^2\theta_1+f_n^2\sin^2\theta_2)] \tag{3.14}$$

$$\sigma_{zz}=\frac{1}{2rsin(\theta_2-\theta_1)}[f_s(\sin^2\theta_2 \\ -\sin^2\theta_1)-\frac{1}{2}(f_n^1\sin2\theta_1+f_n^2 sin2\theta_2)] \tag{3.12}$$

Obviously, $e = 4/\pi-1$ for $\theta_2-\theta_1 = \pi/2$. If $\theta_1= 0$, the principal stress axes are coincident with the principal fabric axes, so

$$\sigma_{xx} = \frac{f_1^n}{2r} \tag{3.16}$$

$$\sigma_{yy} = \frac{f_2^n}{2r} \tag{3.17}$$

$$\sigma_{xy}=\frac{f^s}{2r} \tag{3.18}$$

The above equations show that the stress is equal to the contact force per unit length for the square four-point contact

3.3 STRESS-STRAIN RELATION

3.3.1 Constitutive Law of Local Contact

In the previous section we have obtained an expression for the average stress tensor from the contact force. However, the calculation of the average stress tensor requires exact knowledge of contact forces and contact vector terms for all particles. In this section by establishing the relation of contact force with contact displacement and the relation of contact force with average stress tensor, the stress-strain relations are then derived. The tensor of contact stiffness for three-dimensions is given by Chang (1990a)

$$D_{ij}=D_n\, n_i\, n_j+D_s\, s_i\, s_j+D_t\, t_i\, t_j \qquad (i,\ j=x,\ y,\ z) \tag{3.19}$$

where D_n, D_s and D_t are the local contact stiffnesses (e.g., D_n is normal contact stiffness; D_s and D_t are tangent contact stiffness) in the directions of n, s, and t, respectively, as shown in Figure 3.1, and are independent of one another. In addition

$$\begin{aligned} n_x&=\sin\gamma\cos\beta \\ n_y&=\sin\gamma\sin\beta \\ n_z&=\cos\gamma \end{aligned} \tag{3.20}$$

$$
\begin{aligned}
s_x &= \cos\gamma\cos\beta \\
s_y &= \cos\gamma\sin\beta \\
s_z &= -\sin\gamma
\end{aligned}
\tag{3.21}
$$

$$
\begin{aligned}
t_x &= -\sin\beta \\
t_y &= \cos\beta \\
t_z &= 0
\end{aligned}
\tag{3.22}
$$

For the case of two-dimensions

$$D_{ij}=D_n n_i\, n_j+D_s s_i\, s_j \qquad (i,\, j=x,\, y) \tag{3.23}$$

where

$$
\begin{aligned}
n_x &= \cos\theta \qquad & n_y &= \sin\theta \\
s_x &= -\sin\theta \qquad & s_y &= \cos\theta
\end{aligned}
\tag{3.24}
$$

The incremental form of the local constitutive law describing the relation of contact force with contact displacement is given by

$$\Delta f_i=D_{ij}\Delta u_j \qquad (i,\, j=x,\, y,\, z) \tag{3.25}$$

3.3.2 Constitutive Law of Particulate Assembly

Combining equation (3.4), equation (3.10), equation (3.19) and equation (3.25), we have

$$\Delta\sigma_{ij}=A_{ijkl}\Delta\varepsilon_{kl} \qquad (i,\ j=x,\ y,\ z) \tag{3.26}$$

where

$$A_{ijkl}=\frac{3}{2(1+e)N_1\pi r}\sum_{q=1}^{m_1}(n_i^q n_j^q n_k^q n_l^q D_n+B_{ijkl}^q D_s+E_{ijkl}^q D_t) \tag{3.27}$$

where m_1 and N_1 represent the numbers of contact points and particles within the interested microelement, respectively. If the microelement is an individual particle, m_1=m. B_{ijkl} and E_{ijkl} are given by

$$B_{ijkl}^q=\frac{1}{4}(n_i^q\ s_j^q\ n_k^q\ s_l^q\ +\ n_j^q\ s_i^q\ n_k^q\ s_l^q \\ +\ n_i^q\ s_j^q\ n_l^q\ s_k^q\ +\ n_j^q\ s_i^q\ n_l^q\ s_k^q\ ) \tag{3.28}$$

$$E_{ijkl}^q=\frac{1}{4}(n_i^q\ t_j^q\ n_k^q\ t_l^q\ +\ n_j^q\ t_i^q\ n_k^q\ t_l^q \\ +\ n_i^q\ t_j^q\ n_l^q\ t_k^q\ +\ n_j^q\ t_i^q\ n_l^q\ t_k^q\ ) \tag{3.29}$$

Obviously, since the resultant moment is zero, the stiffness tensor of assembly satisfies the symmetry of the stress tensor and the strain tensor, i.e.,

$$A_{ijkl}=A_{jikl}=A_{klij} \tag{3.30}$$

3.3.3 Stress-Strain Relation for Two-Dimensional Regular Packing

3.3.3.1 General Stress-Strain Relation for Two-Dimensional Regular Packing

For the case of two-dimension, equation (3.27) becomes

$$A_{ijkl}=\frac{2}{(1+e)N_1\pi}\sum_{q=1}^{m_1}(n_i^q n_j^q n_k^q n_l^q D_n+B_{ijkl}^q D_s) \tag{3.31}$$

For a regular packing assembly, the behaviour of a microelement is same as that of a representative-unit. Therefore in this case m_1 =m. The matrix form of the stress-strain relation is

$$\begin{pmatrix}\Delta\sigma_{xx}\\ \\ \Delta\sigma_{yy}\\ \\ \Delta\sigma_{xy}\end{pmatrix}=\begin{pmatrix}C_{11} & C_{12} & C_{13}\\ \\ C_{21} & C_{22} & C_{23}\\ \\ C_{31} & C_{32} & C_{33}\end{pmatrix}\begin{pmatrix}\Delta\varepsilon_{xx}\\ \\ \Delta\varepsilon_{yy}\\ \\ \Delta\gamma_{xy}\end{pmatrix} \tag{3.32}$$

In order to make our model for complicated load directions, we assume the principal fabric axes not to coincide with the principal stress axes, such as in Figure 3.3. We only discuss an individual particle of regular packing. The angle θ^q is the q^{th} contact angle, which is equal to $\theta_1+(q-1)\Delta\theta$. Therefore we have

$$C_{11}=H_1D_n+H_5D_s$$

$$C_{22}=H_2D_n+H_5D_s$$

$$C_{33}=H_5D_n+\frac{1}{4}(H_1+H_2-2H_5)D_5$$

$$C_{31}=C_{13}=H_3D_n+\frac{H_4-H_3}{2}D_s$$

$$C_{32}=C_{23}=H_4D_n+\frac{H_3-H_4}{2}D_s$$

$$C_{21}=C_{12}=H_5(D_n-D_s)$$

where

$$H_1=\frac{2}{(1+e)\pi}\sum_{q=1}^{\frac{m}{2}}\cos^4\theta^q$$

$$H_2=\frac{2}{(1+e)\pi}\sum_{q=1}^{\frac{m}{2}}\sin^4\theta^q$$

$$H_3=\frac{2}{(1+e)\pi}\sum_{q=1}^{\frac{m}{2}}\cos^3\theta^q\sin\theta^q$$

$$H_4=\frac{2}{(1+e)\pi}\sum_{q=1}^{\frac{m}{2}}\sin^3\theta^q\cos\theta^q$$

$$H_5=\frac{2}{(1+e)\pi}\sum_{q=1}^{\frac{m}{2}}\sin^2\theta^q$$

3.3.3.2 Four-Point Square Symmetric Contact

In the case of four-point square symmetric contact as shown in Figure 3.4a. The void ratio, e= $4/\pi-1$; and the incremental contact angle $\Delta\theta=90°$, $\theta^q=\theta_0$. The stiffness components are

$$C_{11}=C_{22}=\frac{1}{2}[2D_n-(D_n-2D_s)\sin^2 2\theta_0]$$

$$C_{33}=\frac{1}{2}[D_s+(2D_n-\frac{3}{2}D_s)\sin^2 2\theta_0]$$

$$C_{21}=C_{12}=\frac{1}{2}(D_n-D_s)\sin^2 2\theta_0$$

$$C_{31}=C_{12}=C_{23}=C_{32}=D_n sin2\theta_0$$

If θ_0 =0, i.e., the principal fabric axes are coincident with the principal stress axes, and we have

$$\begin{pmatrix}\Delta\sigma_{xx}\\ \Delta\sigma_{yy}\\ \Delta\sigma_{xy}\end{pmatrix}=\frac{1}{2}\begin{pmatrix}2D_n & 0 & 0\\ 0 & 2D_n & 0\\ 0 & 0 & D_s\end{pmatrix}\begin{pmatrix}\Delta\varepsilon_{xx}\\ \Delta\varepsilon_{yy}\\ \Delta\gamma_{xy}\end{pmatrix} \tag{3.33}$$

3.3.3.3 Six-Point Dense Contact

For the six-point dense contact packing as shown in Figure 3.4b. The void ratio, e=$4\sin(\pi/3)/\pi$, and $\Delta\theta=\pi/3$, $\theta_0=0$, so

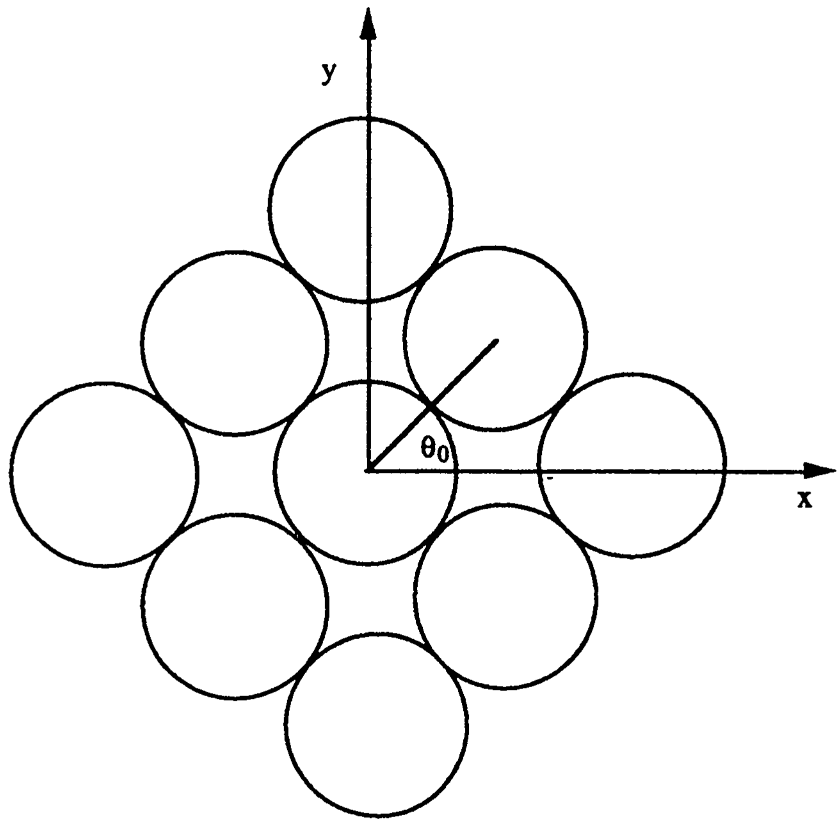

(a) Four-Point Contact

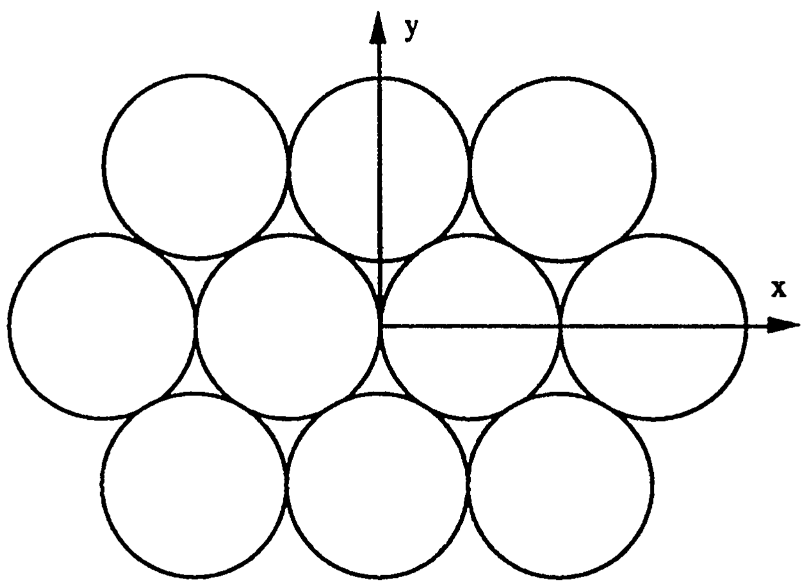

(b) Six-Point Contact

Figure 3.4 Two-Dimensional Rhombic Packing

$$H_1=H_2=\frac{3\sqrt{3}}{4}, \qquad H_5=\frac{\sqrt{3}}{4}, \qquad H_3=H_4=0$$

The stress-strain relation is

$$\begin{pmatrix} \Delta\sigma_{xx} \\ \Delta\sigma_{yy} \\ \Delta\sigma_{xy} \end{pmatrix} = \frac{\sqrt{3}}{4}\begin{pmatrix} 3D_n+D_s & D_n-D_s & 0 \\ D_n-D_s & 3D_n+D_s & 0 \\ 0 & 0 & D_n+D_s \end{pmatrix}\begin{pmatrix} \Delta\varepsilon_{xx} \\ \Delta\varepsilon_{yy} \\ \Delta\gamma_{xy} \end{pmatrix} \tag{3.34}$$

3.3.4 Stress-Strain Relation for Three-Dimensional Regular Packing

3.3.4.1 General Stress-Strain Relation for Three-Dimensional Regular Packing

In the following expressions, γ_q and γ'^q are the angles between the qth coordinate vector $\mathbf{r}^\alpha$ and coordinate axes x and y, respectively. We define

$$\beta_q = \arccos\left(\frac{\cos\gamma'^q}{\sin\gamma}\right) \tag{3.35}$$

Therefore, the stress-strain relation for a symmetric contact assembly is

$$\begin{pmatrix} \Delta\sigma_{xx} \\ \Delta\sigma_{yy} \\ \Delta\sigma_{zz} \\ \Delta\sigma_{xy} \\ \Delta\sigma_{xz} \\ \Delta\sigma_{yz} \end{pmatrix} = \begin{pmatrix} C_{11} & C_{12} & C_{13} & C_{14} & C_{15} & C_{16} \\ C_{21} & C_{22} & C_{23} & C_{24} & C_{25} & C_{26} \\ C_{31} & C_{32} & C_{33} & C_{34} & C_{35} & C_{36} \\ C_{41} & C_{42} & C_{43} & C_{44} & C_{45} & C_{46} \\ C_{51} & C_{52} & C_{53} & C_{54} & C_{55} & C_{56} \\ C_{61} & C_{62} & C_{63} & C_{64} & C_{65} & C_{66} \end{pmatrix} \begin{pmatrix} \Delta\varepsilon_{xx} \\ \Delta\varepsilon_{yy} \\ \Delta\varepsilon_{zz} \\ \Delta\varepsilon_{xy} \\ \Delta\varepsilon_{xz} \\ \Delta\varepsilon_{yz} \end{pmatrix} \tag{3.36}$$

Assuming

$$C_{ij}(\gamma,\beta)=\frac{3}{2(1+e)\pi r}\sum_{q=1}^{m} C'_{ij}(\gamma^q,\beta^q)$$

The components of stiffness tensor ($C_{ij}'=C_{ji}'$) are obtained by

$$C'_{11}=\sin^4\gamma^q\cos^4\beta^q D_n+I^2\cos^4\beta^q D_s+J^2\sin^2\gamma^q D_t$$

$$C'_{22}=\sin^4\gamma^q\cos^4\beta^q D_n+I^2\sin^4\beta^q D_s+J^2\sin^2\gamma^q D_t$$

$$C'_{33}=\cos^4\gamma^q D_n+I^2 D_s$$

$$C'_{44}=J^2\sin^4\gamma^q D_n+I^2J^2D_s+\frac{\sin^2\gamma^q}{4}J^2D_s$$

$$C'_{55}=I^2\cos^2\beta^q D_n+\frac{I^2\cos^2\beta^q}{4}D_s+\frac{1}{4}\cos^2\gamma^q\sin^2\beta^q D_t$$

$$C'_{66}=I^2\sin^2\beta^q D_n+\frac{I^2\sin^2\beta^q}{4}D_n+\frac{1}{4}\cos^2\gamma^q\cos^2\beta^q D_t$$

$$C'_{21}=J^2\sin^4\gamma^q D_n+I^2J^2D_s-J^2\sin^2\gamma^q D_t$$

$$C'_{31}=I^2\cos^2\beta^q(D_n-D_s)$$

$$C'_{32}=I^2\sin^2\beta^q(D_n-D_s)$$

$$C'_{41}=J\sin^4\gamma^q\cos^2\beta^q D_n+I^2Jcos^2\beta^q D_s+\frac{IJ_1}{2}\sin^2\gamma^q D_t$$

$$C'_{42}=Jsin^4\gamma^q\sin^2\beta^q D_n+I^2Jsin^2\beta^q D_s-\frac{JJ_1}{2}\sin^2\gamma^q D_t$$

$$C'_{43}=I^2J(D_n-D_s)$$

$$C'_{51}=Isin^2\gamma^q\cos^3\beta^q D_n+\frac{II_1}{2}\cos^3\beta^q D_s+\frac{IJ}{2}\sin\beta^q D_t$$

$$C'_{52}=IJ\sin^2\gamma^q\sin\beta^q D_n+\frac{II_1J\sin\beta^q}{2}D_s-\frac{IJ}{2}\sin\beta^q D_t$$

$$C'_{53}=IJ\cos^2\gamma^q\cos\beta^q D_n-\frac{II_1}{2}\cos\beta^q D_s$$

$$C'_{54}=IJ\sin^2\gamma^q\cos\beta^q D_n+\frac{II_1J}{2}\cos\beta^q D_s-\frac{IJJ_1}{2}\cos\beta^q D_t$$

$$C'_{61}=IJ\sin^2\gamma^q\cos\beta^q D_n+\frac{II_1J}{2}\cos\beta^q D_s+\frac{IJ\cos\beta^q\cos^2\gamma^q}{2}D_t$$

$$C'_{62}=I\sin^2\gamma^q\sin^3\beta^q D_n+\frac{II_1\sin^3\beta^q}{2}D_s+\frac{I\sin^3\beta^q\cos^2\gamma^q}{2}D_t$$

$$C'_{63}=I\cos^2\gamma^q\sin\beta^q D_n-\frac{II_1}{2}\sin\beta^q D_s$$

$$C'_{64}=IJ\sin^2\gamma^q\sin\beta^q D_n+\frac{II_1J}{2}\sin\beta^q D_s+\frac{II_1}{4}\cos\beta^q D_t$$

$$C'_{65}=I^2JD_n+\frac{I_1J}{4}D_s$$

$$I=\frac{1}{4}\sin 2\gamma^q$$

$$J=\frac{1}{4}\sin 2\beta^q$$

$$I_1=\cos^2\gamma^q-\sin^2\gamma^q$$

$$J_1=\cos^2\beta^q-\sin^2\beta^q$$

3.3.4.2 Three-Dimensional Cubic Packing

The packing model is shown in Figure 3.5. The void ratio, e is 0.9099 and the coordination number, m is 6. The stress-strain relation is obtained by

$$\begin{pmatrix}\Delta\sigma_{xx}\\ \Delta\sigma_{yy}\\ \Delta\sigma_{zz}\\ \Delta\sigma_{xy}\\ \Delta\sigma_{xz}\\ \Delta\sigma_{yz}\end{pmatrix}=\frac{3}{2(1+e)\pi r}\begin{pmatrix}2D_n & 0 & 0 & 0 & 0 & 0\\ 0 & 2D_n & 0 & 0 & 0 & 0\\ 0 & 0 & 2D_n & 0 & 0 & 0\\ 0 & 0 & 0 & D_s & 0 & 0\\ 0 & 0 & 0 & 0 & D_s & 0\\ 0 & 0 & 0 & 0 & 0 & D_n\end{pmatrix}=\begin{pmatrix}\Delta\varepsilon_{xx}\\ \Delta\varepsilon_{yy}\\ \Delta\varepsilon_{zz}\\ \Delta\gamma_{xy}\\ \Delta\gamma_{xz}\\ \Delta\gamma_{yz}\end{pmatrix} \tag{3.37}$$

3.3.4.3 Three-Dimensional Face-Centred Packing

The packing model is shown in Figure 3.6. The void ratio, e is 0.6540 and the coordination number, m is 8. The stress-strain relation is obtained by

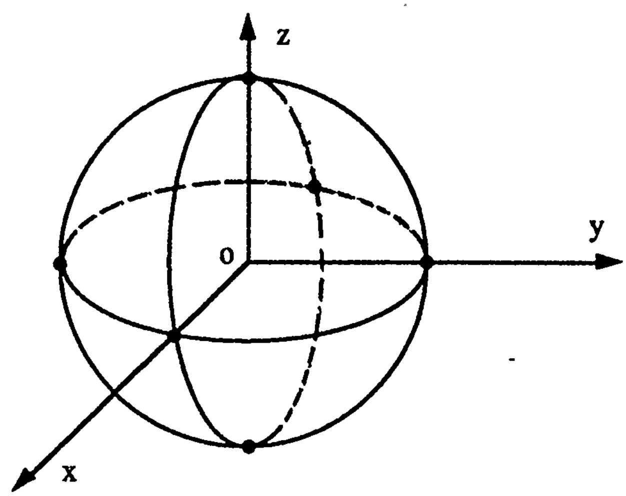

(a)

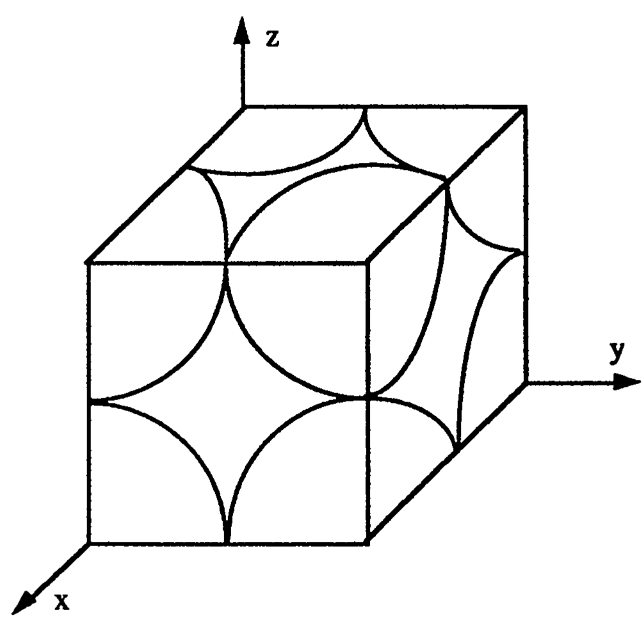

(b)

Figure 3.5 Three-Dimensional Cubic Packing

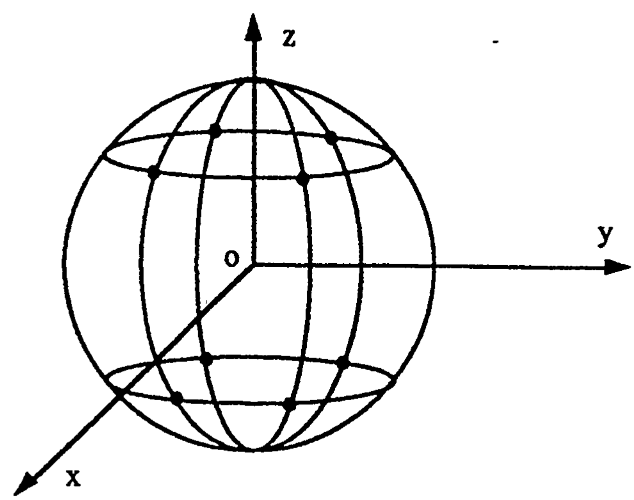

Figure 3.6 Three-Dimensional Face Central Packing

$$\begin{pmatrix}\Delta\sigma_{xx}\\ \Delta\sigma_{yy}\\ \Delta\sigma_{zz}\\ \Delta\sigma_{xy}\\ \Delta\sigma_{xz}\\ \Delta\sigma_{yz}\end{pmatrix} = \frac{3}{2(1+e)\pi r}\begin{pmatrix}C_1 & C_4 & C_5 & 0 & 0 & 0\\ C_4 & C_1 & C_5 & 0 & 0 & 0\\ C_5 & C_5 & C_1 & 0 & 0 & 0\\ 0 & 0 & 0 & C_2 & 0 & 0\\ 0 & 0 & 0 & 0 & C_3 & 0\\ 0 & 0 & 0 & 0 & 0 & C_3\end{pmatrix}\begin{pmatrix}\Delta\varepsilon_{xx}\\ \Delta\varepsilon_{yy}\\ \Delta\varepsilon_{zz}\\ \Delta\gamma_{xy}\\ \Delta\gamma_{xz}\\ \Delta\gamma_{yz}\end{pmatrix} \tag{3.38}$$

where

$$C_1=\frac{1}{4}(2D_n+D_s+3D_t)$$

$$C_2=2D_n+D_s$$

$$C_3=2D_n+\frac{1}{4}(D_n+3D_t)$$

$$C_4=2D_n+D_s-3D_t$$

$$C_5=2(D_n-D_s)$$

3.3.4.4 Three-Dimensional Dense Packing

The packing model is shown in Figure 3.7. The void ratio, e is 0.3504 and

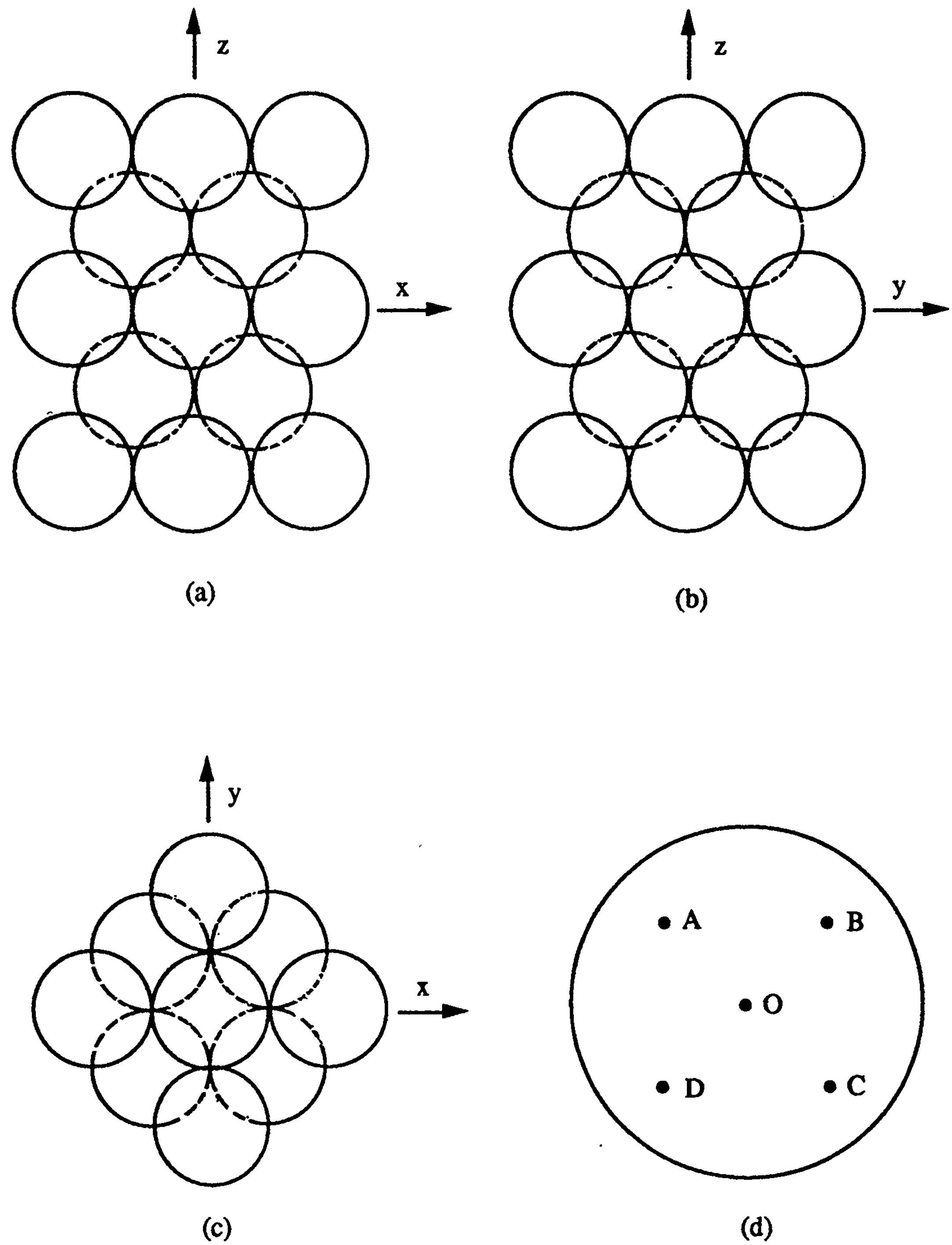

Figure 3.7 Three-Dimensional Dense Twelve Contact Packing

coordination number m is 12. The stress-strain relation is obtained by

$$\begin{pmatrix} \Delta\sigma_{xx} \\ \Delta\sigma_{yy} \\ \Delta\sigma_{zz} \\ \Delta\sigma_{xy} \\ \Delta\sigma_{xz} \\ \Delta\sigma_{yz} \end{pmatrix} = \frac{3}{2(1+e)\pi r} \begin{pmatrix} C_1 & C_5 & C_6 & 0 & 0 & 0 \\ C_5 & C_1 & C_6 & 0 & 0 & 0 \\ C_6 & C_6 & C_2 & 0 & 0 & 0 \\ 0 & 0 & 0 & C_3 & 0 & 0 \\ 0 & 0 & 0 & 0 & C_4 & 0 \\ 0 & 0 & 0 & 0 & 0 & C_4 \end{pmatrix} \begin{pmatrix} \Delta\varepsilon_{xx} \\ \Delta\varepsilon_{yy} \\ \Delta\varepsilon_{zz} \\ \Delta\gamma_{xy} \\ \Delta\gamma_{xz} \\ \Delta\gamma_{yz} \end{pmatrix} \tag{2.39}$$

where

$$C_1=\frac{1}{4}(5D_n+D_s+2D_t)$$

$$C_2=D_n+D_s$$

$$C_3=\frac{1}{4}(D_n+D_s+2D_t)$$

$$C_4=\frac{1}{4}(2D_n+D_s+D_t)$$

$$C_5=\frac{1}{4}(D_n+D_s-2D_t)$$

$$C_6=\frac{1}{2}(D_n-D_s)$$

If D_t=D_s, we have C_1-C_5=$2C_4$. Equation (2.39) shows that five stiffness constants are independent.

3.4 CONCLUSION

Based on principles of micro-mechanics we have derived the stress-strain relations of contact deformation for two-dimensional and three-dimensional regular packing assemblies. The derived stiffness constants are functions of the particle size, void ratio, coordination number, and interparticle contact stiffness. If the interparticle contact interaction is assumed to be linear elastic with no sliding at the contact, the behaviour of assembly deformation is elastic. If the nonlinear constant stiffness given by the Hertz-Mindlin theory of friction contact is used, nonlinear deformation will occur due to nonlinear deformation at the contacts. It is noted that the stiffness tensor is derived for an increment of load based on the packing structure at the instant of load increment. The packing structure , however, changes during the deformation process. Therefore, for the cases with a large change of packing structure such as at high levels of deviatoric stress, the evolution of the packing structure with load should be defined in order to obtain the complete stress-strain relation. For cases with negligibly small changes in packing structure such as for packing under low levels of deviatoric stress, the proposed stress-strain relation can be directly applied in analyses of practical problems.

All the solutions can be used in the cases of different complicated load stress because here we assume the principal stress axis to be coincident with the principal fabric axis. No matter what case, two-dimensions or three-dimensions, if the assembly is isotropic and $D_s=D_t$, only two stiffness constants are independent. If the assembly is isotropic on the cross plane for the case of three-dimensions, five stiffness constants are independent. These conclusions are the same as those obtained by the theory of continuum mechanics. In addition, The stiffness constants are dependent on the different fabric constants. The mechanical behaviours are controlled by the corresponding fabrics.

CHAPTER 4

STRESS-STRAIN RELATION OF A RANDOM PACKING ASSEMBLY UNDER CONTACT DEFORMATION

4.1 INTRODUCTION

Based on the microconstructed continuum, the relation between the fabric tensor and the contact density distribution function, and the relation between the fabric tensor and the stress tensor have been analyzed for assemblies of regular packing in the previous chapter. In this chapter, the analysis is extended to the cases of two-dimensional and three-dimensional random packings.

4.2 STRESS-STRAIN RELATION FOR TWO-DIMENSIONAL RANDOM PACKING

Because natural granular assemblies are usually anisotropic and randomly packed, it is very important to study the mechanical characteristics of random packing assemblies with different fabrics.

For the random packing, the form of summation in equation (3.31) can be replaced by an integral form. For the case of two-dimensions, equation (3.31) becomes

$$A_{ijkl}=\frac{2m}{(1+e)\pi}\int_0^{2\pi}(n_i\ n_j\ n_k\ n_l\ D_n+\ B_{ijkl}D_s)E(\theta)d\theta \tag{4.1}$$

where the form of the density function $E(\theta)$ is the same as that of equation (2.2). However, the fabric constants A, B, and C are determined from the total contact normals within the concerned representative-unit.

4.2.1 Two-Dimensional Isotropic Random Packing

The contact density function is $E(\theta)=1/\pi$ for two-dimensional isotropic packing. Therefore, integrating equation (4.1) using $E(\theta)= 1/\pi$, $n_x = \cos\theta$ and $n_y = \sin\theta$, we obtain

$$\begin{pmatrix} \Delta\sigma_{xx} \\ \Delta\sigma_{yy} \\ \Delta\sigma_{xy} \end{pmatrix} = \frac{m}{4(1+e)\pi} \begin{pmatrix} 3D_n+D_s & D_n-D_s & 0 \\ D_n-D_s & 3D_n+D_s & 0 \\ 0 & 0 & D_n+D_s \end{pmatrix} \begin{pmatrix} \Delta\varepsilon_{xx} \\ \Delta\varepsilon_{yy} \\ \Delta\gamma_{xy} \end{pmatrix} \tag{4.2}$$

From the above equation we can obtain the Bulk Modulus **K** and Shear Modulus **G**, i.e.

$$K=\frac{m}{2(1+e)\pi}D_n \tag{4.3}$$

and

$$G=\frac{m}{4(1+e)\pi}(D_n+D_s) \tag{4.4}$$

Equation (4.3) and equation (4.4) mean that the bulk modulus of the assembly relates only to the normal contact stiffness, and the shear modulus relates to both the normal contact stiffness and the tangent contact stiffness.

The corresponding Poisson's ratio is given by

$$\nu = \frac{D_n - D_s}{3D_n + D_s} = \frac{1-\xi}{3(1+\xi)} \tag{4.5}$$

where ξ (= D_s/D_n) is the contact stiffness ratio. Obviously, ν =1/3 for ξ = 0.

4.2.2 Two-Dimensional Anisotropic Packing

Substituting equation (2.2) into equation (4.1) and integrating we obtain

$$\begin{pmatrix} \Delta\sigma_{xx} \\ \Delta\sigma_{yy} \\ \Delta\sigma_{xy} \end{pmatrix} = \begin{pmatrix} C_{11} & C_{12} & C_{13} \\ C_{21} & C_{22} & C_{23} \\ C_{31} & C_{32} & C_{33} \end{pmatrix} \begin{pmatrix} \Delta\varepsilon_{xx} \\ \Delta\varepsilon_{yy} \\ \Delta\gamma_{xy} \end{pmatrix} \tag{4.6}$$

where

$$C_{11} = C_{22} = \frac{m}{8(1+e)\pi}[(5A+B)D_n + 2D_s]$$

$$C_{33} = \frac{m}{4(1+e)\pi}(D_n + D_s)$$

$$C_{21} = C_{12} = \frac{m}{4(1+e)\pi}(D_n - D_s)$$

$$C_{31}=C_{32}=C_{13}=C_{23}=\frac{m\ C}{4(1+e)\pi}D_n$$

Analysing the above stiffness constants we find C_{33}, C_{21} and C_{12} are independent of the fabric constants. In addition, C_{31}, C_{13}, C_{32}, and C_{23}, which relate to the shear deformation, are dependent on fabric constant **C**. This conclusion is consistent with the analysis in Chapter 3. In other words, the shear compression and dilation of an assembly is caused by the rotation of principal fabric axes.

4.3 STRESS-STRAIN RELATION FOR THREE-DIMENSIONAL RANDOM PACKING

To consider anisotropic random packing in the case of three-dimensions, we introduce a spherical harmonious function to describe the distribution of contact normal directions. The tensorial representation of the distribution function is given by

$$E(\Omega) = \frac{1}{4\pi}\ N_{ij}\ n_i\ n_j$$

$$=\frac{1}{4\pi}(N_{xx}\sin^2\gamma\cos^2\beta+N_{yy}\sin\gamma^2\sin^2\beta \tag{4.7}$$

$$+N_{zz}\cos^2\gamma+2N_{xy}\sin^2\gamma\cos\beta\sin\beta$$

$$+2N_{xz}\sin\gamma\cos\gamma\cos\beta+2N_{yz}\sin\gamma\cos\gamma\sin\beta)$$

where the fabric tensor can be expressed in terms of matrix, i.e.,

$$N_{ij}=\begin{pmatrix} N_{xx} & N_{xy} & N_{xz} \\ N_{xy} & N_{yy} & N_{yz} \\ N_{xz} & N_{yz} & N_{zz} \end{pmatrix} \tag{4.8}$$

Because

$$\int_{\Omega}\frac{1}{4\pi}N_{ij}n_i n_j d\Omega \ =1 \tag{4.9}$$

it requires

$$\begin{aligned}\int_{\Omega}E(\Omega)d\Omega &= \frac{1}{4\pi}\int_0^{2\pi}d\beta\int_0^{\pi} N_{ij}\ n_i\ n_j\ \sin\gamma d\gamma \\ &=\frac{1}{4\pi}\int_0^{2\pi}\int_0^{\pi}(N_{xx}\sin^2\gamma\cos^2\beta+N_{yy}\sin\gamma^2\sin^2\beta \\ &+N_{zz}\cos^2\gamma+2N_{xy}\sin^2\gamma\cos\beta\sin\beta+2N_{xz}\sin\gamma\cos\gamma\cos\beta \\ &+2N_{yz}\sin\gamma\cos\gamma\sin\beta)\sin\gamma d\gamma \\ &=\frac{1}{3}(N_{xx}+N_{yy}+N_{zz})\end{aligned} \tag{4.10}$$

Therefore

$$N_{xx}+N_{yy}+N_{zz}=3 \tag{4.11}$$

For the case of three-dimensional random packing, considering an assembly of a large volume with a large number of particles, the form of summation in equation (3.27) can be replaced by an integral form

$$A_{ijkl}=\frac{3m}{2(1+e)\pi r}\int_0^{\pi}\int_0^{2\pi}(n_i n_j n_k n_l D_n + B_{ijkl}D_s + E_{ijkl}D_t)E(\Omega)\sin\gamma\, d\beta\, d\gamma \tag{4.12}$$

where B_{ijkl} and E_{ijkl} are given by

$$B_{ijkl}=\frac{1}{4}(n_i\, s_j\, n_k\, s_l + n_j\, s_i\, n_k\, s_l + n_i\, s_j\, n_l\, s_k + n_j\, s_i\, n_l\, s_k) \tag{4.13}$$

$$E_{ijkl}=\frac{1}{4}(n_i\, t_j\, n_k\, t_l + n_j\, t_i\, n_k\, t_l + n_i\, t_j\, n_l\, t_k + n_j\, t_i\, n_l\, t_k) \tag{4.14}$$

Considering the practical applications of constitutive relations, the following solutions can be used in the cases where the principal stress axes are not coincident with the principal fabric axes. Substituting the equation (4.7) into equation (4.12), we obtain the stress-strain relations for the three-dimensional random packing assembly. The matrix form is expressed by

$$
\begin{pmatrix} \Delta\sigma_{xx} \\ \Delta\sigma_{yy} \\ \Delta\sigma_{zz} \\ \Delta\sigma_{xy} \\ \Delta\sigma_{xz} \\ \Delta\sigma_{yz} \end{pmatrix} = \frac{3m}{8(1+e)\pi r} \begin{pmatrix} C_{11} & C_{12} & C_{13} & C_{14} & C_{15} & C_{16} \\ C_{21} & C_{22} & C_{23} & C_{24} & C_{25} & C_{26} \\ C_{31} & C_{32} & C_{33} & C_{34} & C_{35} & C_{36} \\ C_{41} & C_{42} & C_{43} & C_{44} & C_{45} & C_{46} \\ C_{51} & C_{52} & C_{53} & C_{54} & C_{55} & C_{56} \\ C_{61} & C_{62} & C_{63} & C_{64} & C_{65} & C_{66} \end{pmatrix} \begin{pmatrix} \Delta\varepsilon_{xx} \\ \Delta\varepsilon_{yy} \\ \Delta\varepsilon_{zz} \\ \Delta\gamma_{xy} \\ \Delta\gamma_{xz} \\ \Delta\gamma_{yz} \end{pmatrix}
$$

(4.15)

If the subscripts x, y, and z are replaced by the subscripts 1, 2, and 3, respectively, the stiffness constants in the above equation are given by

$$C_{11}=\int_0^\pi\int_0^{2\pi}[(N_{11}n_1^6+N_{22}n_1^4n_2^2+N_{33}n_1^4n_3^2)D_n$$

$$+(N_{11}n_1^4s_1^2+N_{22}n_1^2n_2^2s_1^2+N_{33}n_1^2n_3^2s_1^2)D_s$$

$$+(N_{11}n_1^4t_1^2+N_{22}n_1^2n_2^2t_1^2+N_{33}n_1^2n_3^2t_1^2)D_t]\sin\gamma d\gamma d\beta$$

$$=3I_1D_n+J_1D_s+J_4D_t\ ,$$

$$C_{22}=\int_0^\pi\int_0^{2\pi}[(N_{11}n_1^2n_2^4+N_{22}n_2^6+N_{33}n_2^4n_3^2)D_n$$

$$+(N_{11}n_1^2n_2^2s_2^2+N_{22}n_2^4s_2^2+N_{33}n_2^2n_3^2s_2^2)D_s$$

$$+(N_{11}n_1^2n_2^2t_2^2+N_{22}n_2^4t_2^2+N_{33}n_2^2n_3^2t_2^2)D_t]\sin\gamma d\gamma d\beta$$

$$=3I_2D_n+J_2D_s+J_4D_t\ ,$$

$$C_{33}=\int_0^\pi\int_0^{2\pi}[(N_{11}n_1^2n_3^4+N_{22}n_2^2n_3^4+N_{33}n_3^6)D_n$$

$$+(N_{11}n_1^2n_3^2s_3^2+N_{22}n_2^2n_3^2s_3^2+N_{33}n_3^2s_3^4)D_s]\sin\gamma d\gamma d\beta$$

$$=3I_3D_n+8J_3D_s\ ,$$

$$C_{44}=\frac{1}{4}\int_0^\pi\int_0^{2\pi}\{4(N_{11}n_1^4n_2^2+N_{22}n_1^2n_2^4+N_{33}n_1^2n_2^2n_3^2)D_n+N_{11}(n_1^4s_2^2$$

$$+n_1^2n_2^2s_1^2+2n_1^3n_2s_1s_2)+N_{22}(n_1^2n_2^2s_2^2+n_2^4s_1^2+2n_1n_2^3s_1s_2)$$

$$+N_{33}(n_1^2n_2^2s_2^2+n_2^2n_3^2s_1^2+2n_1n_2n_3^2s_1s_2)]D_s+[N_{11}(n_1^4t_2^2$$

$$+n_1^2n_2^2t_1^2+2n_1^3n_2t_1t_2)+N_{22}(n_1^2n_2^2t_2^2+n_2^4t_1^2+2n_1n_2^3t_1t_2)$$

$$+N_{33}(n_1^2n_3^2t_2^2+n_2^2n_3^2t_1^2+2n_1n_2n_3^2t_1t_2)]D_t\}\sin\gamma\, d\gamma\, d\beta$$

$$=I_4D_n+J_3D_s+J_4D_t\ ,$$

$$C_{55}=\frac{1}{4}\int_0^\pi\int_0^{2\pi}\{4(N_{11}n_1^4n_3^2+N_{22}n_1^2n_2^2n_3^2+N_{33}n_1^2n_3^4)D_n$$

$$+N_{11}(n_1^4s_3^2+n_1^2n_3^2s_1^2+2n_1^3n_3s_1s_3)+N_{22}(n_1^2n_2^2s_3^2+n_2^2n_3^2s_1^2$$

$$+2n_1n_2^2n_3s_1s_3)+N_{33}(n_1^2n_3^2s_3^2+n_3^4s_1^2+2n_1n_3^3s_1s_3)]D_s$$

$$+(N_{11}n_1^2n_2^2n_3^2+N_{22}n_2^2n_3^2t_1^2+N_{33}n_3^4t_1^2)D_t\}\sin\gamma\, d\gamma\, d\beta$$

$$=I_4D_n+J_3D_s+J_4D_t\ ,$$

$$C_{66}=\frac{1}{4}\int_0^{\pi}\int_0^{2\pi}\{4(N_{11}n_1^2n_2^2n_3^2+N_{22}n_2^4n_3^2+N_{33}n_2^2n_3^4)D_n$$

$$+[N_{11}(n_2^4s_3^2+n_2^2n_3^2s_2^2+2n_2^3n_3s_2s_3)+N_{22}(n_1^2n_2^2s_3^2+n_1^2n_3^2s_2^2$$

$$+2n_1^2n_2n_3s_2s_3)+N_{33}(n_2^2n_3^2s_3^2+n_3^4s_2^2+2n_2n_3^3s_2s_3)]D_s$$

$$+(N_{11}n_1^2n_3^2t^2+N_{22}n_2^2n_3^2t_2^2+N_{33}n_3^4t_2^2)D_t\}\sin\gamma d\gamma d\beta$$

$$=I_6D_n+J_6D_s+J_8D_t\ ,$$

$$C_{21}=C_{12}=\int_0^{\pi}\int_0^{2\pi}\{(N_{11}n_1^4n_2^2+N_{22}n_2^4n_3^2+N_{33}n_2^2n_3^4)D_n$$

$$+(N_{11}n_1^2n_2^2s_3^2+N_{22}n_2^4s_3^2+N_{33}n_2^2n_3^2s_3^2)D_s+(N_{11}n_1^3n_2t_1t_2$$

$$+N_{22}n_1n_2^3t_1t_2+N_{33}n_1n_2n_3^2t_1t_2)D_t\}\sin\gamma d\gamma d\beta$$

$$=I_4D_n+J_3D_s-J_4D_t\ ,$$

$$C_{31}=C_{13}=\int_0^{\pi}\int_0^{2\pi}[(N_{11}n_1^4n_3^2+N_{22}n_1^2n_2^2n_3^2+N_{33}n_1^2n_3^4)D_n$$

$$+(N_{11}n_1n_3^3s_1s_3+N_{22}n_1n_2^2n_3s_1s_3$$

$$+N_{33}n_1n_3^3s_1s_3)D_s]\sin\gamma d\gamma d\beta$$

$$=I_5(D_n-D_s)\ ,$$

$$C_{32}=C_{23}=\int_0^\pi\int_0^{2\pi}[(N_{11}n_1^2n_2^2n_3^2+N_{22}n_2^4n_3^2+N_{33}n_2^2n_3^4)D_n$$

$$+(N_{11}n_1^3n_3s_1s_3+N_{22}n_1n_2^2n_3s_1s_3$$

$$+N_{33}n_1n_3^3s_1s_3)D_s]\sin\gamma d\gamma d\beta$$

$$=I_6(D_n-D_s)\ ,$$

$$C_{41}=C_{14}=\int_0^\pi\int_0^{2\pi}[N_{22}[2n_1^4n_2^2D_n+(n_1^3n_2s_1s_2+n_1^2n_2^2s_1^2)D_s$$

$$+(n_1^3n_2y_1t_2+n_1^2n_2^2t_1^2)D_t]\sin\gamma d\gamma d\beta$$

$$=\frac{4N_{12}}{105}(6D_n+D_s)\ ,$$

$$C_{42}=C_{24}=\int_0^\pi\int_0^{2\pi}N_{12}[2n_1^2n_2^4D_n+(n_1^2n_2^2s_2^2+n_1n_2^3s_1s_2)D_s$$

$$+(n_1^2n_2^2t_2^2+n_1n_2^3t_1t_2)D_t]\sin\gamma d\gamma d\beta$$

$$=\frac{4N_{12}}{105}(6D_n+2D_s-D_t)\ ,$$

$$C_{43}=C_{34}=\int_0^\pi\int_0^{2\pi}N_{12}[2n_1^2n_2^2n_3^2D_n+(n_1^2n_2n_3s_2s_3$$

$$+n_1n_2^2n_3s_1s_3)D_s]\sin\gamma d\gamma d\beta$$

$$=\frac{8N_{12}}{105}(D_n-D_s)\ ,$$

$$C_{51}=C_{15}=\int_0^{\pi}\int_0^{2\pi}N_{13}[2n_1^4n_3^2D_n+(n_1^3n_3s_1s_3$$

$$+n_1^2n_3^2s_1^2)D_s+n_1^2n_3^2t_1^2D_t]\sin\gamma d\gamma d\beta$$

$$=\frac{N_{13}}{105}(24D_n-3D_s+7D_t)\ ,$$

$$C_{52}=C_{25}=\int_0^{\pi}\int_0^{2\pi}2N_{13}[n_1^2n_2^2n_3^2D_n+(n_1^2n_2n_3s_2s_3$$

$$+n_1n_2n_3^2s_1s_2)D_s+n_1n_2n_3^2t_1t_2D_t]\sin\gamma d\gamma d\beta$$

$$=\frac{N_{13}}{105}(8D_n-D_s-7D_t)\ ,$$

$$C_{53}=C_{35}=\int_0^{\pi}\int_0^{2\pi}N_{13}[2n_1^2n_3^4D_n+(n_1^2n_3^2s_3^2$$

$$+n_1n_3^3s_1s_3)D_s]\sin\gamma d\gamma d\beta$$

$$=\frac{4N_{13}}{105}(6D_n+D_s)\ ,$$

$$C_{54}=C_{45}=\frac{1}{2}\int_0^{\pi}\int_0^{2\pi}N_{23}[4n_1^2n_2^2n_3^2D_n+(n_1^2n_2n_3s_2s_3$$

$$+n_1n_2n_3^2s_1s_2+n_1n_2^2n_3s_1s_3+n_2^2n_3^2s_1^2)D_s$$

$$+(n_1n_2n_3^2t_1t_2+n_2^2n_3^2t_2^2)D_t]\sin\gamma d\gamma d\beta$$

$$=\frac{N_{23}}{105}(8D_n-D_s+7D_t)\ ,$$

$$C_{61}=C_{16}=\int_0^{\pi}\int_0^{2\pi}N_{23}[2n_1^2n_2^2n_3^2D_n+(n_1n_2^2n_3s_1s_3$$

$$+n_1n_2n_3^2s_1s_2)D_s+n_1^2n_3^2t_1^2D_t]\sin\gamma d\gamma d\beta$$

$$=\frac{N_{23}}{105}(8D_n-D_s-7D_t)\ ,$$

$$C_{62}=C_{26}=\int_0^{\pi}\int_0^{2\pi}N_{23}[2n_2^4n_3^2D_n+(n_2^3n_3s_1s_3$$

$$+n_2^2n_3^2s_2^2)D_s+n_2^2n_3^2t_2^2D_t]\sin\gamma d\gamma d\beta$$

$$=\frac{N_{23}}{105}(24D_n-3D_s+7D_t)\ ,$$

$$C_{63}=C_{36}=\int_0^{\pi}\int_0^{2\pi}N_{23}[2n_2^2n_3^4D_n+(n_2^2n_3^2s_3^2$$

$$+n_2n_3^3s_2s_3)D_s]\sin\gamma d\gamma d\beta$$

$$=\frac{4N_{23}}{105}(6D_n+D_s)\ ,$$

$$C_{64}=C_{46}=\frac{1}{2}\int_0^{\pi}\int_0^{2\pi}N_{13}[4n_1^2n_2^2n_3^2D_n+4(n_1^2n_2n_3s_3$$

$$+n_1^2n_3^2s_2^2+n_1n_2n_3^2s_1s_2+n_1n_2^2n_3s_1s_2)D_s$$

$$+(n_1^2n_3^2t_2^2+n_1n_2n_3^2t_1t_2)D_t]\sin\gamma d\gamma d\beta$$

$$=\frac{N_{23}}{105}(8D_n-D_s+7D_t))\ ,$$

$$C_{65}=C_{56}=\frac{1}{2}\int_0^{\pi}\int_0^{2\pi}N_{12}[4n_1^2n_2^2n_3^2D_n+(n_1^2n_2n_3s_2s_3$$

$$+n_1^2n_2^2s_3^2+n_1n_2n_3^2s_1s_2+n_1n_2^2n_3s_1s_3)D_s$$

$$+n_1n_2n_3^2t_1t_2D_t]\sin\gamma d\gamma d\beta$$

$$=\frac{N_{12}}{105}(8D_n-\frac{19}{2}D_s-\frac{7}{2}D_t)) \ ,$$

$$I_1=\frac{4}{105}(5N_{xx}+N_{yy}+N_{zz}) \ ,$$

$$I_2=\frac{4}{105}(N_{xx}+5N_{yy}+N_{zz}) \ ,$$

$$I_3=\frac{4}{105}(N_{xx}+N_{yy}+5N_{zz}) \ ,$$

$$I_4=\frac{4}{105}(3N_{xx}+3N_{yy}+N_{zz}) \ ,$$

$$I_5=\frac{4}{105}(3N_{xx}+N_{yy}+3N_{zz}) \ ,$$

$$I_6=\frac{4}{105}(N_{xx}+3N_{yy}+3N_{zz}) \ ,$$

$$J_1=\frac{1}{105}(10N_{xx}+2N_{yy}+9N_{zz}) \ ,$$

$$J_2=\frac{1}{105}(2N_{xx}+10N_{yy}+9N_{zz}) \ ,$$

$$J_3=\frac{1}{105}(2N_{xx}+2N_{yy}+3N_{zz}) \ ,$$

$$J_4=\frac{1}{105}(2N_{xx}+2N_{yy}+N_{zz}) \ ,$$

$$J_5=\frac{1}{420}(57N_{xx}+19N_{yy}+22N_{zz}) \ ,$$

$$J_6=\frac{1}{420}(19N_{xx}+57N_{yy}+22N_{zz}) \ ,$$

$$J_7=\frac{1}{60}(N_{xx}+3N_{yy}+6N_{zz}) \ ,$$

and

$$J_8=\frac{1}{60}(3N_{xx}+N_{yy}+6N_{zz}) \ ,$$

If $D_s=D_t$, the stiffness constants become

$$C_{11}=\frac{4}{35}(4N_{xx}+3)D_n+\frac{8}{105}(6+N_{xx})D_s\ ,$$

$$C_{22}=\frac{4}{35}(4N_{yy}+3)D_n+\frac{8}{105}(6+N_{yy})D_s\ ,$$

$$C_{33}=\frac{4}{35}(4N_{zz}+3)D_n+\frac{8}{105}(6+N_{zz})D_s\ ,$$

$$C_{44}=\frac{4}{105}(9-2N_{zz})D_n+\frac{2}{35}(8-N_{zz})D_s\ ,$$

$$C_{55}=\frac{4}{105}(9-2N_{yy})D_n+\frac{2}{35}(8-N_{yy})D_s\ ,$$

$$C_{66}=\frac{4}{105}(9-2N_{xx})D_n+\frac{2}{35}(8-N_{xx})D_s\ ,$$

$$C_{21}=C_{12}=\frac{4}{105}(9-2N_{zz})(D_n-D_s)\ ,$$

$$C_{31}=C_{13}=\frac{4}{105}(9-2N_{yy})(D_n-D_s)\ ,$$

$$C_{32}=C_{23}=\frac{4}{105}(9-N_{xx})(D_n-D_s)\ ,$$

$$C_{41}=C_{14}=C_{42}=C_{24}=\frac{4}{105}N_{xy}(6D_n+D_s)\ ,$$

$$C_{43}=C_{34}=\frac{8}{105}N_{xy}(D_n-D_s)\ ,$$

$$C_{51}=C_{15}=C_{53}=C_{35}=\frac{4}{105}N_{yz}(6D_n+D_s) ,$$

$$C_{52}=C_{25}=\frac{8}{105}N_{xz}(D_n-D_s) ,$$

$$C_{54}=C_{45}=\frac{4}{105}N_{yz}(2D_n+\frac{3}{2}D_s) ,$$

$$C_{61}=C_{16}=\frac{8}{105}N_{yz}(D_n-D_s) ,$$

$$C_{62}=C_{26}=C_{63}=C_{36}=\frac{4}{105}N_{yz}(6D_n+D_s) ,$$

$$C_{64}=C_{46}=\frac{4}{105}N_{xz}(2D_n+\frac{3}{2}D_s) ,$$

and

$$C_{65}=C_{56}=\frac{4}{105}N_{xy}(2D_n+\frac{3}{2}D_s)$$

4.4 CORRESPONDING RELATIONS BETWEEN THE FABRIC TENSOR AND THE STIFFNESS TENSOR

In the previous section we have obtained the stiffness tensor. It is shown that all 21 stiffness constants are independent of each other for the case of anisotropic packing and $D_n \neq D_s \neq D_t$. In this section we discuss the corresponding relationships between the stiffness tensor and the fabric tensor for five different fabrics. The following analyses use the previous stress-strain relations for D_s=D_t.

4.4.1 Fully Anisotropic Assembly

For the fully anisotropic assembly, we have $N_{xx} \neq N_{yy} \neq N_{zz} \neq N_{xy} \neq N_{xz} \neq N_{yz} \neq 0$. The corresponding relation is given by

$$\begin{pmatrix} N_{xx} & N_{xy} & N_{xz} \\ N_{yx} & N_{yy} & N_{yz} \\ N_{zx} & N_{zy} & N_{zz} \end{pmatrix} \leftrightarrow \begin{pmatrix} C_{11} & C_{21} & C_{31} & Q & S & C_{61} \\ C_{21} & C_{22} & C_{32} & Q & C_{52} & R \\ C_{31} & C_{32} & C_{33} & C_{43} & S & R \\ Q & Q & C_{43} & C_{44} & C_{54} & C_{64} \\ S & C_{52} & S & C_{54} & C_{55} & C_{65} \\ C_{61} & R & R & C_{64} & C_{65} & C_{66} \end{pmatrix} \tag{4.16}$$

Fabric Tensor $\Leftrightarrow$ Stiffness Tensor

Three sets of stiffness constants are equal, i.e.

$$Q=\frac{4}{105}N_{xy}(6D_n+D_s)$$

$$S=\frac{4}{105}N_{xz}(6D_n+D_s)$$

$$R=\frac{4}{105}N_{yz}(2D_n+\frac{3}{2}D_s)$$

Therefore, for $D_t = D_s$, in the case of the fully anisotropic packing the number of independent stiffness constants reduces from 21 to 18.

4.4.2 Anisotropic Assembly

In this case, $N_{xx} \neq N_{yy} \neq N_{zz} \neq 0$, and $N_{xy} = N_{xz} = N_{yz} = N \neq 0$. The corresponding relation is given by

$$\begin{pmatrix} N_{xx} & N & N \\ N & N_{yy} & N \\ N & N & N_{zz} \end{pmatrix} \leftrightarrow \begin{pmatrix} C_{11} & C_{21} & C_{31} & Q & Q & S \\ C_{21} & C_{22} & C_{32} & Q & S & Q \\ C_{31} & C_{32} & C_{33} & S & Q & Q \\ Q & Q & S & C_{44} & R & R \\ Q & S & Q & R & C_{55} & R \\ S & Q & Q & R & R & C_{66} \end{pmatrix} \tag{4.17}$$

Fabric Tensor $\Leftrightarrow$ Stiffness Tensor

Likewise, three sets of stiffness constants are equal. However the number of the constants with equal value increases. The number of independent stiffness constants reduces from 18 to 12, where

$$Q=\frac{4}{105}N(6D_n+D_s)$$

$$S=\frac{4}{105}N(6D_n+D_s)$$

$$R=\frac{4}{105}N_{yz}(2D_n+\frac{3}{2}D_s)$$

4.3 Normal Anisotropic Assembly

For the normal anisotropic fabrics, $N_{xx} \neq N_{yy} \neq N_{zz} \neq 0$ and $N_{xy} = N_{xz} = N_{yz} = 0$. The corresponding relation is given by

$$\begin{pmatrix} N_{xx} & 0 & 0 \\ 0 & N_{yy} & 0 \\ 0 & 0 & N_{zz} \end{pmatrix} \leftrightarrow \begin{pmatrix} C_{11} & C_{21} & C_{31} & 0 & 0 & 0 \\ C_{21} & C_{22} & C_{32} & 0 & 0 & 0 \\ C_{31} & C_{32} & C_{33} & 0 & 0 & 0 \\ 0 & 0 & 0 & C_{44} & 0 & 0 \\ 0 & 0 & 0 & 0 & C_{55} & 0 \\ 0 & 0 & 0 & 0 & 0 & C_{66} \end{pmatrix} \tag{4.18}$$

Fabric Tensor $\Leftrightarrow$ Stiffness Tensor

The number of independent stiffness constants reduces from 12 to 9.

4.4.4 Transversely Isotropic Assembly

The transversely isotropic material symmetry means that the material fabrics are in the same directions on a plane perpendicular to the plane of transversely isotropy. Here we assume the intersection plane to be perpendicular to the Z axis, so

$$N_{xx}=N_{yy}=\frac{3-N_{zz}}{2}$$

$$N_{xy} = N_{xz} = N_{yz} = 0$$

The corresponding relation is given by

$$\begin{pmatrix} \frac{3-N_{zz}}{2} & 0 & 0 \\ 0 & \frac{3-N_{zz}}{2} & 0 \\ 0 & 0 & N_{zz} \end{pmatrix} \leftrightarrow \begin{pmatrix} Q & C_{21} & S & 0 & 0 & 0 \\ C_{21} & Q & S & 0 & 0 & 0 \\ S & S & C_{33} & 0 & 0 & 0 \\ 0 & 0 & 0 & C_{44} & 0 & 0 \\ 0 & 0 & 0 & 0 & R & 0 \\ 0 & 0 & 0 & 0 & 0 & R \end{pmatrix} \tag{4.19}$$

Fabric Tensor $\Leftrightarrow$ Stiffness Tensor

where

$$Q=2C_{44}+C_{21}=\frac{m}{70(1+e)\pi r}[3(9-2N_{zz})D_n+(15-N_{zz})D_s]$$

$$S=\frac{m}{70(1+e)\pi r}(6+N_{zz})(D_n-D_s)$$

$$R=\frac{m}{70(1+e)\pi r}[(6+N_{zz})D_n+\frac{3}{4}(13+N_{zz})D_s]$$

The number of independent stiffness constants reduces from 9 to 5.

4.4.5 Isotropic Assembly

If the fabric tensor is an identity tensor, δ_{ij}, Kronecker delta, i.e., $N_{xx} = N_{yy} = N_{zz} = 1$ and $N_{xy} = N_{xz} = N_{yz} = 0$, the stiffness matrix represents a packing with isotropic material symmetry. The corresponding relation is given by

$$\begin{pmatrix} 1 & 0 & 0 \\ 0 & 1 & 0 \\ 0 & 0 & 1 \end{pmatrix} \Leftrightarrow \begin{pmatrix} Q & S & S & 0 & 0 & 0 \\ S & Q & S & 0 & 0 & 0 \\ S & S & Q & 0 & 0 & 0 \\ 0 & 0 & 0 & R & 0 & 0 \\ 0 & 0 & 0 & 0 & R & 0 \\ 0 & 0 & 0 & 0 & 0 & R \end{pmatrix} \tag{4.20}$$

Fabric Tensor $\Leftrightarrow$ Stiffness Tensor

where

$$Q = \frac{m}{10(1+e)\pi r}[3D_n + 2D_s]$$

$$S=\frac{m}{10(1+e)\pi r}(D_n-D_s)$$

$$R=\frac{Q-S}{2}$$

$$=\frac{m}{20(1+e)\pi r}(2D_n+3D_n)$$

For the isotropic assembly only two stiffness constants are independent.

4.5 RELATIONS OF FABRICS TO MODULI OF ASSEMBLY

4.5.1 Moduli of Isotropic Assembly for Three-Dimensions

The moduli of an isotropic assembly can be directly obtained from equation (4.20). The bulk modulus of assembly is:

$$K=S+\frac{2}{3}R \tag{4.21}$$

$$=\frac{m}{6(1+e)\pi r}D_n$$

The shear modulus is

$$G=\frac{mD_n}{20(1+e)\pi r}(2+3\xi) \tag{4.22}$$

The Young's modulus is

$$E=\frac{mD_n}{2(1+e)\pi r}\frac{(2+3\xi)}{(4+\xi)} \tag{4.23}$$

where $\xi = D_s/D_n$. Obviously, Poisson's ratio is determined by

$$\nu = \frac{1-\xi}{4-\xi} \tag{4.24}$$

Obviously, if the packing is made of cemented frictionless particles such that the shear stiffness $D_s = D_t = 0$, we obtain a value of 0.5 for the Poisson's ratio ν.

4.5.2 Moduli of Transversely Isotropic Assembly for Three-Dimensions

Assuming the transverse plane to be perpendicular to the Z axis, we obtain three shear moduli on the two different planes.

On the *yoz* plane and *xoz* plane, the shear moduli are

$$G_{yz}=G_{xz}=\frac{m}{70(1+e)\pi r}[(6+N_{zz})D_n+\frac{3}{4}(13+N_{zz})D_s] \tag{4.25}$$

$$G_{xy}=\frac{Q-R}{2}=\frac{m}{70(1+e)\pi r}[(9-2N_{zz})D_n+\frac{3}{2}(8-N_{zz})D_s] \tag{4.26}$$

On the *zoz* plane, the Young's modulus is

$$E_{zz}=\frac{mD_n}{10(1+e)\pi r}\frac{2(18+24N_{zz}-7N_{zz}^2)+(90+15N_{zz})\xi}{4(9-2N_{zz})+(6+N_{zz})\xi} \tag{4.27}$$

The Poisson's ratio is

$$\nu=\frac{(6+N_{zz})(1-\xi)}{4(9-2N_{zz})+(6+N_{zz})\xi} \tag{4.28}$$

The relations among shear modulus, Young's modulus, Poisson's ratio, contact siffness ratio, and fabric constant N_{zz} are plotted in Figure 4.1 to Figure 4.3. It shows that G_{xy} is equal to G_{xz} only in the case of $N_{zz} = 1$. In other words, if assembly is isotropic,

G_{xy} is equal to G_{xz}.

4.6 CONCLUSION

In this chapter, the stress-strain relations of a granular assembly of random packing under contact deformation are derived considering the fabric distribution and orientation, and micromechanics. The main conclusions are consistent with those from the conclusions from the continuum theory. These conclusions include:

(1) The stress-strain relations are related to fabrics of assembly and to the local contact stiffness.

(2) For a fully anisotropic assembly, if the three local contact stiffness constants are not equal to one another, the stress-strain relation is controlled by 21 stiffness constants. If the two tangent stiffness constants are equal, i.e., $D_s = D_t$, the independent stiffness constants reduce from 21 to 18.

(3) If the directions of the principal fabric axes are the same as those of principal stress axes, though it is anisotropic, the number of independent stiffness constants is only nine.

(4) For the case of the transversely isotropic assembly, only five independent stiffness constants determine the stress-strain relation.

(5) For an isotropic assembly, the number of independent constants is two.

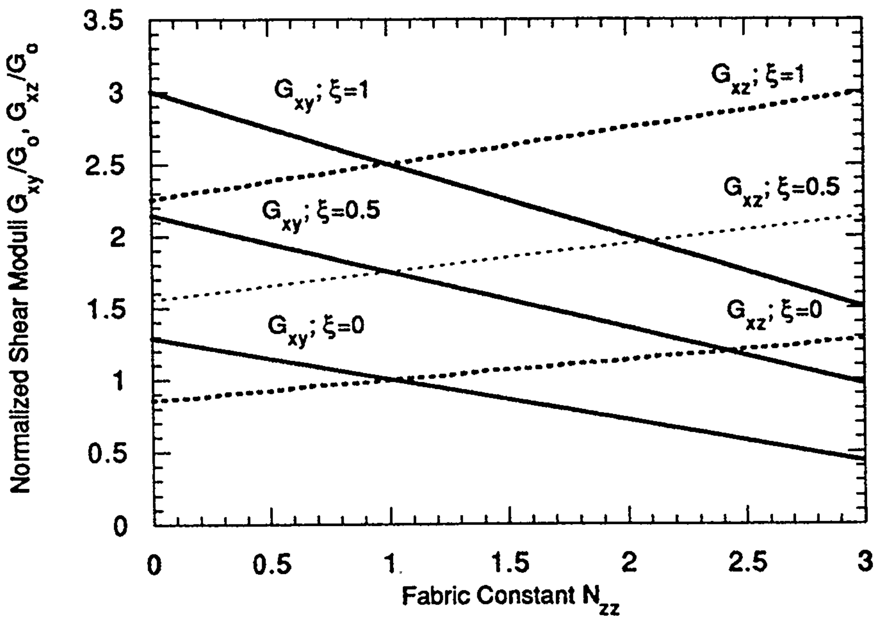

Figure 4.1 Relations among Shear Modulus, Contact Stiffness Ratio and Fabric Constant

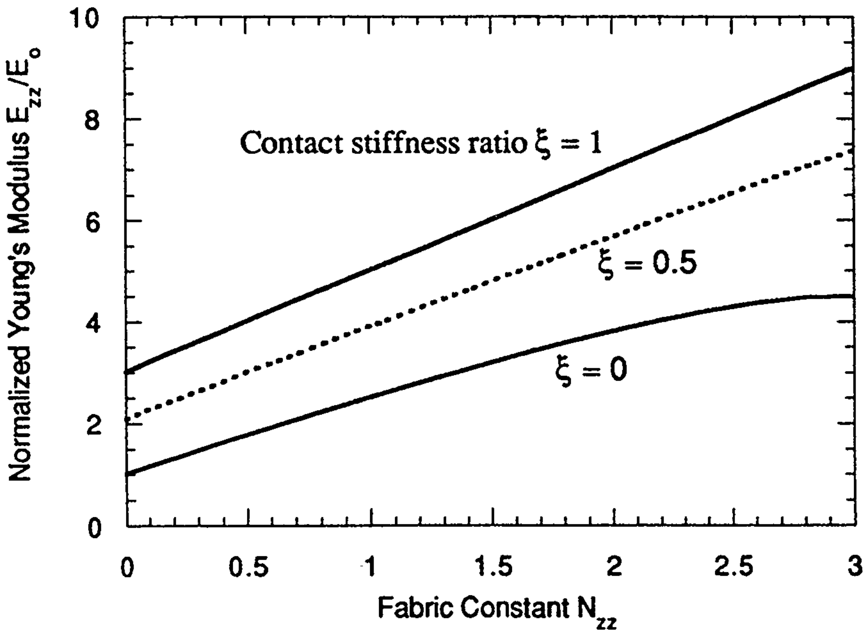

Figure 4.2 Relations among Young's Modulus, Contact Stiffness Ratio and Fabric Constant

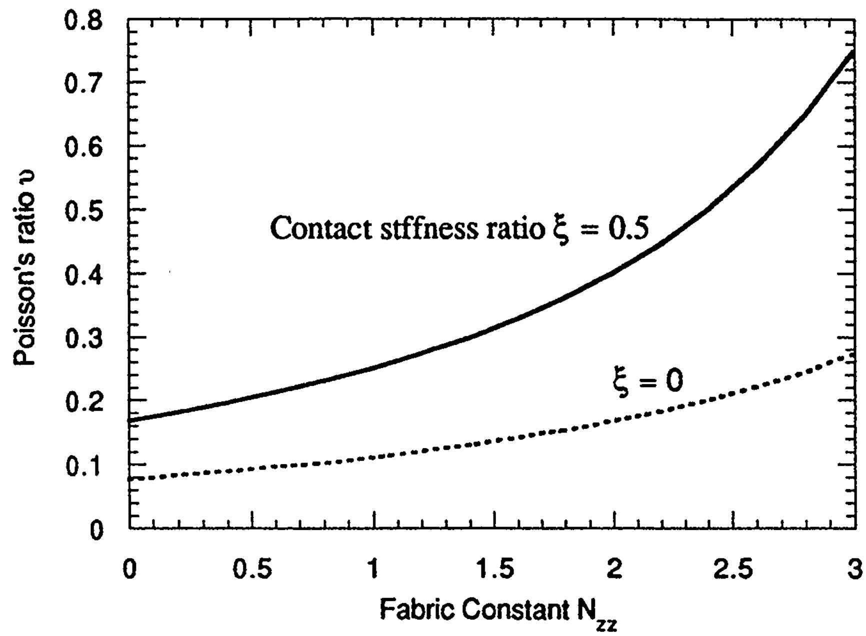

Figure 4.3 Relations among Poisson's Ratio, Contact Stiffness Ratio and Fabric Constant

CHAPTER 5

ANISOTROPIC SWELLING MODEL FOR CLAY

5.1 INTRODUCTION

In previous chapters we have analyzed the characteristics of the granular materials and derived the stress-strain relations by introducing the concepts of fabrics. The stress-strain models are based on the contact density and contact distribution of the particle assembly. The conclusions obtained from these models indicate that the mechanical behaviours of granular materials are controlled by the changes of contact stiffness, void ratio and fabrics. However, these models have limitations when they are used in the analysis of swelling clay. First, the relevant particles in swelling clay are not spherical or elliptical particles but "plate-like" particles. Second, the swelling behaviour of swelling clay is not controlled by the particle slip or the gain and loss of contact points but by the mechanism of "double-layer" swelling. Therefore, we have to find a new model to predict quantitatively the swelling deformation behaviour of clay. In this chapter, the constitutive relations for two-dimensional and three-dimensional anisotropic swelling are derived. In addition, theoretical results and test data are compared.

5.2 SWELLING MECHANISM IN CLAY

Natural clays normally contain a significant portion of structured assemblages composed of clay mineral particles (Figure 5.1). Clay mineral particles are of "plate-like"

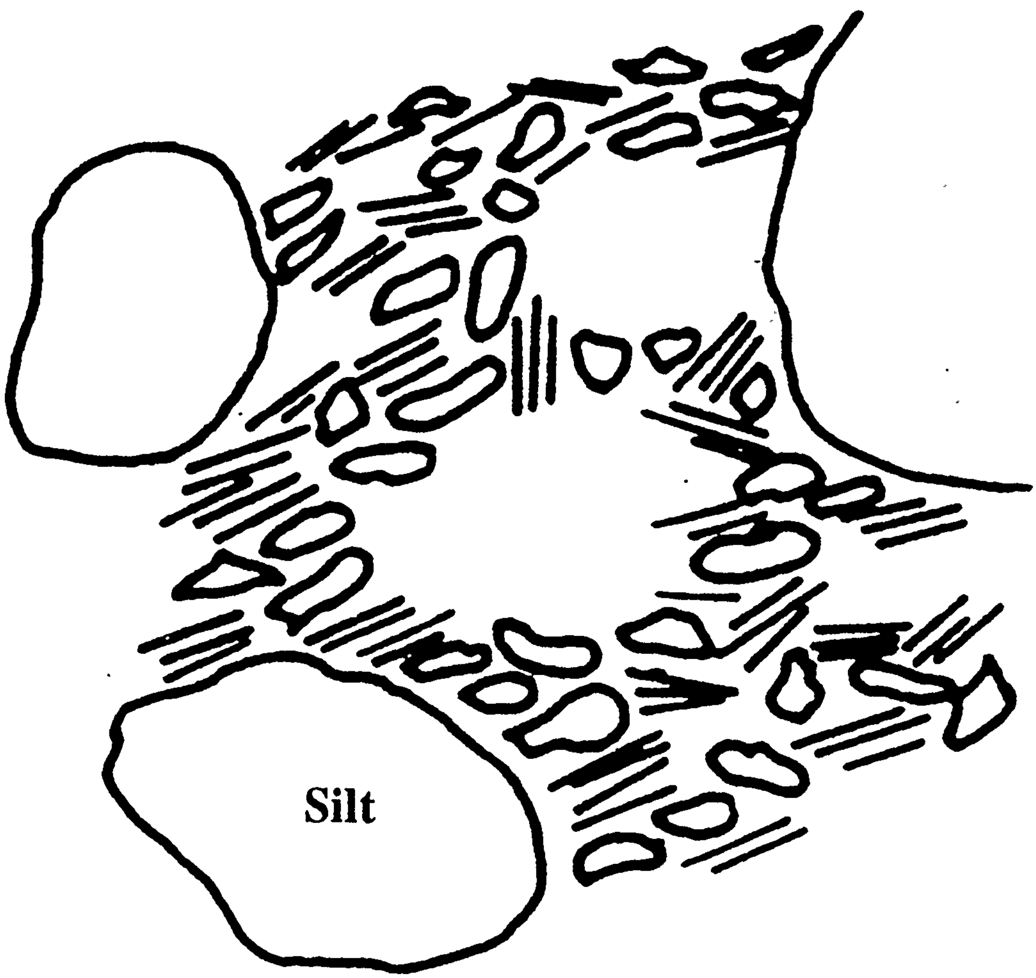

Figure 5.1 Fabric Structure of A Nature Clay

form having a high specific surface area. The surfaces of clay mineral particles carry residual negative charges, mainly as a result of the isomorphous substitution of aluminum or silicon atoms of basic clay mineral structural units by atoms of lower valency, but also due to dissociation of hydroxyl ions. The negative charges on the clay particles surface result in cations present in the water in the void space being attracted to the particles. The net effect is that the cations form a dispersed layer adjacent to the particle, the cation concentration decreasing with increasing distance from the surface until the concentration becomes equal to that in the "normal" water-pore fluid in the void space. The negatively charged particle surface and dispersed layer of cations is termed a 'double layer" structure. For a given particle, the thickness of the cation layer or double layer depends on the valency and concentration of the cations.

When a natural clay sample is exposed to fresh or pure water, the water molecules have a tendency to diffuse into the double layer according to the ionic concentration gradient between the void space and the external, i.e., osmotic process. Water molecules are adsorbed to the particle surface causing an increase in the double layer thickness, i.e., swelling (Figure 5.2). Adsorbed water molecules can move relatively freely parallel to the particle, but movement perpendicular to the surface is restricted. The amount of swelling on exposed to fresh water is dependent on the freedom allowed in swelling. A sufficiently high external pressure can be imposed on the clay sample to inhibit any water migration from outside into the clay particles. This pressure is called swelling pressure, σ_s , at which no swelling is induced. If the external pressure σ is less than the value of σ_s, swelling will occur. There exists a relation linking the swelling between clay particles

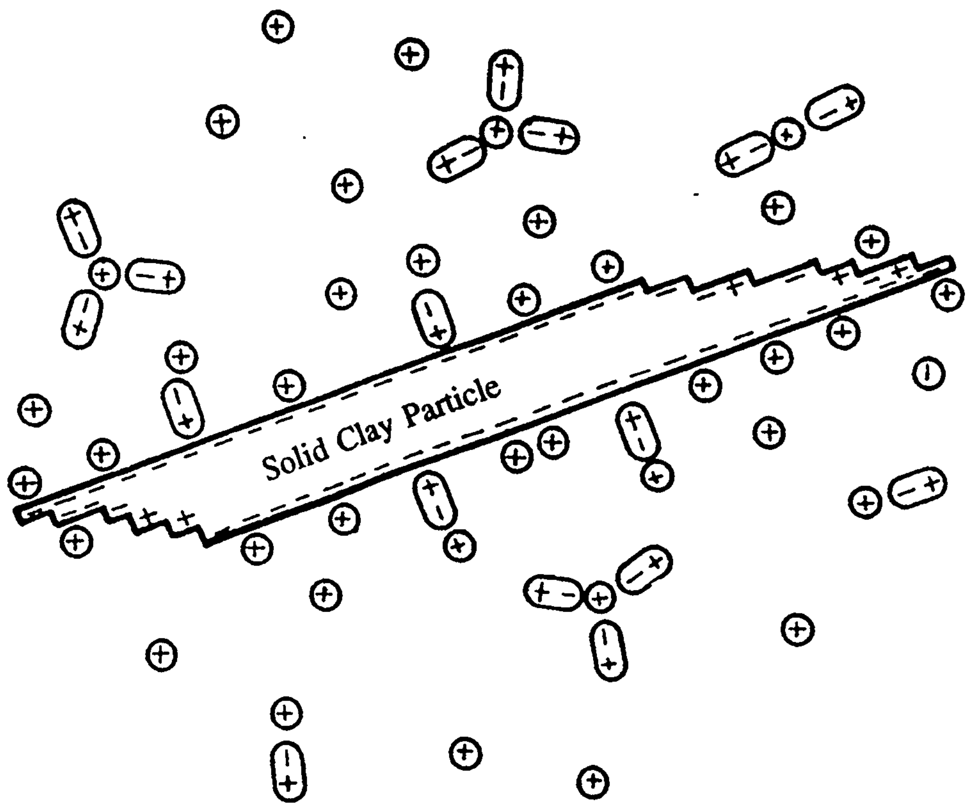

Figure 5.2 Negatively Charged Clay Particle and Surrounding Aqueous Solution

and the external normal pressure. This relation may be linear or non-linear. In this study, we assume a linear relation as follows (Figure 5.3):

$$\delta = C_{se}(\sigma_s - \sigma) \tag{5.1}$$

where δ is the swell per unit length between clay particles; σ_s is the swelling pressure; σ is the imposed normal pressure; and C_{se} is the slope or coefficient of swell.

5.3 ANISOTROPIC SWELLING MODEL

5.3.1 Two-Dimensional Model

The density function used to describe the clay particle distribution is similar to that for a granular particle, except that the orientation of the clay particle is defined by its normal instead of the contact angle (Figure 5.4). Here the normal direction is defined as the direction perpendicular to the clay particle. So the density function used is similar to equation (2.2)

$$a(\theta) = \frac{1}{\pi}(A\cos^2\theta + B\sin^2\theta + C\sin 2\theta) \tag{5.2}$$

where A, B, and C are fabric constants, θ is the angle between the normal and horizontal axis.

When a vertical stress σ_{yy} and a horizontal stress σ_{xx} are applied to a sample consisting of clay particles (Figure 5.4), the induced normal stress, σ^i, and shear stress, τ^i at the i^{th} particle with an angle θ^i between the normal and the horizontal plane is given by

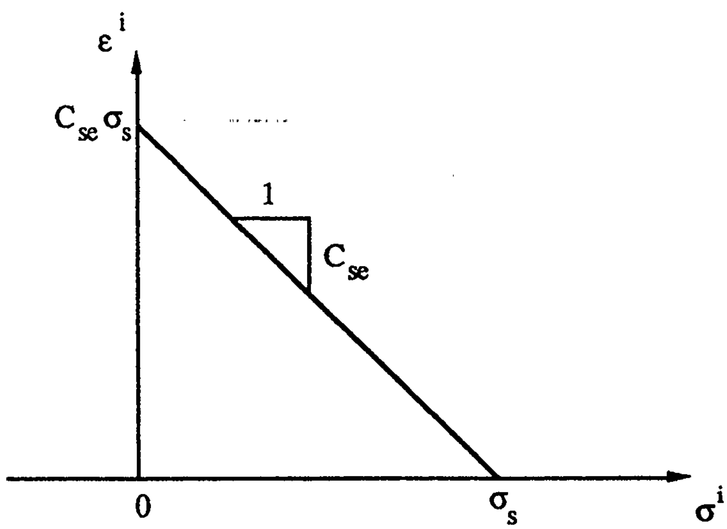

Figure 5.3 Swell Model for Individual Clay Particle

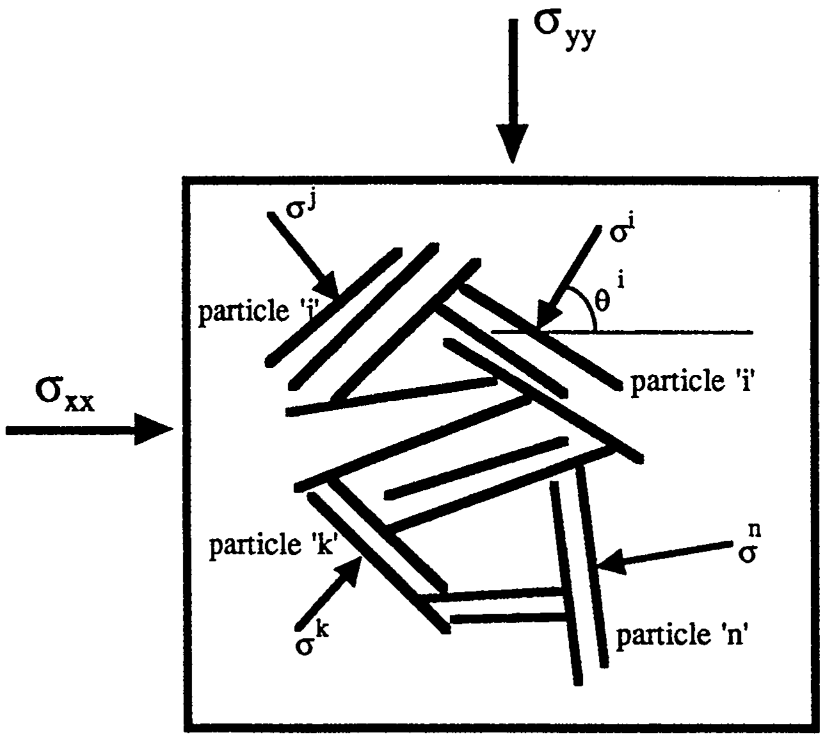

Figure 5.4 Clay Particle Orientation

$$\sigma^i(\theta)=\sigma_{xx}\cos^2\theta^i+\sigma_{yy}\sin^2\theta^i$$

$$\tau^i(\theta)=\frac{\sigma_{xx}-\sigma_{yy}}{2}\sin 2\theta^i \tag{5.3}$$

It is important to note that stresses, σ^i and τ^i, are average stresses acting on the clay particle surfaces. They are not interparticle or contact stresses. It is assumed that shear stress has no effect on the swelling. Hence, if the induced normal stress is less than the swelling pressure σ_s, swelling will occur. The normal swell strains for the ith clay particle is given by

$$\delta^i=C_{se}[\sigma_s-\sigma^i(\theta^i\ )] \tag{5.4}$$

Resolving the normal swell into its x- and y- components and summing up all components for all particles in a unit volume, the resultant x- and y- swell are obtained by integration

$$\begin{aligned}\delta_{xx}&=C_{se}\int_{-\frac{\pi}{2}}^{\frac{\pi}{2}}[\sigma_s-\sigma(\theta)]\cos\theta\ a(\theta)d\theta\\&=II_1-II_2\end{aligned} \tag{5.5}$$

$$\begin{aligned}\delta_{yy}&=C_{se}\int_0^{\pi}[\sigma_s-\sigma(\theta)]\sin\theta\ a(\theta)d\theta\\&=JJ_1-JJ_2\end{aligned} \tag{5.6}$$

where

$$II_1=\frac{C_{se}}{\pi}\int_{-\frac{\pi}{2}}^{\frac{\pi}{2}}\sigma_s\ \cos\theta(A\cos^2\theta+B\sin^2\theta+C\sin2\theta)d\theta$$

$$=\frac{2C_{se}\sigma_s}{3\pi}(2A+B)$$

$$II_2=\frac{C_{se}}{\pi}\int_{\frac{\pi}{2}}^{-\frac{\pi}{2}}(\sigma_{xx}\cos^2\theta+\sigma_{yy}\sin^2\theta)(A\cos^2\theta+B\sin^2\theta+C\sin2\theta)\cos\theta d\theta$$

$$=\frac{C_{se}}{\pi}\int_{-\frac{\pi}{2}}^{\frac{\pi}{2}}[\sigma_{xx}(A\cos^5\theta+B\cos^3\theta\sin^2\theta+C\cos^3\theta\sin2\theta)$$

$$+\sigma_{yy}(A\sin^2\theta\cos^3\theta+B\sin^4\theta\cos\theta+C\sin^2\theta\sin2\theta\cos\theta)]d\theta$$

$$=\frac{2C_{se}}{15\pi}[2\sigma_{xx}(4A+B)+\sigma_{yy}(2A+3B)]$$

$$JJ_1=\frac{C_{se}}{\pi}\int_0^{\pi}\sigma_s\ \sin\theta(A\cos^2\theta+B\sin^2\theta+C\sin2\theta)d\theta$$

$$=\frac{2C_{se}\sigma_s}{3\pi}(A+2B)$$

$$JJ_2=\frac{C_{se}}{\pi}\int_0^{\pi}(\sigma_{xx}\cos^2\theta+\sigma_{yy}\sin^2\theta)(A\cos^2\theta+B\sin^2\theta+C\sin2\theta)\sin\theta d\theta$$

$$=\frac{C_{se}}{\pi}\int_0^{\pi}[\sigma_{xx}(A\cos^4\theta\sin\theta+B\cos^2\theta\sin^3\theta+C\cos^2\theta\sin2\theta\sin\theta)$$

$$+\sigma_{yy}(A\sin^3\theta\cos^2\theta+B\sin^5\theta+C\sin^3\theta\sin2\theta)]d\theta$$

$$=\frac{2C_{se}}{15\pi}[\sigma_{xx}(3A+2B)+2\sigma_{yy}(A+4B)]$$

Since the integrations in equations (5.5) and (5.6) are performed per unit value, the displacements are equal to the strain. Therefore, in the case of two-dimensions the stress-strain relations for swelling soil are given by

$$\varepsilon_{xx}=\frac{2C_{se}}{15\pi}\{5\sigma_s(2A+B)-[2\sigma_{xx}(4A+B)+\sigma_{yy}(2A+3B)]\} \tag{5.7}$$

$$\varepsilon_{yy}=\frac{2C_{se}}{15\pi}\{5\sigma_s(A+2B)-[\sigma_{xx}(3A+2B)+2\sigma_{yy}(A+4B)]\} \tag{5.8}$$

Equations (5.7) and (5.8) indicate that swelling strains are dependent on the clay particle swelling properties, the fabric distribution and the imposed stress. The external stresses or swelling pressures, σ_{xx} and σ_{yy}, to prevent any swelling (i.e., $\varepsilon_{xx} = \varepsilon_{yy} = 0$) are a function of fabrics.

5.3.2 Three-Dimensional Model

The density function of the normal directions to clay particles for the case of three-dimensions is:

$$a(\gamma,\beta)=\frac{1}{4\pi}(N_{xx}\sin^2\gamma\cos^2\beta+N_{yy}\sin^2\gamma\sin^2\beta+N_{zz}\cos^2\gamma) \tag{5.9}$$

where γ and β are coordinate angles as defined and shown in Figure 3.1; N_{xx}, N_{yy} and N_{zz} are fabric constants. From equation (4.11) we have $N_{xx} + N_{yy} + N_{zz} = 3$. The normal stress to the clay particle for three-dimensions is:

$$\sigma^i(\gamma^i,\beta^i)=\sigma_{xx}\sin^2\gamma^i\cos^2\beta^i+\sigma_{yy}\sin^2\gamma^i\sin^2\beta^i+\sigma_{zz}\cos^2\gamma^i \tag{5.10}$$

Similar to the case of two-dimensions. the swelling strain components are given by

$$\varepsilon_{xx}=C_{se}\int_{-\frac{\pi}{2}}^{\frac{\pi}{2}}d\beta\int_0^{\pi}[\sigma_s-\sigma(\gamma,\ \beta)]a(\gamma,\ \beta)\sin^2\gamma\cos\beta d\gamma \tag{5.11}$$

$$\varepsilon_{yy}=\frac{C_{se}}{4\pi}\int_0^{\pi}d\beta\int_0^{\pi}[\sigma_s-\sigma(\gamma,\ \beta)]a(\gamma,\ \beta)\sin^2\gamma\sin\beta d\gamma \tag{5.12}$$

$$\varepsilon_{zz}=\frac{C_{se}}{4\pi}\int_0^{2\pi}d\beta\int_0^{\frac{\pi}{2}}[\sigma_s-\sigma(\gamma,\ \beta)]a(\gamma,\ \beta)\sin\gamma\cos\gamma d\gamma \tag{5.13}$$

Substituting equations (5.9) and (5.10) into equation (5.11) we have

$$\begin{aligned}\varepsilon_{xx}=&\frac{C_{se}}{4\pi}\int_{-\frac{\pi}{2}}^{\frac{\pi}{2}}d\beta\int_0^{\pi}[\sigma_s-(\sigma_{xx}\sin^2\gamma\cos^2\beta+\sigma_{yy}\sin^2\gamma\sin^2\beta+\sigma_{zz}\cos^2\gamma)]\\&[N_{xx}\sin^2\gamma\cos^2\beta+N_{yy}\sin^2\gamma\sin^2\beta+N_{zz}\cos^2\gamma]\sin^2\gamma\cos\beta d\gamma\\=&\frac{C_{se}}{4\pi}(HX_0+HX_1+HX_2+HX_3+HX_4+HX_5+HX_6+HX_7+HX_8+HX_9)\end{aligned} \tag{5.14}$$

where

$$\begin{aligned}HX_0=&\sigma_s\int_{-\frac{\pi}{2}}^{\frac{\pi}{2}}d\beta\int_0^{\pi}(N_{xx}\sin^4\gamma\cos^3\beta+N_{yy}\sin^4\\&\gamma\sin^2\beta\cos\beta+N_{zz}\cos^2\gamma\sin^2\gamma\cos\beta)d\gamma\\=&\frac{\pi\sigma_s}{4}(2N_{xx}+N_{yy}+N_{zz})\\=&\frac{\pi\sigma_s}{4}(N_{xx}+3)\ ,\end{aligned}$$

$$HX_1=\sigma_{xx}N_{xx}\int_{-\frac{\pi}{2}}^{\frac{\pi}{2}}d\beta\int_0^{\pi}\sin^6\gamma\cos^5\beta d\gamma=\frac{\pi\sigma_{xx}N_{xx}}{3}\ ,$$

$$HX_2=\sigma_{xx}N_{yy}\int_{-\frac{\pi}{2}}^{\frac{\pi}{2}}d\beta\int_0^{\pi}\sin^6\gamma\cos^3\beta\sin^2\beta\, d\gamma=\frac{\pi\sigma_{xx}N_{xx}}{12}\ ,$$

$$HX_3=\sigma_{xx}N_{zz}\int_{-\frac{\pi}{2}}^{\frac{\pi}{2}}d\beta\int_0^{\pi}\sin^4\gamma\cos^3\beta\cos^2\gamma\, d\gamma=\frac{\pi\sigma_{xx}N_{xx}}{12}\ ,$$

$$HX_4=\sigma_{yy}N_{xx}\int_{-\frac{\pi}{2}}^{\frac{\pi}{2}}d\beta\int_0^{\pi}\sin^6\gamma\sin^2\beta\cos^3\beta\, d\gamma=\frac{\pi\sigma_{yy}N_{xx}}{12}\ ,$$

$$HX_5=\sigma_{yy}N_{yy}\int_{-\frac{\pi}{2}}^{\frac{\pi}{2}}d\beta\int_0^{\pi}\sin^6\gamma\sin^4\beta\cos\beta\, d\gamma=\frac{\pi\sigma_{yy}N_{yy}}{8}\ ,$$

$$HX_6=\sigma_{yy}N_{zz}\int_{-\frac{\pi}{2}}^{\frac{\pi}{2}}d\beta\int_0^{\pi}\sin^4\gamma\cos^2\gamma\cos\beta\sin^2\beta\, d\gamma=\frac{\pi\sigma_{yy}N_{zz}}{24}\ ,$$

$$HX_7=\sigma_{zz}N_{xx}\int_{-\frac{\pi}{2}}^{\frac{\pi}{2}}d\beta\int_0^{\pi}\sin^4\gamma\cos^2\gamma\cos^3\beta\, d\gamma=\frac{\pi\sigma_{zz}N_{xx}}{12}\ ,$$

$$HX_8=\sigma_{zz}N_{yy}\int_{-\frac{\pi}{2}}^{\frac{\pi}{2}}d\beta\int_0^{\pi}\sin^4\gamma\cos^2\gamma\sin^2\beta\cos\beta\, d\gamma=\frac{\pi\sigma_{zz}N_{yy}}{24}\ ,$$

and

$$HX_9=\sigma_{zz}N_{zz}\int_{-\frac{\pi}{2}}^{\frac{\pi}{2}}d\beta\int_0^{\pi}\sin^2\gamma\cos^4\gamma\cos\beta\, d\gamma=\frac{\pi\sigma_{zz}N_{zz}}{8}$$

So we obtain the strain component in the x-direction

$$\varepsilon_{xx}=\frac{1}{16}\{C_{se}\sigma_s(N_{xx}+3)-\frac{1}{6}C_{se}[(8\sigma_{xx}+2\sigma_{yy}+2\sigma_{zz})N_{xx}$$
$$+(2\sigma_{xx}+3\sigma_{yy}+\sigma_{zz})N_{yy}+(2\sigma_{xx}+\sigma_{yy}+3\sigma_{zz})N_{zz})]\} \tag{5.15}$$

Substituting equations (5.9) and (5.10) into equation (5.13) we have

$$\varepsilon_{yy}=\frac{C_{se}}{4\pi}\int_0^{\pi}d\beta\int_0^{\pi}[\sigma_s-(\sigma_{xx}\sin^2\gamma\cos^2\beta+\sigma_{yy}\sin^2\gamma\sin^2\beta+\sigma_{zz}\cos^2\gamma)]$$
$$[N_{xx}\sin^2\gamma\cos\beta^2\beta+N_{yy}\sin^2\gamma\sin^2\beta+N_{zz}\cos^2\gamma]\sin^2\gamma\sin\beta d\gamma \tag{5.16}$$
$$=\frac{C_{se}}{4\pi}(HY_0+HY_1+HY_2+HY_3+HY_4+HY_5+HY_6+HY_7+HY_8+HY_9)$$

where

$$HY_0=\sigma_s\int_0^{\pi}d\beta\int_0^{\pi}(N_{xx}\sin^4\gamma\cos^2\beta\sin\beta$$
$$+N_{yy}\sin^4\gamma\sin^3\beta+N_{zz}\cos^2\gamma\sin^2\gamma\sin\beta)d\gamma$$
$$=\frac{\pi\sigma_s}{4}(N_{xx}+2N_{yy}+N_{zz})$$
$$=\frac{\pi\sigma_s}{4}\ (N_{yy}+3)$$

$$HY_1=\sigma_{xx}N_{xx}\int_0^{\pi}d\beta\int_0^{\pi}\sin^6\gamma\cos^4\beta\sin\beta d\gamma=\frac{\pi\sigma_{xx}N_{xx}}{8}\ ,$$

$$HY_2=\sigma_{xx}N_{yy}\int_0^{\pi}d\beta\int_0^{\pi}\sin^6\gamma\cos^2\beta\sin^3\beta d\gamma=\frac{\pi\sigma_{xx}N_{yy}}{12}\ ,$$

$$HY_3=\sigma_{xx}N_{zz}\int_0^{\pi}d\beta\int_0^{\pi}\sin^4\gamma\cos^2\beta\cos^2\gamma\sin\beta d\gamma=\frac{\pi\sigma_{xx}N_{zz}}{24}\ ,$$

$$HY_4=\sigma_{yy}N_{xx}\int_0^{\pi}d\beta\int_0^{\pi}\sin^6\gamma\sin^3\beta\cos^2\beta d\gamma=\frac{\pi\sigma_{yy}N_{xx}}{12}\ ,$$

$$HY_5=\sigma_{yy}N_{yy}\int_0^{\pi}d\beta\int_0^{\pi}\sin^6\gamma\sin^5\beta d\gamma=\frac{\pi\sigma_{yy}N_{yy}}{3}\ ,$$

$$HY_6=\sigma_{yy}N_{zz}\int_0^{\pi}d\beta\int_0^{\pi}\sin^4\gamma\cos^2\gamma\sin^3\beta d\gamma=\frac{\pi\sigma_{yy}N_{zz}}{12}\ ,$$

$$HY_7=\sigma_{zz}N_{xx}\int_0^{\pi}d\beta\int_0^{\pi}\sin^4\gamma\cos^2\gamma\cos^2\beta\sin\beta d\gamma=\frac{\pi\sigma_{zz}N_{xx}}{24}\ ,$$

$$HY_8=\sigma_{zz}N_{yy}\int_0^{\pi}d\beta\int_0^{\pi}\sin^4\gamma\cos^2\gamma\sin^3\beta d\gamma=\frac{\pi\sigma_{zz}N_{yy}}{12}\ ,$$

and

$$HY_9=\sigma_{zz}N_{zz}\int_0^{\pi}d\beta\int_0^{\pi}\sin^2\gamma\cos^4\gamma\sin\beta d\gamma=\frac{\pi\sigma_{zz}N_{zz}}{8}$$

So we obtain the strain component on the y-direction

$$\begin{aligned}\varepsilon_{yy}=\frac{1}{16}\{&C_{se}\sigma_s(N_{yy}+3)-\frac{1}{6}C_{se}[(3\sigma_{xx}+2\sigma_{yy}+\sigma_{zz})N_{xx}\\&+(2\sigma_{xx}+8\sigma_{yy}+2\sigma_{zz})N_{yy}+(\sigma_{xx}+2\sigma_{yy}+3\sigma_{zz})N_{zz})]\}\end{aligned}\tag{2.17}$$

Substituting equations (5.8) and (5.9) into equation (5.12) we have

$$\varepsilon_{zz}=\frac{C_{se}}{4\pi}\int_0^{2\pi}d\beta\int_0^{\frac{\pi}{2}}[\sigma_s-(\sigma_{xx}\sin^2\gamma\cos^2\beta+\sigma_{yy}\sin^2\gamma\sin^2\beta+\sigma_{zz}\cos^2\gamma)]$$

$$[N_{xx}\sin^2\gamma\cos^2\beta+N_{yy}\sin^2\gamma\sin^2\beta+N_{zz}\cos^2\gamma]\sin\gamma\cos\gamma d\gamma \tag{5.18}$$

$$=\frac{C_{se}}{4\pi}(HZ_0+HZ_1+HZ_2+HZ_3+HZ_4+HZ_5+HZ_6+HZ_7+HZ_8+HZ_9)$$

where

$$HZ_0=\sigma_s\int_0^{2\pi}d\beta\int_0^{\frac{\pi}{2}}(N_{xx}\sin^3\gamma\cos^2\beta\cos\gamma$$

$$+N_{yy}\sin^3\gamma\sin^2\beta\cos\gamma+N_{zz}\cos^3\gamma\sin\gamma)d\gamma$$

$$=\frac{\pi\sigma_s}{4}(N_{xx}+N_{yy}+2N_{zz})$$

$$=\frac{\pi\sigma_s}{4}(N_{zz}+3)\ ,$$

$$HZ_1=\sigma_{xx}N_{xx}\int_0^{2\pi}d\beta\int_0^{\frac{\pi}{2}}\sin^5\gamma\cos\gamma\cos^4\beta d\gamma=\frac{\pi\sigma_{xx}N_{xx}}{8}\ ,$$

$$HZ_2=\sigma_{xx}N_{yy}\int_0^{2\pi}d\beta\int_0^{\frac{\pi}{2}}\sin^5\gamma\cos^2\beta\sin^2\beta\cos\gamma d\gamma=\frac{\pi\sigma_{xx}N_{yy}}{24}\ ,$$

$$HZ_3=\sigma_{xx}N_{zz}\int_0^{2\pi}d\beta\int_0^{\frac{\pi}{2}}\sin^3\gamma\cos^2\beta\cos^3\gamma d\gamma=\frac{\pi\sigma_{xx}N_{zz}}{12}\ ,$$

$$HZ_4=\sigma_{yy}N_{xx}\int_0^{2\pi}d\beta\int_0^{\frac{\pi}{2}}\sin^5\gamma\sin^2\beta\cos^2\beta\cos\gamma d\gamma=\frac{\pi\sigma_{yy}N_{xx}}{24}\ ,$$

$$HZ_5=\sigma_{yy}N_{yy}\int_0^{2\pi}d\beta\int_0^{\frac{\pi}{2}}\sin^5\gamma\sin^4\beta\cos\gamma d\gamma=\frac{\pi\sigma_{yy}N_{yy}}{8} ,$$

$$HZ_6=\sigma_{yy}N_{zz}\int_0^{2\pi}d\beta\int_0^{\frac{\pi}{2}}\sin^3\gamma\cos^3\gamma\sin^2\beta d\gamma=\frac{\pi\sigma_{yy}N_{zz}}{12} ,$$

$$HZ_7=\sigma_{zz}N_{xx}\int_0^{2\pi}d\beta\int_0^{\frac{\pi}{2}}\sin^3\gamma\cos^3\gamma\cos^2\beta d\gamma=\frac{\pi\sigma_{zz}N_{xx}}{12} ,$$

$$HZ_8=\sigma_{zz}N_{yy}\int_0^{2\pi}d\beta\int_0^{\frac{\pi}{2}}\sin^3\gamma\cos^3\gamma\sin^2\beta d\gamma=\frac{\pi\sigma_{zz}N_{yy}}{12} ,$$

and

$$HZ_9=\sigma_{zz}N_{zz}\int_0^{2\pi}d\beta\int_0^{\frac{\pi}{2}}\sin\gamma\cos^5\gamma d\gamma=\frac{\pi\sigma_{zz}N_{zz}}{3}$$

So we obtain the strain component on the z-direction

$$\varepsilon_{zz}=\frac{1}{16}\{C_{se}\sigma_s(N_{zz}+3)-\frac{1}{6}C_{se}[(3\sigma_{xx}+\sigma_{yy}+2\sigma_{zz})N_{xx} \\ +(\sigma_{xx}+3\sigma_{yy}+2\sigma_{zz})N_{yy}+(2\sigma_{xx}+2\sigma_{yy}+8\sigma_{zz})N_{zz})]\} \tag{5.19}$$

We rearrange equations (5.15), (5.17) and equation (5.19), so

$$\varepsilon_{xx}=\frac{1}{16}\{C_{se}\sigma_s(N_{xx}+3)-\frac{C_{se}}{6}[(2(4N_{xx}+N_{yy}+N_{zz})\sigma_{xx}$$
$$+(2N_{xx}+3N_{yy}+N_{zz})\sigma_{yy}+(2N_{xx}+N_{yy}+3N_{zz})\sigma_{zz}]\} \tag{5.20}$$

$$\varepsilon_{yy}=\frac{1}{16}\{C_{se}\sigma_s(N_{yy}+3)-\frac{C_{se}}{6}[((3N_{xx}+2N_{yy}+N_{zz})\sigma_{xx}$$
$$+2(N_{xx}+4N_{yy}+N_{zz})\sigma_{yy}+(N_{xx}+2N_{yy}+3N_{zz})\sigma_{zz}]\} \tag{5.21}$$

$$\varepsilon_{zz}=\frac{1}{16}\{C_{se}\sigma_s(N_{zz}+3)-\frac{C_{se}}{6}[((3N_{xx}+N_{yy}+2N_{zz})\sigma_{xx}$$
$$+(N_{xx}+3N_{yy}+2N_{zz})\sigma_{yy}+2(N_{xx}+N_{yy}+4N_{zz})\sigma_{zz}]\} \tag{5.22}$$

In order to obtain the stress-strain relations from the theoretical model we have to find the fabric constants N_{xx}, N_{yy}, and N_{zz}. By using the relation $N_{xx} + N_{yy} + N_{zz} = 3$, the constitutive relations become

$$\varepsilon_{xx}=\frac{C_{se}}{96}[18\sigma_s-3(2\sigma_{xx}+\sigma_{yy}+3\sigma_{zz})+(6\sigma_s$$
$$-6\sigma_{xx}-\sigma_{yy}+\sigma_{zz})N_{xx}-2(\sigma_{yy}-\sigma_{zz})N_{yy}] \tag{5.23}$$

$$\varepsilon_{yy}=\frac{C_{se}}{96}[18\sigma_s-3(\sigma_{xx}+2\sigma_{yy}+3\sigma_{zz})-2(\sigma_{xx}$$
$$-\sigma_{zz})N_{xx}+(6\sigma_s-\sigma_{xx}-6\sigma_{yy}+\sigma_{zz})N_{yy}] \tag{5.24}$$

$$\varepsilon_{zz}=\frac{C_{se}}{96}[36\sigma_s-2(\sigma_{xx}+\sigma_{yy}+4\sigma_{zz})-(6\sigma_s+\sigma_{xx}$$
$$-\sigma_{yy}-6\sigma_{zz})N_{xx}-(6\sigma_s-\sigma_{xx}+\sigma_{yy}-6\sigma_{zz})N_{yy}] \tag{5.25}$$

The fabric constants are given by

$$N_{xx}=\frac{(g_2\varepsilon_{xx}-f_3\varepsilon_{yy})(h_1\varepsilon_{xx}-f_1\varepsilon_{zz})-(f_1\varepsilon_{yy}-g_1\varepsilon_{xx})(f_3\varepsilon_{zz}-h_3\varepsilon_{xx})}{(f_2\varepsilon_{yy}-g_3\varepsilon_{xx})(f_3\varepsilon_{zz}-h_3\varepsilon_{xx})-(h_2\varepsilon_{xx}-f_2\varepsilon_{zz})(g_2\varepsilon_{xx}-f_3\varepsilon_{yy})} \tag{5.26}$$

$$N_{yy}=\frac{(h_1\varepsilon_{xx}-f_1\varepsilon_{zz})(g_3\varepsilon_{xx}-f_2\varepsilon_{yy})-(f_1\varepsilon_{yy}-g_1\varepsilon_{xx})(f_2\varepsilon_{zz}-h_2\varepsilon_{xx})}{(f_3\varepsilon_{yy}-g_2\varepsilon_{xx})(f_2\varepsilon_{zz}-h_2\varepsilon_{xx})-(h_3\varepsilon_{xx}-f_3\varepsilon_{zz})(g_3\varepsilon_{xx}-f_2\varepsilon_{yy})} \tag{5.27}$$

where

$$f_1=18\sigma_s-3(2\sigma_{xx}+\sigma_{yy}+3\sigma_{zz})\ ,$$

$$f_2=6\sigma_s-(6\sigma_{xx}+\sigma_{yy}-\sigma_{zz})\ ,$$

$$f_3=2(\sigma_{zz}-\sigma_{yy})\ ,$$

$$g_1=18\sigma_s-2(\sigma_{xx}+2\sigma_{yy}+3\sigma_{zz})\ ,$$

$$g_2=6\sigma_s-\sigma_{xx}-6\sigma_{yy}+\sigma_{zz}\ ,$$

$$g_3=2(\sigma_{zz}-\sigma_{xx})\ ,$$

$$h_1=2[18\sigma_s-(\sigma_{xx}+\sigma_{yy}+4\sigma_{zz})]\ ,$$

$$h_2=-6\sigma_s-(\sigma_{xx}-\sigma_{yy}-6\sigma_{zz})\ ,$$

and

$$h_3=-6\sigma_s+\sigma_{xx}-\sigma_{yy}+6\sigma_{zz}$$

Equations (5.20) to (5.27) provide a theoretical framework for the anisotropic swelling behaviour of clay. The model states that the swelling strains are dependent on clay particle swelling properties, clay particle fabrics, and the imposed stresses. The application of stress in one principal direction not only suppresses the swelling in that direction but also reduces swelling in the orthogonal directions. The model predicts a linear relationship between the imposed stress and the swelling strain because a linear stress-strain law for the clay particle is assumed. The power and semi-log laws can be introduced to describe non-linear swelling behaviour.

According the definition of elastic theory, we obtain corresponding Young's moduli

$$E_{xx}=-\frac{12}{C_{se}(4N_{xx}+N_{y}+N_{z})} \tag{5.28}$$

$$E_{yy}=-\frac{12}{C_{se}(N_{xx}+4N_{y}+N_{z})} \tag{5.29}$$

$$E_{zz}=-\frac{12}{C_{se}(N_{xx}+N_{y}+4N_{z})} \tag{5.30}$$

Obviously, for transversely isotropic swelling clay, we have

$$\begin{aligned} E_{xx}=E_{yy}&=-\frac{24}{C_{se}(15-3N_{zz})} \\ E_{zz}&=-\frac{4}{C_{se}(1+N_{zz})} \end{aligned} \tag{5.31}$$

For isotropic swelling soil, the Young's moduli become

$$E_{xx}=E_{yy}=E_{zz}=-\frac{2}{C_{se}} \tag{5.32}$$

The Poisson's ratio is -0.5 for isotropic swelling clay. The negative value of

Poisson's ratio means that the clay sample will swell, instead of contract, in three orthogonal directions when the imposed stress is less than the swelling pressure.

5.4 COMPARISON OF THEORETICAL RESULTS WITH EXPERIMENTAL DATA

In this section, the proposed anisotropic swelling model will be used to analyze the experimental results of swelling tests on Southern Ontario Queenston clay shale cores. Details of testing methods and results are reported by Lo and Lee (1990). They found that the swelling behaviour is orthotropic and highly stress dependent. The application of stress in one principal direction not only suppresses the swelling in that principal direction but also in the orthogonal directions. However, they did not bring forward a theory to account for the behaviour observed from their tests.

5.4.1 Experimental Data

5.4.1.1 Shale Samples

The samples of Queenston shale studied were obtained at depths between 80m and 122m from a borehole near Niagara Falls, Southern Ontario. The directions and magnitudes of the in situ principal horizontal stresses determined from hydrofracturing tests are: 7.9 MPa along the major principal horizontal-stress direction (HM) direction, and 5.2 MPa along the major principal horizontal-stress direction (HN direction). The direction of the minor principal stress is N45°E. The in situ vertical stress (V direction) is due to the overburden of depth about 105m.

The average unit weight of Queenston shale is 26.7 KN/m^3. The water content is about 2.6 %, and the porosity is approximately 7%. The calcite content varies from 3% to 7%. The salinity of the pore fluid is in the range of 108-265 g/L. The elastic moduli vary from 9 to 13 GPa, with Poisson's ratios of 0.35-0.40. There is no significant trend of variation in physical and mechanical properties with depth.

5.4.1.2 Test Detail and Results

To study the directional swelling behaviour, two types of swelling tests, the free swelling tests and the semiconfined swell test, were used to measure the swelling deformations in the directions of the three principal stress, i.e., V, HM, and HN directions

In the free swelling test, a cylindrical sample (61mm in diameter and 62mm in height) was immersed in a bath of water, and no vertical stress, σ_a, was applied to the sample. Eleven free swelling tests were performed on shale samples prepared from the vertically drilled cores where orientations were shown in Figure 5.5a. The test results are shown in Table 5.1.

The swelling strains are expressed in swelling potential, i.e., the swelling strains which occurred between 10 and 100 days. The horizontal strains in the major and minor principal stress directions (HM and HN directions, respectively) are virtually identical,

Table 5.1 Summary of Free Swelling Test Results

On Queenston Shale from SABNGS No. 3 Site

Year of test	Sample No.	σ_a (MPa)	Swelling potential HM (%)	HN	V
1985	FS1	0	0.32	0.32	0.48
	FS2	0	0.24	0.24	0.39
	FS3	0	0.24	0.24	0.45
1986	FS1	0	0.31	0.31	0.41
	FS2	0	0.34	0.34	0.51
	FS3	0	0.27	0.27	0.42
1987	FS1	0	0.30	0.30	0.49
	FS2	0	0.34	0.34	0.54
	FS3	0	0.24	0.24	0.38
	FS4	0	0.24	0.24	0.41
	FS5	0	0.22	0.22	0.37

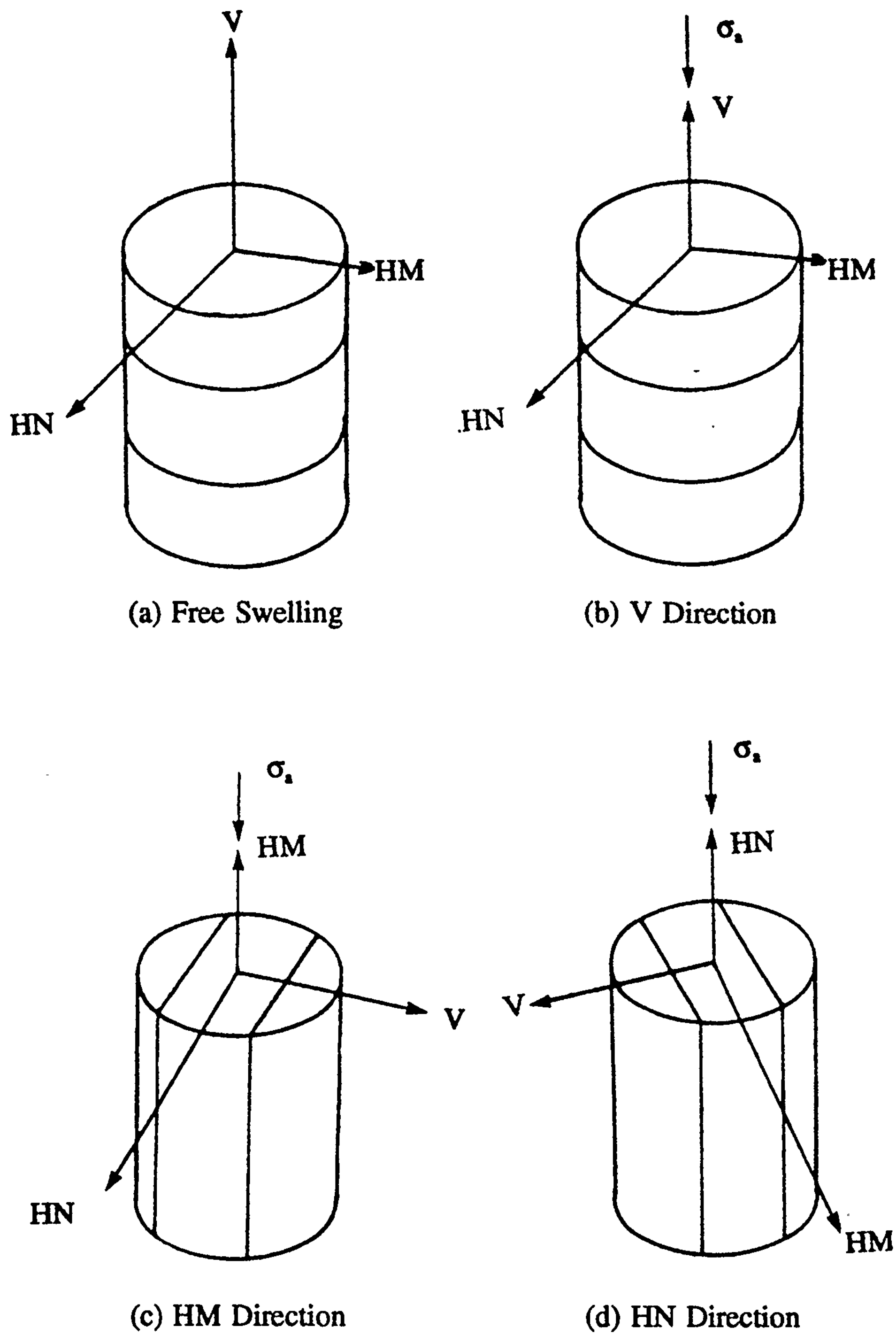

Figure 5.5 Various Specimen Orientation with Respect to Applied Stress Direction

indicating the swelling behaviour in the horizontal directions is isotropic. It is also observed from Table 5.1 that (1) there is no definite trend in variation of vertical and horizontal swelling potential with depth, and (2) swelling potentials in the vertical direction are approximately 1.6 times these in the horizontal directions.

In the semiconfined swelling test, a cylindrical sample was immersed in a bath of water and a vertical stress, σ_a, was applied to the top of the sample. Test samples of three different orientations coaxial with the in situ stress were prepared for the semiconfined swelling test, as shown in Figure 5.5b to 5.5d. The swelling potentials measured in 27 tests were summarized in Table 5.2. Test results indicate that the applied stress in the vertical direction suppresses the swelling in the horizontal directions, on which external stresses are applied. Swelling potentials in all three directions decrease with increasing applied stress. Swelling potentials in the vertical direction are generally higher than horizontal swelling potentials, suggesting that the swelling behaviour of Queenston shale is transversely isotropic. However, the swelling potentials in the horizontal directions are isotropic.

5.4.2 Model Prediction

In this section, we determine the swelling pressure σ_s, swelling coefficient C_{se} and fabric constants N_{xx}, N_{yy} and N_{zz} from the free swell results using the model. With these determined values, we use the model to predict the swelling potentials under the semiconfined condition and compare the predicted results with those observed in the semiconfined tests.

Table 5.2 Summary of Modified Semiconfined Swell Test

Results on Queenston Shale from SABNGS No.3 Site

Year of test	Sample No.	σ_a (MPa)	Swelling potential		
			HM	HN	V
1985	MSC/V1	0.027	0.20	0.210	0.265
	MSC/V2	0.131	0.19	0.170	0.220
	MSC/V3	0.691	0.17	0.155	0.140
	MSC/HM1	0.036	0.19	0.120	0.245
	MSC/HM2	0.342	0.15	0.135	0.180
	MSC/HM3	1.855	0.04	0.115	0.150
	MSC/HN1	0.036	0.24	0.150	0.260
	MSC/HN2	0.342	0.18	0.125	0.220
	MSC/HN3	1.860	0.11	0.040	0.145
1986	MSC/V1	0.019	0.210	0.210	0.240
	MSC/V2	0.131	0.230	0.170	0.202
	MSC/V3	0.687	0.140	0.140	0.195
	MSC/HM1	0.036	0.180	0.165	0.220
	MSC/HM2	0.358	0.125	0.120	0.220
	MSC/HM3	1.866	0.040	0.125	0.165
	MSC/HN1	0.036	0.160	0.150	0.270
	MSC/HN2	0.355	0.160	0.160	0.205
	MSC/HN3	1.868	0.060	0.025	0.160
1987	MSC/V1	0.025	0.175	0.140	0.220
	MSC/V2	0.250	0.125	0.105	0.185
	MSC/V3	2.380	0.150	0.100	0.080
	MSC/HM1	0.025	0.155	0.210	0.250
	MSC/HM2	0.250	0.125	0.180	0.240
	MSC/HM3	2.420	0.050	0.105	0.190
	MSC/HN1	0.025	0.220	0.195	0.300
	MSC/HN2	0.260	0.220	0.145	0.290
	MSC/HN3	2.420	0.110	0.040	0.130

In free swelling conditions, equations (5.26) to (5.27) are simplified to

$$N_{xx}=\frac{3(3\varepsilon_{xx}-\varepsilon_{yy}-\varepsilon_{zz})}{\varepsilon_{xx}+\varepsilon_{yy}+\varepsilon_{zz}} \tag{5.33}$$

$$N_{yy}=\frac{3(3\varepsilon_{yy}-\varepsilon_{xx}-\varepsilon_{zz})}{\varepsilon_{xx}+\varepsilon_{yy}+\varepsilon_{zz}} \tag{5.34}$$

After averaging the data of swelling potentials listed in Table 5.1 for each year, and then substituting those data into the equations (5.33) and (5.34), we obtain the fabric constants N_{xx} and N_{yy}. The assumed swelling pressure σ_s is 3.26 MPa which is larger than the in-situ vertical stress. Using the relations $N_{xx}+N_{yy}+N_{zz}=3$, the swell coefficient C_{se}, fabric constants N_{xx} , N_{yy} and N_{zz} and elastic moduli E_{xx}, E_{yy}, and E_{zz} are calculated and presented in Table 5.3.

Table 5.3 Summary of Fabric Constants and C_{se}

Year of test	σ_s (MPa)	C_{se} (1/GPa)	Fabric constants N_{xx}	N_{yy}	N_{zz}	Elastic moduli (GPa) E_{xx}	E_{yy}	E_{zz}
1985	3.26	0.2910	0.2879	0.2879	2.4243	10.7	10.7	4.0
1986	3.26	0.2908	0.4717	0.4717	2.0565	9.3	9.3	4.5
1987	3.26	0.2216	0.3018	0.3018	2.3963	13.9	13.9	5.3

The fabric constant N_{zz} and elastic modulus in the vertical direction E_{zz} are larger than fabric constants N_{xx} and N_{yy} and elastic moduli E_{xx} and E_{yy} in the horizontal directions, indicating that the vertical swelling potential is larger than the horizontal. In

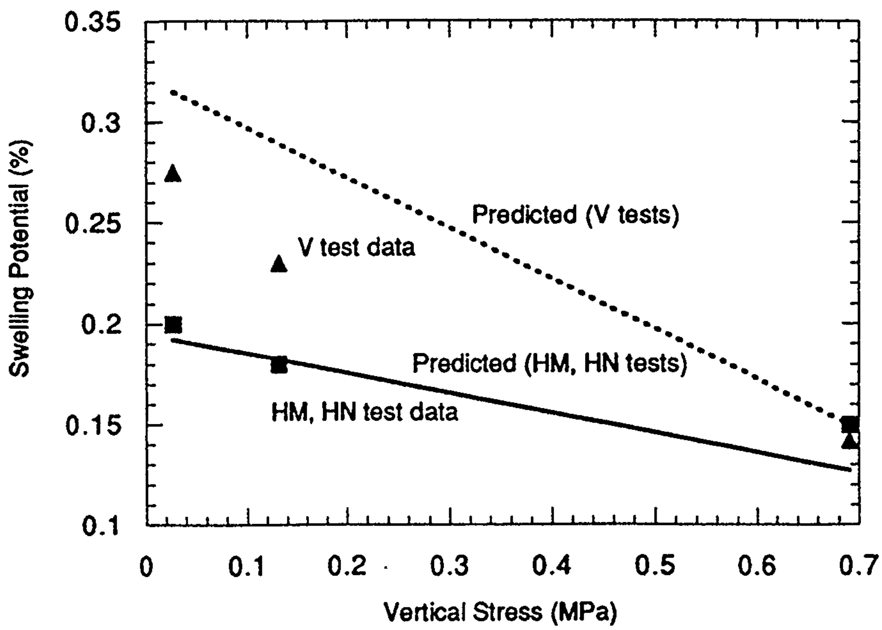

Figure 5.6 Comparison of Predicted and Experimental Results

(1985 Tests, V Direction)

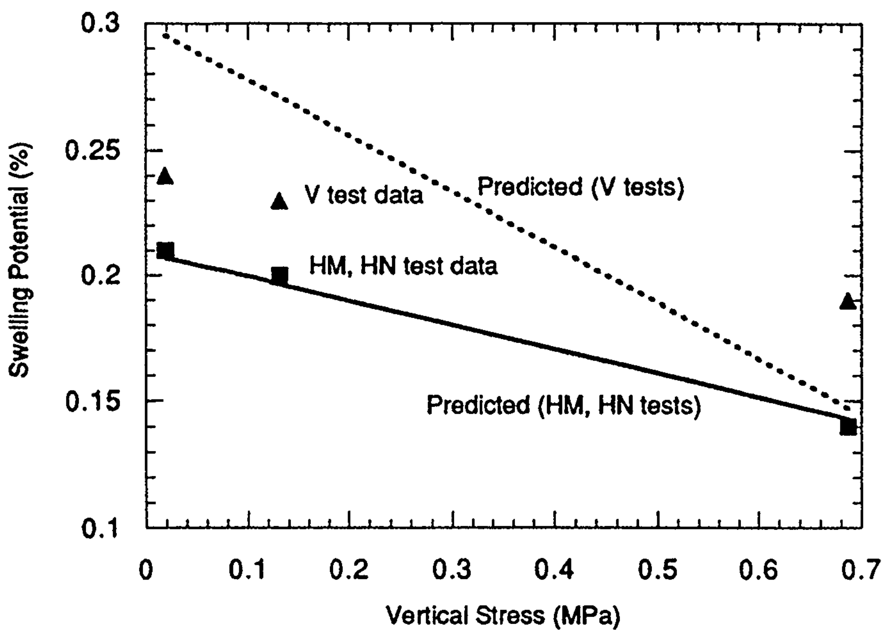

Figure 5.7 Comparison of Predicted and Experimental Results

(1986 Tests, V Direction)

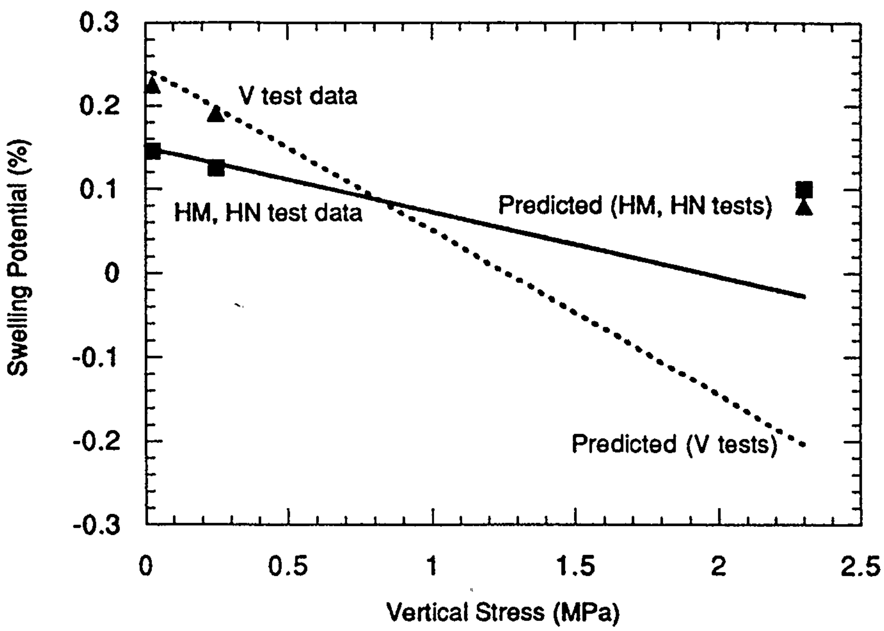

Figure 5.8 Comparison of Predicted and Experimental Results

(1987 Tests, V Direction)

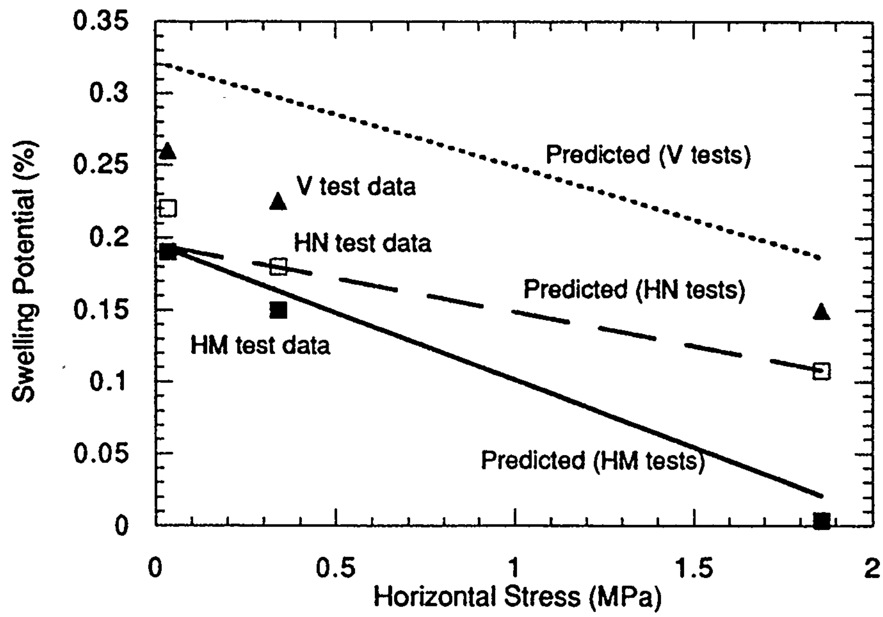

Figure 5.9 Comparison of Predicted and Experimental Results

(1985 Tests, HM and HN Directions)

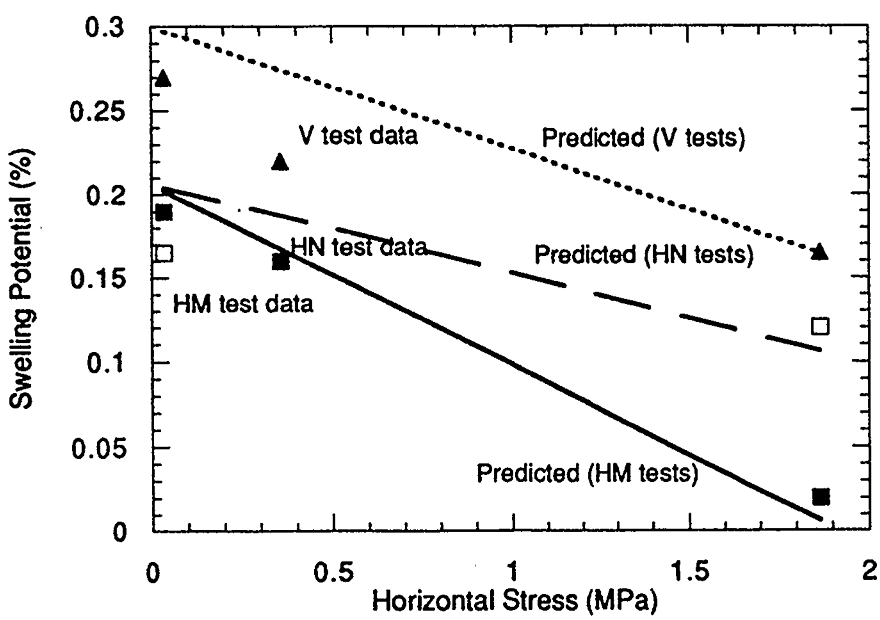

Figure 5.10 Comparison of Predicted and Experimental Results

(1986 Tests, HM and HN Directions)

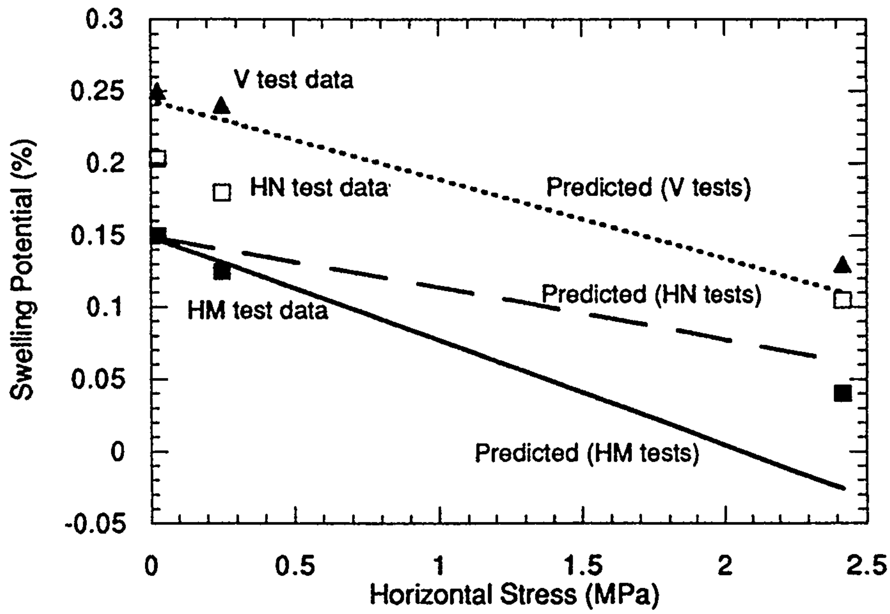

Figure 5.11 Comparison of Predicted and Experimental Results

(1987 Tests, HM and HN Directions)

addition, $N_{xx} = N_{yy}$ and $E_{xx} = E_{yy}$ suggests isotropic swelling deformation in the horizontal directions.

Using the swelling constants and fabric constants determined from the free swell tests, the swelling potential under semiconfined condition listed in Table 5.2 are calculated from the model, and plotted in Figures 5.6 to 5.11. In these figures experimental data are also plotted for comparison. The predicted swelling behaviour are generally consistent with those observed in the tests. However, in some V tests, there are differences between the predicted results and experimental measurements. This is probably due to the heterogeneity of the samples. The application of confining stress in one direction suppresses the swelling in its direction as well as the orthogonal directions. The difference between the predicted and observed results are mainly due to the assumption of the linear swelling behaviour of clay particles, i.e., C_{se} becomes independent of stress. A non-linear behaviour obeying power or semi-log law may yield a better match between the predicted and observed results. However, no analytical solution will be obtained and numerical analysis is required if a non-linear swell relation is used.

5.5 CONCLUSION

In this chapter, a stress-strain model based on micromechanics has been developed to predict anisotropic swelling behaviour of clay. The model predicts that the swelling is dependent on clay particle swelling properties, fabrics and imposed principal stresses. The application of stress in one direction suppresses the swelling in that direction as well as in orthogonal directions. The model has been evaluated by comparing the predicted results with those from experiments.

CHAPTER 6

CONCLUSIONS AND RECOMMENDATIONS

6.1 INTRODUCTION

Particulate, discrete and frictional materials such as sands, form a separate class of materials. Stress and strain at a point, as defined for continuous media, are not valid for assemblies consisting of granular sands and swell particles. Instead, stress and strain have to be redefined for these assemblies, as the force and displacement averaged over a representative-unit or a finite volume within the system. This process of averaging is performed by summation of the total contact normals for regular packing or integration using a density function of contact normals for random packing.

The constitutive relations are dependent on the microstructure or fabric of a particulate assembly. Different types of regular packing have different stress-strain relations which can be reflected by the corresponding constitutive coefficients. For a random packing assembly, the stiffness tensor can be obtained in an explicit form which is expressed in terms of the contact stiffness of the particles and the fabric tensor of the assembly.

Based on analysis of the micromechanics of particulate assemblies, including assemblies of rigid particles, deformable particles, and swelling particles, stress-strain relations are derived from the concepts of a sliding plane and micromechanical continuum. The conclusions presented are applicable to granular sands and swelling clays.

6.2 CONCLUSIONS

The shear behaviour of a granular assembly of rigid particles in simple shear and biaxial compression conditions have been studied using the principle of micromechanics. Analytical solutions are derived to describe the stress ratio, the change in fabric distribution and orientation, and the strain ratio during the process of shear deformation. Development of a stress-strain model based on micromechanics requires an additional relation linking the change in fabrics, and the change in contact number to the strain. The main advantages of this micromechanical model are that the model considers the effects of the fabric anisotropy, and the rotation of principal stress on the shear deformation of granular medium. The model provides a sound basis to explain some empirical correlations in soil mechanics such as Rowe's stress-dilatancy law and critical state. Since the model includes the effects of fabrics, the model can be applicable to any granular assembly of particles of different size distribution.

Based on the principles of micro-mechanics we have derived the stress-strain relations of contact deformation for two-dimensional and three-dimensional regular packing assemblies. The derived stiffness constants are functions of the particle size, void ratio, coordination number, and interparticle contact stiffness. If the interparticle contact interaction is assumed to be linear elastic with no sliding at the contact, the assembly deformation is elastic. If the nonlinear constant stiffness given by the Hertz-Mindlin theory of friction contact is used, nonlinear deformation will occur due to plastic deformation at the contacts. It is noted that the stiffness tensor is derived for an increment of load based on the packing structure at the instant of load increment. The packing structure , however, changes during the deformation process. Therefore, for cases with a large change of packing structure such as at high levels of deviatoric stress, the evolution of the packing structure with load should be defined in order to obtain the complete stress-strain relation. For cases with negligibly small changes in packing structure such as for packing under low levels of deviatoric stress, the proposed stress-strain relation can be directly applied in analyses of practical problems. All the solutions can be used in the cases of different complicated loads because here we assume the principal stress axis not to be coincident with the principal fabric axis. No matter what case, two dimensional or three-dimensional, if the assembly is isotropic and D_s=D_t, only two stiffness constants are independent. If the assembly is isotropic on the cross plane for the case of three-dimensions, five stiffness constants are independent. These conclusions are the same as those obtained by the theory of continuum mechanics. In addition, stiffness constants are dependent on the different fabric constants.

For random packing assemblies the stress-strain relations under contact deformation are derived considering the fabric distribution and orientation, and micromechanics. The main conclusions are consistent with those from the conclusions from continuum theory. These conclusions include: (1) The stress-strain relations are related to the fabrics of assembly and to the local contact stiffnesses. (2) For a fully anisotropic assembly, if the three local contact stiffness constants are not equal to one another, the stress-strain relation is controlled by 21 stiffness constants. If the two tangent stiffness constants are equal, i.e. $D_s = D_t$, the independent stiffness constants reduce from 21 to 18. (3) If the directions of the principal fabric axes are the same as those of principal stress axes, though it is anisotropic, the number of independent stiffness constants is only nine. (4) For the case of the isotropic assembly on the intersection plane, only five independent stiffness constants determine the stress-strain relation. (5) For an isotropic assembly, there are two independent constants.

In addition, a stress-strain model based on micromechanics has been developed to predict anisotropic swelling behaviour of clay. The model predicts that the swelling is dependent of clay particle swelling properties, fabrics and imposed principal stresses. The application of stress in one direction suppresses the swelling in that direction as well as the orthogonal directions. The model has been evaluated by comparing the predicted results with these from experiments.

6.3 RECOMMENDATIONS

In Chapter 2, the model can be applied to a particulate assembly with any shape and size of particles. A versatile three-dimensional model can be obtained using the same approach as presented in this chapter. In this case, we have to introduce a three-dimensional density function same as equation (4.7) and analyze the equilibrium of contact forces (f_{nx}, f_{ny}, and f_{nz}) and external stresses (σ_{xx}, σ_{yy}, and $_{zz}$).

In Chapters 3 and 4, the derived stress-stain relations are based on a system of equal size spherical particles. It is possible to extend this model to a system with different size distribution but still spherical particles if we introduce a density function describing particle dimension or void ratio.

In Chapter 5, we assume the swelling coefficient is a constant and the local constitutive law of swelling particles depends on the first-power of normal pressure. There are two ways to improve this model, namely, we assume a local constitutive law

$$\delta^{t}=C_{sw}(\sigma)[\sigma_{s}-\sigma(\gamma,\beta)]$$

or

$$\delta^{t}=C_{sw}[\sigma_{s}-\sigma(\gamma,\beta)]^{\eta}$$

where η is a test parameter.

BIBLIOGRAPHY

Arthur, J. R. F.(1975). "Homogeneous and layered sand in triaxial compression." Geotechnique, Vol. 25, No. 4, pp. 799-815.

Arthur, J. R. F., and Menzies, B. K. (1977). "Induced anisotropy in a sand." Geotechnique, Vol. 27, No. 1, pp. 13-30.

Atukorala, U. D. (1989). "Stress-strain relations for sand based on particulate consideration." Ph.D. Dissertation, University of British Columbia. British Columbia, Canada.

Barden, L., and Nhightman. (1969). "Plane strain deformation of granular materials at low and high pressures." Geotechnque, Vol. 19, No. 4, pp. 441-452.

Bathurst, R. J. (1985). "A study of stress and anisotropy in idealized granular assembly." Ph.D. Dissertation, Queen's University, Ontario, Canada.

Bathurst, R. J., and Rothenburg, L. (1988a). "Micromechanical aspects of isotropic granular assembles with linear contact interaction." J. Applied. Mech., ASME, Vol. 55, No. 1, pp. 17-13.

Bathurst, R. J., and Rothenburg, L. (1988b). "Note on a random isotropic granular material with negative Poisson's ratio." Int. J. Engrg Sci., Vol. 26, No. 4, pp. 373-384.

Bazant, Z. P. (1975). "Micromechanics model for creep of anisotropic clay." J. Engrg. Mech. Div., Vol. 101, No. EM1., pp. 57-78.

Bernal, J. D. (1960). "Co-ordination of randomly packed spheres." Nature, Vol. 108, pp. 901-911.

Bishop, A. W. (1950). Discussion of "The measurement of the shear strength of soil." by Skempton and Bishop, Geotechnigue, Vol. II, No. 2, pp. 113-116.

Brown, C. B. (1976). "The use of maximum entropy in the characterization of granular media." Proc. U. S. - Japan Seminar on Continuum Mechanical and Statistical Approach in The Mechanics of Granular Materials, Sendai, Japan.

Brown, C. B. (1988). "Experiments on disc arrays, coordination and void entropies." Micromechanics of Granular Materials, Ed. by M. Satake and J. T. Jenkins, pp. 142-152.

Caquot (1934). "Equilibre des massifs a frottement interne." Stabilite des Terres Pulverents et Coherentes, Gauthier Villars, Paris, France.

Casagrande, A. N. (1936). "Characteristics of cohesionless soils affecting the stability of slopes and earth fills." J. Boston Soci. Civil Engrg., pp.257-276.

Chang, C. S. (1985). "Dilatancy modelling for granular sand in simple shear condition." Proc. 11th Int. Conf. on Soil Mech. and Found. Engrg., San Francisco, pp. 419-422.

Chang, C. S. (1988). "Micromechanical modelling of constitutive relation for granular materials." Micromechanics of Granular Materials, Ed. by M. Satake and J. T. Jenkins, pp. 271-278.

Chang, C. S. (1990a). "Strain tensor and deformation for granular materials." J. of Engrg. Mech., Vol 116, No. 4, pp. 792-804.

Chang, C. S. (1990b) "Packing structure and mechanical properties of granular." J. Engrg. Mech., Vol. 116, No. 5, pp. 1077-1093.

Chang, C. S., (1990c) "Constitutive relation for a particulate medium with the effect of particle rotation." Int. J. Solids Strut., Vol. 26, No. 4, pp. 437-453.

Chang, C. S., Cahng, Y. and Kabir, M. G. (1992a). "Micromechanics modelling for stress-strain behaviour of granular soils. I: theory." J. of Geotech. Engrg., Vol. 118, No. 12, pp. 1959-1974.

Chang, C. S., Cahng, Y. and Kabir, M. G. (1992b). "Micromechanics modelling for stress-strain behaviour of granular soils. I: evaluation." J. of Geotech. Engrg., Vol. 118, No. 12, pp. 1975-1992.

Chang, C. S., and Ma, L. (1990e) "Modelling of discrete granulates as micropolar continuum." J. Engrg. Mech., Vol. 116, No. 12, pp. 2703-2712.

Chang, C. S. and Misra, A. (1989b). "Theoretical and experimental study of regular packing of granulates." J. Engrg. Mech., Vol. 115, No. 4, pp. 705-720.

Chang, C. S. and Misra, A. (1989c). "Computer simulation and modelling of mechanical properties of particulate." Computers and Geotechnics, Vol. 7, pp. 269-287.

Chang, C. S. and Misra, A. (1990d). "Application of uniform strain theory to heterogeneous granular solids." J. Engrg. Mech., Vol. 116, No. 10, pp. 2310-2328.

Chang, C. S., Weeraratne, S. P., and Misra, A. (1989a). "Slip mechanism-based on constitutive model for granular soils." J. Engrg. Mech., Vol. 115, No. 3, pp. 790-807.

Christoffersen, J., Mehrabadi, M. M., and Nemat-Nasser, S. (1981). "A micromechanical description of granular material behaviour." J. Applied Mech., ASME, Vol. 48, pp. 339-344.

Collins, K. and Megowu, A. (1974) "The form and function of microfabric feature in a variety of natural soils." Geotechnique, Vol. 24, No. 2, 1974.

Coulomb, C. A. (1773). "Essaisur une application des regles de maximis et minimis a quelgues problemes de statique relatifes a l'architecture." Memoires de Mathematique and de Physique, l'Acdemie Royale des Sciences Par Divers Savans, and Las Dans Ses Assemblees, Vol. 7, pp.343-382.

Cowin, S. C., and Satake, M. (1978). "Continuum mechanical model for granular assemblies." Geotechnique, Vol. 29, No. 1, pp. 47-65.

Cundall, P. A. and Strack, O. D. L. (1979). "A discrete Numerical model for granular assemblies." Geotechnique, Vol. 29, No. 1, pp. 47-65.

Cundall, P. A. (1988). "Computer simulation of dense sphere assemblies." Micromechanics of Granular Materials, Ed. by M. Satake and J. T. Jenkins, pp. 113-123.

Davis, R. A. (1977). " A discrete probabilistic model for mechanical response of a granular medium." ACTA, Mechanics, Vol. 27, pp. 69-89.

Deresiewicz, H. (1958). "Stress-strain relation for a simple model of a granular medium." J. Applied Mech., ASME, Vol. 25, No. 3, pp. 402-406.

Digby, P. J. (1981). "The effective elastic moduli of porous granular rock." J. Applied Mech., ASME, Vol. 48, pp. 803-808.

Drescher, A. and Dejosseline, Dejong, G. (1972). "Photoelastic verification of a mechanical model for the flow of a granular material." J. Mech. and Physics of Solids, Vol. 20, No. 2, pp. 337-351.

Duffy, J. (1959). "A differential stress-strain relation for the hexagonal close-packed array of elastic spheres." J. Applied Mech., ASME, Vol. 26, pp. 88-94.

Duffy, J. and Mindlin, R. D. (1957). "Stress-strain relation and vibrations of a granular medium." J. Applied Mech., ASME, Vol. 24, pp. 585-593.

Field, W. G. (1963). "Towards the statistical deformation of a granular mass." Proc. 4th Aust. and N. Z. Conf. on Soil, pp. 143-148.

Gassmann, F. "Elastic waves through a packing of spheres." Geophysics, Vol. 16, pp. 673-685.

Ghaboussi, J. (1990). "Three-dimensional discrete element method for granular materials." Int. J. Num. and Analy. Methods in Geomech., Vol. 14, pp. 451-472.

Gray, W. A. (1968). "The packing of solid particles." Chapman and Hall Ltd. Landon.

Grivas, D. A., and Harr, M. E. (1975) "Particle contacts in discrete materials." Abstracts of Indiana Academy of Science, Engrg. Div., 1975.

Hara, G. (1935). "Theorie der akustischen Schwingungsbreitung in gekornten substanzen und experimentelle untersuchung an kohlepulrer." Elektrische Nachrichten-Technik, Vol. 12, pp. 191-200.

Horne, M. R. (1965). "The behaviour of an assembly of rotund, rigid, cohesionless particles, Part I and II." Proc. Royal Society, Series A, Vol. 286, pp. 62-92.

Iida, K. (1939). "velocity of elastic waves in a granular substance." Bulletin of the Earthquake Research Institute, Tokyo University, Vol. D, pp. 783-808.

Ishihara, K., and Okada, S. (1970). "Effects of stress history on cyclic behaviour of sand." Soils and Foundations, Vol. 18, No. 4, pp. 31-45.

Jenkins, J. T. (1988). "Volume change in small strain-axisymmetric deformations of granular materials." in Micromechanics of Granular Materials, Ed. by M. Satak and J. T. Jenkins.

Jenkins, J. T. and Satake, M. (1983). "Mechanics of Granular Materials: New Models and Constitutive Relations." Elasevier, New York, N. Y..

Johnson, K. L. (1976). "Adhesion at the contact of solids, in Theoretical and Applied Mechanics, Ed. by W. T., Koiter, Amsterdam, North Holland Publishing Company, 133-143.

Johnson, K. L. (1985). "Contact Mechanics.". London, Cambridge, University Press.

Kanatani, K. (1980). "An entropy model for shear deformation of granular materials." Lett. Applied Engrg. Sci., Vol. 16, pp. 989-998.

Kanatani, K. (1988). "Distribution of directional data and fabric tensors, Int. J. Engrg

Sci. Vol. 22, No. 2, pp. 149-164.

Kishino, Y. (1983). "A generalized relationship between the stress and the dilatancy in granular materials." Mechanics of Granular Materials, Ed. by J. T. Jenkins and M. Satake, pp. 117-126.

Kishino, Y. (1988). "Disc model analysis of micromechanics of granular materials." Ed. by M. Satake and J. T. Jenkins, pp. 143-152.

Kitainura, R. (1985) "A Markov model of particulate material with anisotropic fabrics." Proc. of the NUMETA Conference on Num. Methods. in Geomech., Nagaya, pp. 455-464.

Ko. H. Y. and Scott, R. F. (1967). "Deformation of sand in shear." J. Soil Mech. Found. Div., ASCE, Vol. 93, No. 5, pp. 283-310.

Konishi, J. (1983). "Induced aisotropiy in assemblies of oval-section rods in the biaxial compression." Mechanics of Granular Materials, Ed. by J. T. Jenkins and M. Satake, pp. 31-39.

Krizek, R. J. (1977) "Fabric effects on strength and deformation of Kaolin clay." Proc. 9th ICSMFE, Vol. 1, pp. 169-176.

Lee, K. L. and Farhoomand, I. (1967). "Compressibility and crushing of granular soil in anisotropic triaxial compression." Canadian Geotechnique Journal, Vol. IV, pp. 68-86.

Lo, K. Y. and Lee, Y. N. (1990). "Time-dependent deformation behaviour of Queeston shale." Can. Geotech. J., Vol. 27, pp. 461-471.

Lubkin, J. L. (1951). " The torsion of elastic sphere in contact." J. Applied Mech., ASME, Vol. 18, No. 2, pp. 183-186.

Makhlouf, H. and Stewart, J. J. (1967). "Elastic constants of cubical-tetrahedral and tetragonal spheroid array of uniform sphere." Proc. Int. Symp. of Wave Propagation and Dynamic Properties of Earth Materials, Albuqyerque, N. M., pp 825-837.

Marsal, R. J. (1963). "Contact forces in soil and rockfill materials." Proc. of the Second Panamerican Conference on Soil Mechanics and Foundation Engineering, Vol. 2, 67-90.

Marsal, R. J. (1964). " Stochastic process in the grain skeleton of soil." Proc. 6th ICSMFE, Vol. 1, pp. 303-307.

Matsuo, S. and Kamon, M. (1977). "Microscopic study on deformation and strength of clays." Proc. 9th ICSMEF, Vol. 1, pp. 201-204.

Matsuoka, H. (1974). "A microscopic study on shear mechanism of granular materials." Soils and Foundations. Vol. 14, No. 1, pp. 29-43.

Matsuoka, M. and Nakai, T. (1977). " Stress-strain relation of soils based on the SMP." Proc. of Speciality Session 9, 9th ICSMFE, pp. 155-161.

Mehrabadi, M. M. (1980). "On statistical description of stress and fabric in granular materials." Int. J. Num. Analy. Methods. in Geomech., Vol. 6, pp. 95-108.

Mehrabadi, M. M. (1983). "A micromechanically based on rate constitutive description of granular materials." Int. Conference on Constitutive Laws for Engineering Materials, Theory and Application, Tuscan, Arizona, Jan., pp. 10-14.

Mindlin, R. D. and Deresiewicz, H. (1953). "Elastic spheres in contact under varying oblique forces." J. Applied Mech., AMSE, Vol. 20, No. 3, pp. 327-344.

Mogami, T. (1965). "A statistical approach to the mechanics of granular materials." Soils and Foundations, Vol. 5, No. 2, pp. 30-37.

Nemat-Nasser, S. (1980). "On behaviour of granular materials in simple shear." Soils and Foundations, Vol. 20, No. 2.

Newland, P. L. and Allely, B. H. (1957). "Volume changes in drained triaxial test on granular materials." Geotechanique, Vol. 7, No. 1, pp. 17-34.

Oda, M. (1972a). "Initial fabrics and their relations to mechanical properties of granular materials. " Soils and Foundations, Vol. 12, No. 1, pp. 17-36.

Oda, M. (1972b). "The mechanics of fabric changes during compressional deformation of sand." Soils and Foundations, Vol. 12, No. 2, pp. 1-17.

Oda, M. (1974). "A mechanical and statistical model of granular material." Soils and Foundations, Vol. 14, No. 2, pp. 25-28.

Oda, M. (1977). "Co-ordination number and its relation to shear strength of granular materials." Soils and Foundations, Vol. 17, No. 2, pp. 20-41.

Oda, M. (1978). "Experiment study of anisotropic shear strength of sand by plane strain test." Soils and Foundations, Vol. 18, No. 1, pp. 25-38.

Oda, M. (1982). "A statistical study of fabric in a random assembly of spherical granules." Int. J. Num. Analy. Methods. Geomechanics, Vol. 6, No. 1, pp. 77-94.

Oda, M. (1985). "Stress-induced anisotropy in granular masses." Soil and Foundation, Vol. 25, No. 3, 85-97.

Oda, M. (1988). " Introduction of inherent anisotropy of soils in the yield function." Micromechanics of Granular Materials, Ed. by M. Satake and J. T., Jenkins, pp. 81-90.

Rankine, W. J. M. (1857). "On the stability of loose earth:" Phil. Trans. Royal Soc., Landon, England.

Reynolds, O. (1885). "On the dilatancy of media composed of rigid particles in contact." Phil. Magazine, Vol. 20, pp. 469-481.

Rothenburg, L. and Bathurst, R. J. (1989). " Analytical study of induced anisotropy in idealized granular materials." Geotechnique, Vo. 39, No. 4, pp. 601-614.

Rowe, P. W. (1962). " The stress-dilatancy relations for the static equilibrium of an assembly of particles in contact." Proc. of Royal Society, Series A, Vol. 269, pp. 500-527.

Rowe, P. W. (1972) "The relevance of soil fabric to site investigation." Geotechnique, Vol. 22, No. 2, pp. 195-300.

Satake, M. (1983). "Fundamental quantities in the graph approach to granular materials ." in Micromechanics of Granular Materials, Ed. by J. T., Jenkins and Satake, M., pp. 9-20.

Satake, M. and Jenkins, J. T. (1988). "Micromechanics of Granular Materials." Elsevier, New York, N. Y..

Scott, R. F. (1980). "Computer modelling of clay structure and mechanics." J. of Geotech. Engrg. Div. Vol. 106, No. 1, pp.17-33.

Serrano, A. A., and Rodrigues-Ortiz, J. M. (1973) " A contribution to the mechanics of heterogeneous granular media." Proc. Symp. Plasticity and Soil Mechanics, Cambridge, U. K..

Serrano, A. A. and Rodrigues-Ortiz, J. M. (1976). "Force and displacement fields in heterogeneous mechanics." Num. Methods in Soil Mech, and Rock Mech. Kanlarabe.

Smith, W. O., and Richart, P. D. (1989). "Packing of homogeneous spheres." Phys. Rew., Vol. 34, pp. 1271-1274.

Simith, W. O., Foote, P. D., and Busang, P. F. (1929). "Packing of homogeneous spheres." Physical Review, Vol. 34, pp. 1271-1274.

Taylor, D. W. (1938). "Plastic strain in metals." J. Inst. Metals, Vol. 62, No. 1, pp. 307-324.

Taylor, D. W. (1948). "Fundamentals of Soil Mechanics." J. Wiley and Sons, New York, N. Y..

Ting, T. W. and Corkum, B. T. (1988). "Strength of granular materials using discrete numerical modelling." Num. Meth. Geomechanics, Ed. by S. Woboda, Innsbruck, pp. 305-310.

Tobita, Y. (1988). "Yield condition of anisotropic granular materials." Soils and Foundations, Vol. 28, No. 2, pp. 113-126.

Tokue, T. (1979). "A consideration about Rowe's minimum energy ratio principle and a new concept of shear mechanism." Soil and Foundation, Vol. 18, No. 1, pp. 1-10.

Tuncer, B. E. (1975). "A micromechanical formulation for stress-strain response of clay." Int. J. Engrg. Sci., Vol. 13, pp. 831-840.

Tzou-shin Ueng (1990). "Deformation behaviour of sand under shear - particulate approach." J. of Geotech. Engrg., Vol. 116, No. 11, pp. 1625-1640.

Vesic, A. S. and Clough, G. W. (1968). "Behaviour of granular materials under high stress." J. of the Soil Mech. and Found. Engrg. Div., ASCE, Vol. 95, No. SM3, pp.661-687.

Walton, K. (1987). "The effective elastic moduli of random packing of sphere." J. Mech. Phys. Solids. Vol. 35, pp. 213-226.

Wroth, C. P. (1973). " A brief review of the application of plasticity to soil mechanics." Proc. Symp. on Plasticity and Soil Mech., Cambridge.

Yamada, Y. and Ishihara, K. (1979). "Anisotropic deformation characteristics of sand under three dimensional stress condition." Soil and Foundation, Vol. 19, No. 2, pp. 79-94.

Yanngiswa, E. (1983). "Influence of void and stress condition on the dynamic shear modulus of granular media." Adv. in the Mechanics and the Flow of Granular Materials, Vol. 2, pp. 947-960.